NUCLEAR STRUCTURE OF ^{21}Ne AND ^{29}Si

NUCLEAR STRUCTURE OF ^{21}Ne AND ^{29}Si

by

AADU ANDRES PILT, B.Sc., M.Sc.

A Thesis

Submitted to the School of Graduate Studies

in Partial Fulfilment of the Requirements

for the Degree

Doctor of Philosophy

McMaster University

June, 1972

DOCTOR OF PHILOSOPHY
(Physics)

McMASTER UNIVERSITY
Hamilton, Ontario

TITLE: Nuclear Structure of ^{21}Ne and ^{29}Si

AUTHOR: Aadu Andres Pilt, B.Sc. (Toronto)
M.Sc. (Alberta)

SUPERVISOR: Professor John A. Kuehner

NUMBER OF PAGES: v, 129

SCOPE AND CONTENTS:

The properties of the levels of ^{21}Ne and ^{29}Si have been studied via γ-ray angular distribution and linear polarization measurements and γ-γ coincidence studies yielding a number of new spin-parity assignments to the states of both nuclei. Comparison of the results with the Nilsson model for odd nuclei indicate that for ^{21}Ne, good agreement is in general obtained. Nevertheless, a number of interesting discrepancies exist with regard to the negative parity states of ^{21}Ne and explanations have been proposed for some of these. The agreement is also quite good for ^{29}Si with a calculation using a minimum of free parameters, confirming the oblate shape for this nucleus.

ACKNOWLEDGEMENTS

At one time or another during the past two and a half years, I have received advice, assistance and stimulation from almost every nuclear physicist at McMaster. Although it is impossible to mention everyone personally, I would like to extend my thanks to all of them collectively. In particular, moreover, I would like to express my gratitude to:

Professor John Kuehner, my supervisor, for his penetrating insight into matters of importance, his love of physics, his guidance, suggestions, criticisms and encouragement;

Geoff Frank; for his assistance with the experiments, for his willingness to listen to my ideas with such enthusiasm, and who, along with

Bob O'Neil and Bob Price, was responsible for the realization of much of the Nilsson model code;

Present and past members of the group: Al Baxter, Everett Cairns, Russ Elliott, Hubert Grawe, Wayne Greene, Dave Kelly and Ray Spear for their various contributions;

Professors A. B. Volkov and G. R. Piercy of my Supervisory Committee for their sincere interest and help;

Keith Scott for assistance with matters theoretical;

Claus Rolfs of the University of Toronto for help with the initial stages of the ^{21}Ne experiments and for

numerous discussions;

Professor M. W. Johns for affording me the opportunity to work in such a pleasant and stimulating environment, and for his advice at a crucial moment of my research;

Phil Ashbaugh, John McKay and the rest of the accelerator staff for providing more alpha particles than I knew what to do with;

Mrs. Helen Kennelly for typing the manuscript with such incredible speed and finesse;

and The National Research Council of Canada for financial support in the form of Postgraduate Scholarships.

Emale

TABLE OF CONTENTS

INTRODUCTION

At first sight, the atomic nucleus is such an incredibly complex aggregate of particles that it appears distressingly hopeless to envision ever understanding it, and it is quite true that the system of A nucleons (with $A \geq 3$) is completely intractable to an exact analysis. Hence, simplified models of its structure are necessary, based on hopefully reasonable assumptions concerning its dominant features. Some of these models treat the collective properties of the nucleus in which the individual constitutents thereof lose their identity almost entirely. Thus, those aspects of the nucleus which depend primarily on its size and shape are studied, and it is found that modes of excitation apparently exist which are reminiscent of rotations and vibrations of deformed, soft ellipsoids. Other models, perhaps more satisfying, strive to retain the basically particulate nature of the nucleus and explain its excited states in terms of rearranging the "outer" active particles in planetary-like orbits ("shells") with differing energies and angular momenta. Excited states of nuclei have been found corresponding to both of the above (admittedly rather over simplified) pictures, although it is clear that completely microscopic calculations (such as the shell model with

suitable interactions) should reproduce the collective properties of nuclei as well.

The experimental study of the electromagnetic decays of nuclear levels is a useful method of obtaining the parameters, such as excitation energies, spins, parities and lifetimes of the levels and the multipolarity of the transitions which are required to effectuate a realistic comparison with the properties predicted by the various models. The remarkable feature of studying the nucleus through its electromagnetic interactions is its relative independence of the ill-known nuclear force - the quantum mechanical theory of the electromagnetic field being well-known.

In this thesis is described an investigation of the electromagnetic decay properties of two nuclei: ^{21}Ne and ^{29}Si. The former nucleus, ^{21}Ne, is rather well described both by the shell model and the Nilsson collective model, and it was envisaged to place the collective model on a firmer basis by extending the then-known experimental results - and this was quite successful. In the course of the theoretical interpretation of the nucleus as a whole, however, some rather anomalous features were noted and eventually explanations for these were proposed, which showed dramatically that the Nilsson model is apparently incapable of explaining certain states without considerable modification. The study of ^{29}Si proceeded from a rather different, though related, goal: an

attempt to describe this nucleus by the Nilsson model, which had been suggested a number of years ago but due to the lack of experimental data, never carried out beyond a rather rudimentary stage. In the present investigation the properties of a number of states were determined and found to be quite consistent with the predictions of the model.

The study of both nuclei was carried out in part by a rather unique instrument: a planar Ge(Li) γ-radiation detector sensitive to linear polarization. Because of the complexity and poor energy resolution of conventional polarization-sensitive detectors, a group of researchers at Chalk River designed and constructed a polarimeter with the high resolution of a Ge(Li) semiconductor crystal. Thanks to the generosity of Professors Ewan and Litherland, this apparatus was made available to us and extensive use was made of it.

The organization of this thesis is determined by the desirability of discussing the properties of ^{21}Ne and ^{29}Si separately. Chapter I outlines some of the basic theoretical considerations involved in this study: how a study of angular correlations and polarizations of the γ-rays emitted by nuclei may be used to determine level spins and parities and transition multipolarities; and a brief discussion of two of the common nuclear models. Chapter II contains the study of ^{21}Ne states and Chapter III concerns ^{29}Si. The experimental aspect

of this study was rather common to both nuclei and is given in Chapter II. Both Chapters II and III contain separate, extensive sections on the discussion of the results obtained in the respective experiments. A brief conclusion is followed by Appendices.

CHAPTER I

THEORETICAL CONSIDERATIONS

1. Gamma ray angular distributions and linear polarizations

a. Basic theory

Consider nuclei which are prepared in an excited state by a process which is symmetrical about some axis. In this study, axial symmetry results from producing nuclei in states B* in the A(a,b)B* reaction and not observing the outgoing light particles b. Then axial symmetry about the direction of the incoming beam is obtained. The ensemble of final states may then be described by a diagonal density matrix (Ferguson 1967). Equivalently, we consider the proportion of nuclei P(m) prepared with z-component m of the total angular momentum J. The requirement that the residual state have good parity implies symmetry under reflection through a plane perpendicular to the beam direction and imposes the subsidiary requirement $P(m) = P(-m)$. In general, furthermore, $P(m) \neq P(m')$ for m' different from m. Such an ensemble is said to be aligned.

The angular distribution of the γ-ray decay of aligned states has been extensively treated by Rose and Brink (1967) and only the relevant formulae are presented here.

If an aligned state $|J,m\rangle$ decays to another state J' by γ-ray emission, the angular distribution of the radiation, with the residual projection m' and the γ-ray linear

polarization unobserved is,

$$W(\theta) = \sum_k B_k(J) \left\{ \frac{R_k(LLJJ') + 2\delta R_k(LL'JJ') + \delta^2 R_k(L'L'JJ')}{1 + \delta^2} \right\} \cdot P_k(\cos\theta)$$

$$\equiv \sum_k a_k P_k(\cos\theta). \qquad (1.1)$$

In the above expression, the functions B_k and R_k depend on the alignment and geometry of the states in the following manner:

$$B_k(J) = \Sigma P(m)(-)^{J-m} \sqrt{2J+1} \; (JmJ-m|ko)$$

$$R_k(LL'JJ') = (-)^{1+J-J'-L+L'-k} \sqrt{(2J+1)(2L+1)(2L'+1)}$$

$$\times (L1L'-1|ko) W(JJLL';kJ')$$

The quantities (JmJ-m ko) and W(JJLL';kJ') are Clebsch-Gordan and Racah coefficients, respectively (see e.g. Brink and Satchler, 1967). In the above expressions

i) L and L' denote the multipolarities of the radiation (it is sufficient to consider no higher than quadrupole radiation; L' = L+1 = 2);

ii) δ is the multipole mixing ratio defined by

$$\delta = \frac{\langle J||T_L'||J'\rangle}{\langle J||T_L||J'\rangle} \cdot \left(\frac{2L'+1}{2L+1}\right)^{\frac{1}{2}}$$

where $\langle J||T_L'||J'\rangle$ is the reduced matrix element (transition probability) for radiation of multipolarity L';

iii) $P_k(\cos\theta)$ are the Legendre polynomials.

The measured angular distribution is related to a theoretical one by

$$W_{meas}(\theta) = \sum_k a_k Q_k P_k (\cos\theta)$$

where the Q_k are attenuation coefficients taking account of the finite solid angle of the detector.

The γ-radiation from an aligned state will be in general linearly polarized. (Circular polarization, since it arises from parity mixing of nuclear states, is in general extremely small.) The direction linear-polarization correlation may be written

$$W(\theta,\gamma) = \sum_k a_k [P_k(\cos\theta)+(-1)^{\pi}\cos 2\gamma\ K_k(LL')P_k^2(\cos\theta)] \quad (1.2)$$

where a_k is defined as before, γ is the angle between the electric vector of the emitted γ-ray and the reaction plane, $P_k^2(\cos\theta)$ is an associated Legendre polynomial and the functions $K_k(LL')$ have been tabulated by Fagg and Hanna (1959). The parity dependence of the polarization is introduced by the phase $(-1)^{\pi}$, where π is 0 or 1 depending on whether the L' radiation is electric or magnetic. The effects of finite detector angle are not included in (1.2) but are discussed in Appendix I.

The γ-ray polarization is then defined (Frauenfelder and Steffen 1965) by

$$P(\theta) = \frac{W(\theta,\gamma=0°) - W(\theta,\gamma=90°)}{W(\theta,\gamma=0°) + W(\theta,\gamma=90°)} \quad (1.3)$$

which yields values of the polarization between +1 and -1. A γ-ray completely polarized with the electric vector in the reaction plane has P=+1, while if it is completely polarized perpendicular to the reaction plane P=-1. An unpolarized γ-ray has P=0.

As the measurement of polarizations in this work made use of the dependence of the Compton effect on polarization we briefly review here the salient features. The differential cross section $\sigma_C(\phi,\gamma)$ for Compton scattering of a polarized γ-ray is

$$\sigma_C(\phi,\gamma) = \frac{1}{2}\left(\frac{e^2}{m_o c^2}\right)^2 \left(\frac{k}{k_o}\right)^2 \left(\frac{k}{k_o} + \frac{k_o}{k} - 2\sin^2\phi\cos^2\gamma\right) \quad (1.5)$$

where ϕ is the scattering angle and γ is defined as before. The initial γ ray energy is k_o and k is the energy of the scattered quantum, given by

$$k = \frac{k_o}{1 + (1-\cos\phi)(k_o/m_o c^2)} \quad .$$

The polarization-sensitivity of Compton scattering is contained in the $\cos^2\gamma$ factor in (1.5) which shows that the scattering is a maximum in the plane perpendicular to the electric vector of the incident photon. The manner in which this dependence was used to measure polarizations is discussed in Chapter II.

It is a relatively straightforward matter to derive the formulae for the linear polarization of a γ ray at an arbitrary

angle θ to the beam axis. Limiting ourselves (as usual) to L=1, L'=2, we find for mixed quadrupole-dipole transitions

$$P(\theta) = \frac{\pm[\frac{1}{2}(a_2+b_2)P_2^{\,2}(\cos\theta) - \frac{1}{12}\,a_4P_4^{\,2}(\cos\theta)]}{1 + a_2P_2(\cos\theta) + a_4P_4(\cos\theta)} \qquad (1.6)$$

with

$$b_2 = \frac{-8a_2\delta R_2(LL'J_1J_2)}{3[R_2(LLJ_1J_2) + 2\delta R_2(LL'J_1J_2) + \delta^2 R_2(L'L'J_1J_2)]} \cdot (1.7)$$

The dependence on the angular distribution coefficients a_2, a_4 indicates the necessity of measuring angular distributions simultaneously with the polarization. In fact, as shown in a later chapter, much information can be obtained from such a simultaneous measurement. Usually, the linear polarization is measured at θ=90° since the polarization function is frequently at or near a maximum at that angle (it vanishes of course at 0°). Then

$$P = \pm \frac{3(a_2+b_2) + 5/4\ a_4}{2 - a_2 + 3/4\ a_4} \qquad (1.8)$$

with the positive sign to be taken for E2/M1 radiation and the opposite sign if the admixture is M2/E1. (It should be again emphasized here that the great usefulness of linear polarization measurements is a consequence of this strong parity dependence.) It is noteworthy that for pure dipole or quadrupole radiation $b_2 = 0$ and the polarization can be directly calculated from the a_2, a_4 coefficients.

Inspection of (7) and (8) yields a very interesting

result. Suppose that a particular γ ray angular distribution is isotropic, i.e. $a_2=a_4=0$. This may be due to one of three reasons:

i) the initial state has J=1/2 or 0

ii) the initial state is unaligned, i.e. all population parameters are equal

iii) the initial state is aligned but the population parameters of the state and multipolarity of the γ ray are such as to result in a cancellation of the a_2 and a_4 coefficients.

It is readily seen that for cases i) and ii) zero polarization also obtains. For possibility iii) however this is no longer true; in fact, now in general a non zero polarization is expected. To see this more clearly, we write

$$b_2 = -\frac{8}{3}\frac{\delta}{1+\delta^2} B_2 R_2 \qquad (1.9)$$

so that if $a_2=0$ for reason iii) and the P(m) are not all equal, $b_2\neq 0$ and a nonzero polarization will manifest. Thus, polarization measurements may resolve spin ambiguities associated with isotropic angular distributions. For example, a 3/2→1/2 transition will be isotropic, independent of the substate populations, for two particular values of δ and thus can not be distinguished from a 1/2→1/2 transition. If however the polarization is measured to be different from zero, the J=1/2 possibility is excluded. A zero polarization,

unfortunately, may be consistent with both J=1/2 and 3/2 assignments.

b. χ^2-analysis of data.

Consider now the analysis of the angular distributions. Gamma ray intensities measured at a series of angles $Y(\theta_i)$ are to be compared with the $W(\theta_i)$ calculated assuming certain values for the initial spin J_i, mixing ratio δ and population parameters P(m). The goodness of fit is measured by the statistical quantity

$$\chi^2 = \sum_i \left(\frac{W(\theta_i) - Y(\theta_i)}{E(\theta_i)}\right)^2$$

where $E(\theta_i)$, the variance in $Y(\theta_i)$, is commonly taken to be the statistical error in the measurement. Since the spins and mixing ratios are not linear in the expression for $W(\theta_i)$, the usual method of analysis is to fix spins and the mixing ratio and to vary the P(m) in search for a minimum in χ^2. The mixing ratio is then varied for given J_i and J_f over the range $-\infty<\delta<\infty$; it is customary to step through values of $\tan^{-1}\delta$.

Statistical fluctuations result in variations in the χ^2 minima if an angular distribution measurement is repeated a number of times. The distribution of χ^2 is tabulated for various degrees of freedom (d.f.), the number of d.f. being the number of data points less the number of free parameters. The concept of confidence limit is relevant. By this is meant the probability that for the correct theoretical expression χ^2

will exceed a certain value. For example, with 5 d.f. the 1% confidence limit is 3.5, meaning that if the correct theory is being applied (in this case, the correct spin sequence and mixing ratio) χ^2 is expected to exceed 3.5 in only 1% of the measurements.

In determining J and δ the practice is to reject solutions for which χ^2 exceeds the 0.1% confidence limit. This criterion has been applied in the present work.

The addition of the polarization data (even at only the one angle $\theta=90°$) may do much to further de-limit spins and mixing ratios which otherwise would remain undistinguished by a simple angular distribution measurement (in addition of course to establishing the parity of the transition). One such possible limitation for isotropic angular distributions has already been discussed. A more useful limitation is the following. It is well known that the angular distribution for a "stretched" E2 transition J+2→J is nearly identical to the one obtained for a J→J transition with a suitable δ. The linear polarizations of these transitions are however markedly different, being near unity for the first possibility and near zero for the second. This difference has recently been successfuly exploited in this laboratory to make unambiguous $J^{\pi}=5-$ assignments to levels in some upper s-d shell nuclei (e.g., Greene Kuehner and Pilt 1971). The distinction afforded by a polarization measurement is not always as clear-cut,

unfortunately, and occasionally the most one can do is a reduction of errors on previous determinations of δ.

A question of the best method of simultaneously analyzing angular distribution and polarization data also arises. We have chosen the following method. First, the angular distributions are analyzed using the χ^2 test to obtain the best fit for a given spin sequence for each value of δ (stepped through 5° intervals in $\tan^{-1}\delta$ from -90° to 90° to avoid missing a sharp minimum). Using (9), the polarization is then calculated for each value of δ using the best fit angular distribution parameters. Only if the calculated value of P lies within 2 standard deviations of the experimental result and if the angular distribution χ^2 lies below the 0.1% confidence limit, is the corresponding spin sequence, parity change and mixing ratio accepted as a possible solution.

c. Restriction of population parameters

Experimental considerations require that the polarizations and angular distributions of the γ rays of interest be as large as possible. It will be observed from the structure of eq. (1) and (7) that the extent of anisotropy of the angular distribution and polarization of a γ ray is in general increased as the degree of alignment of the γ emitting state is increased. In other words, it is desirable to prepare the state $|Jm\rangle$ such that only the lowest magnetic substates are populated. Such an ideal can only be realized with certainty

in a very few cases, for example, resonant α particle or proton capture on a zero spin target. Alternatively, one may use a particle counter located along the beam axis and measure particle-γ angular correlations following a nuclear reaction. The quantum numbers of the magnetic substates of the residual nuclei are then restricted to the sum of the spins of the target, incident projectile, and outgoing light particle.

Another technique of producing strong alignment to the residual nuclei uses the reaction near threshold for populating a state of interest; the ℓ value of the outgoing partial waves will usually be predominantly $\ell=0$ and the residual nuclei will be left in magnetic substates with low quantum numbers. Estimates of the nuclear alignment may be based on the calculated penetrabilities for the outgoing particles and assuming that the reaction cross section is dominated by these quantities. Such an analysis depends critically on statistical models of the compound nucleus (Sheldon and van Patter 1965; Pilt 1969) and its use is liable to question in reactions which are known to be highly resonant. Then calculation of the transmission coefficients from (say) optical model analyses may be fraught with serious difficulties.

The question naturally arises, are <u>any</u> model-dependent limitations on the population parameters at all justifiable?

If not, then it may be extremely difficult to obtain unique results: consider the decay of a state of unknown spin J_1 to a state with (say) $J_2 = 7/2$. Then if no limitation be made, it is quite likely that $J_1 = 5/2, 7/2$, and $9/2$ all give acceptable χ^2 fits for some value of δ and the $P(m)$. Since for $J_1=9/2$ we have 4 independent parameters and only 3 experimentally observed quantities (a_2, a_4, P) the fits are underdetermined and ambiguities are to be expected. On the other hand, arbitrarily imposing the kind of severe limits as has been done for reactions in the pf shell where the statistical model is better founded - limits such as $P(3/2)/P(1/2) \leq 0.05$ and $P(m)=0$ for $m>3/2$ - appear overly restrictive in the light of what is known about the fluctuations expected in the s-d shell. These restrictions have been imposed of late even for reactions known to be highly resonant, (Main et al 1971) but have been justified on the grounds that good agreement is obtained with less model dependent techniques (e.g. restricting the substates geometrically by the particle-γ coincidence technique). In other words, the method "works" but the results are somewhat open to question.

In the present work, a compromise approach has been attempted. While it does introduce a certain model-dependence to the analysis which may be annoying to the purist, we believe that this aspect has been minimized whilst permitting unique assignments to be made to otherwise ambiguous spin determinations. It is perhaps worthwhile to point out that

many of the multiple solutions concomitant with completely free varying population parameters are associated with unrealistic combinations of the population parameters where all except one are zero. The very broad limits which were imposed in the present work eliminate many of these "solutions". The remainder of this section explains and seeks to justify the approach tried in the present work.

For α particles incident on a spin zero target and neutrons in the exit channel (as are the reactions used in this work) the substate populations of a final state $|Jm\rangle$ are given by Pilt (1969)

$$P(m) = \Sigma\ (-)^{J_2-\ell_1-j_2-\frac{1}{2}-m}(2\ell_1+1)^{5/2}(\ell_1 o \ell_1 o|ko)(JmJ-m|ko)^{-1}$$

$$\times[W(\ell_1\ell_1\ell_1\ell_1|ko)]^2 W(J_1J_1J_2K_2|kj_2)(T_{\ell_1}T_{\ell_2}/\Sigma T_\ell) \qquad (1.10)$$

with J_1=target spin, J_2=spin of residual state, m=z-component of J_2, $\ell_{1,2}$=incoming and outgoing orbital angular momenta, respectively; $j_2=\ell_2\pm 1/2$, and k=order of Legendre polynomial. The T's are the relevant transmission coefficients assuming a compound statistical process. As a first approximation, we may use Coulomb penetrabilities for the incoming partial waves. The outgoing neutron transmission coefficients may be derived, for example, from the elastic scattering ampltiudes obtained from optical model codes such as DWUCK (Kunz 1965). The relation between these quantities is

$$T_\ell = 4(\mathrm{Im}C_\ell + |C_\ell|^2)$$

where T_ℓ is the transmission coefficient for the ℓ'th partial wave and C_ℓ the corresponding complex scattering amplitude. The use of these averaged transmission coefficients is rather difficult to justify in reactions with light nuclei where Ericson fluctuations (rapid fluctuations in the cross section due to interference from overlapping resonances in the compound nucleus) are prevalent.

A possible approach for determining the effects of fluctuations follows the treatment of Vogt et al. (1964). If the effects of fluctuations over a finite energy range (corresponding to target thickness or beam width) are considered as yielding an energy averaged cross section $\langle\sigma\rangle_s$ which may not be an adequate estimate for the true cross section $\bar{\sigma}$, one may define a probable error ε_s so that the probability of finding $\langle\sigma\rangle_s/\bar{\sigma}$ within $1\pm\varepsilon_s$ is 50%. One has $\varepsilon_s=d_S\, S^{-1/2}$, where d_S is the width (in units of σ) of a χ^2 distribution with S df ($d_\infty=0.6745$, the value for a normal distribution) and the sample size is $S=\Delta E/\Gamma$, where ΔE is the energy averaging interval. One finds for the value of ΔE used that the average cross section may deviate from $\bar{\sigma}$ by 50% or so; a measurement of the yields of the reactions of interest in this work do indeed show fluctuations of this order.

The above considerations indicate that the use of energy averaged transmission coefficients to estimate the magnetic substate populations P(m) of the residual state is a

rather unjustifiable assumption. It can be shown, however, that the effect on the population parameters is not nearly as large as might first be expected. The reason for this is that even if the entire cross section were to occur through (say) the $\ell=1$ outgoing channel, contributions to all substates will still exist, depending on the distribution of spins in the compound nucleus and the appropriate Clebsch-Gordan coefficients. A computer programme has recently been written (Sheldon and van Patter 1966) which may be used to evaluate (10) and hence to estimate the possible effect of varying the transmission coefficients on the population parameters.

Accordingly, the following approach to the analysis was taken:

$^{18}O(\alpha,n\gamma)^{21}Ne$ reaction. Since this reaction is extremely resonant and beam energies corresponding to resonances were chosen because of the increased yield to ^{21}Ne states of interest, the statistical assumption is rather dubious at best. Hence, the population parameters for m=1/2, 3/2, 5/2 were allowed to vary freely. As pointed out earlier, this did not lead, in most cases, to unique spin assignments. Many of these were already known from previous work, however (see Ch. II), and hence the angular distribution and polarization measurements were sufficient to extract the level parities and multipole mixing ratios of the γ-transitions.

$^{26}Mg(\alpha,n\gamma)^{29}Si$. This reaction was not as resonant

near the bombarding energies of interest as the previous one. Since furthermore many level spins were unknown, it was decided to limit the P(m) to the following rather broad limits: a 50% deviation from either side of the value calculated from the Sheldon programme. The subsequent exclusion of rather suspect combinations as $P(1/2) \leq 0.05$, $P(3/2) \leq 0.05$, $P(5/2) \geq 0.90$ allowed a number of unique spin determinations to be made Ch. III.

2. Nuclear models

a Mixed configuration shell model

Consider a nucleus with N nucleons distributed among a number of shells, with n_i nucleons in the i'th shell. This configuration may be written $(j_i)^{n_i}(j_2)^{n_2}\ldots\ldots$. For each configuration there are many ways in which the particle angular momenta and isospins may be combined to give some total angular momentum J and isospin T. It is frequently useful to classify these possible combinations by group theoretic methods such as SU_3. Partially conserved quantum numbers such as the seniority s (the number of nucleons left after removal of all pairs coupled to J=0, T=0) and the reduced isospin t of these remaining nucleons are also useful in the classification of states.

An n-particle state may be reduced by coefficients of fractional parentage (cfp's) to a sum of products of (n-2) particle states and 2 particle states; thus a 2 body matrix

element (say for a residual 2 body interaction) may be reduced to sums of cfp's and matrix elements for 2 particle states. A shell model Hamiltonian

$$H = \sum_i (T_i + V_i) + \sum_{i<j} V_{ij}$$

where V_i represents a soluble potential (say a harmonic oscillator) and V_{ij} the residual 2 body interaction, may then in principle be diagonalized if the single particle energies (eigensolutions of V_i) and the matrix elements of V_{ij} are known and the Racah algebra can be carried out. Energy spectra and wavefunctions may be obtained and matrix elements of one-body operators may be calculated, for example those of electromagnetic transitions or particle transfer amplitudes (spectroscopic factors) and the results compared with the experiments.

Only for a few nuclei near closed shells can exact calculations be carried out. ^{21}Ne, with 5 nucleons outside the ^{16}O shell closure, is one of these happy cases (just!) and a full $(sd)^5$ diagonalization has recently been done for a variety of single particle energies and residual interactions, (Halbert et al. 1971), yielding the properties of many of the low-lying positive parity states in ^{21}Ne. For the negative parity states, however, this has not yet been done, apparently because the problem of 7 "particles" distributed among 4 shells requires severe truncation if it is to be solved. (Recall that negative parity states in the lower 2s1d shell

arise primarily from promoting a particle from the p shell into the sd shell.) In view of the interest that non-normal parity states† have recently awakened, the lack of such calculations is a pity indeed and their completion will be eagerly awaited.

In contrast to ^{21}Ne, ^{29}Si poses a formidable problem indeed for the shell modeler. Situated almost exactly in the middle of the sd shell, 13 particles beyond ^{16}O and 11 particles removed from ^{40}Ca, the next shell closure, an exact calculation is most formidable and will likely remain so for several years. The closed subshell nucleus ^{28}Si (which closes the $d_{5/2}$ subshell) is itself rather intractable to calculation because of the number of particles involved and because the ground state, far from being a good closed subshell, apparently contains appreciable admixtures of various particle-hole configurations. Hartree-Fock calculations indicate that ^{28}Si is strongly deformed and recent experiments tend to confirm this.

Recently, however, Wildenthal and his co-workers at Utrecht, Netherlands have reported shell-model calculations on a number of nuclei in the middle of the sd shell using a restricted basis (de Voigt et al, 1972).

---

† By non-normal parity we mean parity opposite to that of the ground state.

b. Nuclear collective models; the Nilsson model

Nuclear collective motion is founded on the straightforward physical principles of the classical behaviour of a liquid drop, despite the fact that the laws of classical mechanics are clearly inappropriate for a finite system of strongly interacting Fermions. Nevertheless, phenomenological models, which strive to retain the intuitive and pleasing physics of classical behaviour, and yet include quantum effects, have been developed, and with rather good - one might say surprising - success, describe the properties of a large number of nuclei. Unfortunately because of the rather ad hoc manner in which quantum and classical physics have been combined in these models, it is difficult to relate them properly to microscopic many-body theory. The latter, such as the random phase approximation, are undoubtedly much more satisfactory in their quantum-mechanical basis, but calculations of use to an experimentalist (level energies, spins and parities, transition rates) are as yet distressingly far away except for the simplest of nuclei. Furthermore, the formal mathematical manipulations inherent in such calculations defy interpretation in easily understandable terms. Until a closer correspondence between phenomenological and microscopic theories becomes available and understandable, much of collective nuclear behaviour will continue to be interpreted in terms of "macroscopic" models.

The Nilsson model has been extensively discussed elsewhere (Nilsson 1955) and no attempt will be made to derive the well-known results here.

The description is that of an odd nucleon moving in the average field of the remaining nucleons which constitute a deformed "core". The total Hamiltonian, as is well known, is

$$H = H_p + H_c + H_{rpc}$$

where H_p, is the sum of single particle energies for a deformed potential, H_c is the core rotational energy, and H_{rpc} is the rotation-particle-coupling or Coriolis interaction which couples the particle angular momenta j to the total angular momentum J. The particle Hamiltonian has the form

$$H_p = H_o + H_\delta + C\vec{\ell}\cdot\vec{s} + D\vec{\ell}^2$$

where H_o is a spherical harmonic oscillator potential, H_δ represents a quadrupole distortion, and C and D are chosen to reproduce shell model level spacings in the limit of zero deformation. With such a Hamiltonian, the particle angular momentum j_p is no longer conserved but its projection Ω_p along the symmetry axis is. Neglecting "$\Delta N=2$" coupling (N enumerates oscillator shells) the eigenfunctions of H_p may be expanded in terms of shell model eigenfunctions:

$$|\Omega\alpha> = \Sigma\ c^{\alpha}_{j\Omega}\ |\ell j\Omega>$$

$$|\Omega\alpha> = \Sigma\ a^{\alpha}_{\ell\Lambda}\ |\ell\Lambda\Sigma>$$

where Λ is the projection of the orbital angular momentum ℓ and Σ that of the intrinsic spin, along the symmetry axis. Matrix elements of H_δ in these representations may be calculated from the expressions given by Nilsson (1955).

The particle angular momentum $\vec{j}_p$ and that of the core, $\vec{R}$, (neither of which are conserved), combine to give a total spin $\vec{J}$ and projection K along the symmetry axis of the rotating core, both of which are good quantum numbers. The eigenvalues of H_c are

$$E_c = \frac{\hbar^2}{2\mathcal{J}} [J(J+1) - K^2 - \Omega^2 - \vec{j}^2]$$

where the last term, $\frac{\hbar^2}{2\mathcal{J}} \vec{j}^2$ contains only particle coordinates and is usually absorbed in the particle Hamiltonian. For axial symmetry, $K=\Omega$ and the well-known $J(J+1)$ energy spacing of rotational bands obtains. The Coriolis term is

$$H_{rpc} = \frac{\hbar^2}{2\mathcal{J}} (J_+ j_- + J_- j_+)$$

where the operators are given by

$$J_\pm = J_1 \pm iJ_2 \quad ; \quad j_\pm = j_1 \pm ij_2 \ .$$

The operators $J_\pm$ have matrix elements between states for which K differs by 1; thus K is no longer conserved since H_{rpc} mixes in states of $K\pm1$ to a zero-order wavefunction of definite K. This may be treated perturbatively (Kerman 1956) or mixed-K wavefunctions may be written in a good-K basis and the RPC matrix diagonalized. For light nuclei, the latter approach is highly preferred since the off-diagonal RPC matrix elements

are comparable in magnitude to the diagonal terms and the perturbation approach is highly suspect. It is important to note that the RPC term is very crucial in considering K=1/2 bands since the coupling between the two time-reversed orbits gives rise to rotational bands where the J(J+1) structure may be completely lost. The proper rotational formula for K=1/2 is

$$E_J^{K=1/2} = \frac{\hbar^2}{2\mathcal{J}} [J(J+1)-K^2+(-)^{J+1/2}a(J+1/2)]$$

where the decoupling parameter a may be calculated from the RPC matrix element. It is important to point out that RPC is manifested as a general feature of adiabatic rotational models and that the specific form of the RPC matrix elements depend on a model for the intrinsic particle motion (such as the Nilsson model). To see this, we note that the off-diagonal RPC matrix elements are in general given by

$$\langle JK|H_{rpc}|JK\pm1\rangle = \frac{\hbar^2}{2\mathcal{J}} \langle K|j_{\mp}|K\pm1\rangle \sqrt{(J\mp K)(J\pm K+1)} \quad .$$

The single particle matrix element

$$m_{\mp} = \langle K|j_{\mp}|K\pm1\rangle$$

may be calculated from, say, Nilsson wave functions whence

$$m_{\mp} = \sum_j C_{j\ell}^{K} C_{j\ell}^{K\pm1} \sqrt{(j\mp K)(j\pm K+1)}.$$

Alternatively, one may relax the specific model for intrinsic particle motion and consider $m_{\pm}$ as an empirical parameter. This second approach will be considered in part in the discussion of E1 rates in ^{21}Ne.

With the calculation of the wavefunctions, one may evaluate matrix elements of electromagnetic operators and calculate the EM transition rates. The formulae are standard and are presented in Nilsson's article. We mention here that RPC plays an important role here, since a coherent sum of terms involving the various K-components of the wavefunction is to be calculated; thus, small admixtures of other bands may alter the transition rates expected for "pure" bands remarkably. Examples will be presented in the discussion.

3. Electromagnetic Transitions

The measurement of nuclear level energies, spins and parities is seldom an adequate test of a nuclear model. By far more exacting is an attempt to determine the structure of a level through the components of its wavefunction, since this is what determines the nature of a level in a particular nuclear model. One method, frequently used in heavier nuclei, involves single or two-particle-transfer reaction cross sections to explore the predominant shell model or Nilsson configurations. This method is not as powerful in light nuclei since the highest spin particles in the s-d shell are only $d_{5/2}$, thus direct reaction processes will not populate higher spin states except through the small possible particle-hole components of the target. Another sensitive study of nuclear wavefunctions is by measuring the transition matrix elements of electromag-

netic operators. This is a valuable technique since the quantum theory of the electromagnetic field is well understood, and no assumptions about reaction mechanisms (such as the applicability of distorted-waves theory) are necessary. The methods outlined in a previous section yield level spins and parities and multipole mixing ratios of γ transitions; to obtain the absolute transition matrix elements only the level lifetimes are necessary. For the nuclei under consideration in this thesis, a large number of lifetimes have been measured by previous and concurrent workers, so that in conjunction with the present work, a detailed comparison of the experimental transition rates with those predicted by the models discussed earlier is possible.

a. Basic theory

The two kinds of transitions, electric and magnetic, are related to the distribution inside the nucleus of charges and currents, respectively. The probability of emission per unit time of a γ ray of energy $E_\gamma = \hbar\omega$ and multipolarity and projection (L,m) is given by

$$T(L,m) = \frac{8\pi(L+1)}{L[(2L+1)!!]^2} \frac{k^{2L+1}}{\hbar} B(L,m)$$

where

$$k = \omega/c = \frac{E_\gamma}{197} \times 10^{13}\ \text{cm}^{-1} = \frac{E_\gamma}{197}\ \text{fm}^{-1} .$$

The reduced transition rate is defined by

$$B(L,m) = \langle f | \Omega_m^L | i \rangle^2$$

where $|f\rangle$ and $|i\rangle$ are the final and initial states. The operator Ω can be written for electric and magnetic radiations

$$\Omega_L^m(el) = Q'_{Lm} + Q''_{Lm}$$
$$\Omega_L^m(mag) = M'_{Lm} + M''_{Lm}$$

with a parity selection rule

$$el: \pi_\gamma = \pi_i \cdot \pi_f = (-)^L$$
$$mag: \pi_\gamma = \pi_i \cdot \pi_f = (-)^{L+1} .$$

The term $$Q'_{Lm} = \Sigma e_i r_i^L Y_L^m(r_i)$$

and the second term Q''_{Lm} arises from the induced electric moment due to the magnetization density and can be neglected if $E_\gamma << 931$ MeV, which is invariably the case in our work. Furthermore

$$M'_{Lm} = \Sigma [\nabla r_i^L Y_L^m(r_i)] \cdot \frac{2g_i(\ell)}{L+1} \vec{\ell}_i \frac{eh}{2M_p c}$$
$$M''_{Lm} = \Sigma [\nabla r_i^L Y_L^m(r_i)] \cdot g_i^{(s)} \vec{s}_i \, eh/2M_p c .$$

The orbital and spin gyromagnetic ratios $g^{(\ell)}$ and $g^{(s)}$ are proportionality factors which relate the magnetic moments with the orbital and intrinsic angular momenta. For free nucleons we have

$$g^{(\ell)}_{proton} = 1 \qquad g^{(\ell)}_{neutron} = 0$$
$$g^{(s)}_{proton} = 5.585 \qquad g^{(s)}_{neutron} = -3.826 .$$

In a refined theory, the gyromagnetic ratios (as well as the nucleon charges) may be assigned "effective" values to improve

the agreement with experiment.

The Weisskopf units or estimates give a rough idea of the expected magnitude for the total width $\Gamma(L)$ of a state, which is simply related to the transition rate by

$$\Gamma(L) = \hbar T(L) = \frac{8\pi(L+1)}{L[(2L+1)!!]^2} k^{2L+1} B(L)$$

The estimates are based on the following assumptions:

1. The nucleus consists of an inert core and one particle
2. The final state has $\ell=0$, the initial $\ell=L$
3. Spin wavefunctions remain unchanged by the transition
4. The radial part of the initial and final wavefunctions are both given by

$$U(r) = \text{const}, \quad r \leq R$$
$$U(r) = 0 \quad , r > R \ .$$

Then the Weisskopf rates for electric and magnetic transitions are

$$T_W(EL) = \frac{2(L+1)}{L[(2L+1)!!]^2} \left(\frac{3}{L+3}\right)^2 \frac{e^2}{\hbar c} \omega(kR)^{2L}$$

$$T_W(ML) = \frac{20(L+1)}{L[(2L+1)!!]^2} \left(\frac{3}{L+3}\right)^2 \frac{e^2}{\hbar c} \omega(kR)^{2L-2} \ .$$

Using $R=1.2A^{1/3}$ fm we obtain the following well-known expressions for Γ_W in terms of E_γ and A for various multipolarities

$$\Gamma_W(E1) = 6.8\times10^{-2}A^{2/3}E^3\text{eV} \qquad \Gamma_W(M1) = 2.1\times10^{-2}E^3\text{eV}$$
$$\Gamma_W(E2) = 4.9\times10^{-8}A^{4/3}E^5\text{eV}$$

An experimentally determined width Γ can be expressed in Weiss-

kopf units from

$$|\dot{M}|^2 \text{ wu} = \frac{4\pi}{e^2} \left(\frac{L+3}{3}\right)^2 \frac{1}{R^{2L}} B(EL)$$

$$|M|^2 \text{ wu} = \frac{\pi}{10} \left(\frac{L+3}{3}\right)^2 \frac{1}{R^{2L-2}} B(ML) \quad .$$

b. Inhibition of El rates

Even a cursory examination of the available experimental data (e.g. Skorka et al. 1966) reveals that the El transition rates are in general much hindered (by 10^2 - 10^4) from the Weisskopf single-particle estimate. This hindrance can be partially understood both in the collective and shell models. In the vibrational model, for instance, El transitions that arise from (say) $J^\pi = 3^- \rightarrow 2^+$ decays are second order processes requiring the simultaneous destruction of an octupole (λ=3) and creation of a λ=2 phonon. In the shell model, El transitions occur between single-particle states in adjacent major oscillator shells. Unless $\Delta j \leq 1$, with j the orbital angular momentum, the transitions are forbidden and must take place via admixtures of other components. The presence of the giant dipole resonance (gdr) may also cut down El transitions proceeding from other states, since the gdr may exhaust a sizeable fraction of the dipole sum rule (e.g. Brown 1967).

A number of arguments have recently been presented to indicate that El transitions between certain other kinds of

states may also be forbidden. Briefly, the argument goes along the following lines (Ellis and Engeland 1972):

"Physically sound" wavefunctions should not involve any centre-of-mass (cm) excitations; i.e., the cm must be in a 1s state. Consider E1 transitions between states of oscillator energy $n\hbar\omega$ and $(n-1)\hbar\omega$. If these two states differ only in the coordinates of only one kind of particle, say a proton, meaning that the matrix elements of any neutron one-body operator vanish, the matrix element of R_n, the neutron cm operator, must also vanish. Since the two above-mentioned states are in 1s cm states, the matrix element $\langle n|R|(n-1)\rangle = 0$. It follows that the matrix element of R_p must also vanish. But the E1 operator is just $R_n - R_p$; the transition is forbidden. Exactly analogous arguments are readily constructed for neutron transitions. It must be pointed out that it is implicit in the above derivation that it is in fact possible to construct states with the desired properties in a consistent manner. This is by no means trivial to prove or to disprove and recourse must eventually be made, in all probability, to shell model calculations.

As an example, let us consider the applicability of the model to a very simple case: E1 transitions in ^{17}O. The ground state (we assume) is simply $\nu(sd)^1$; negative-parity states are formed by raising a particle from the p-shell to the sd shell. Since we may then couple the two sd particles to T=0 or 1 (i.e., coupling the hole to a T=0 or 1 mass 18

core) we obtain

$$\psi_{T_p=0} = \pi(p^{-1})\ [\pi(sd)^1\nu(sd)^1]_{T=0}$$

$$\psi_{T_p=1} = \alpha\pi(p^{-1})[\pi(sd)^1\nu(sd)^1]_{T=1} + \beta\nu(p^{-1})[\nu(sd^2)]_{T=1}$$

Clearly, $\psi_{T=0}$ differs from the model ground state in only the coordinates of <u>one</u> kind of particle (a proton) so that E1 transitions between these states are not allowed. $\psi_{T=1}$, however, contains both proton and neutron excitations so that the E1 matrix element does not necessarily vanish by the above-mentioned theorem. There may, however, be other selection rules or "accidental" cancellations inhibiting the E1 rate. It is most important to note that we may not argue that $\langle\psi_{T=1}|E1|0\rangle = 0$ along the following lines:

$$\langle\psi_{T=1}|\theta_{E1}|0\rangle = \alpha\langle\nu(p^{-1})\nu(sd)^2|\theta_{E1}|\nu(sd)^1\rangle$$

$$+ \beta\langle\pi(p^{-1})\pi(sd)\nu(sd)|\theta_{E1}|\nu(sd)\rangle.$$

Applying the theorem to both matrix elements separately, they would both vanish! This is not allowable since the individual components $\nu(p^{-1})[\nu(sd)^2]_{T=1}$ and $\pi(p^{-1})[\nu(sd)\pi(sd)]_{T=1}$ are not individually physical wavefunctions of "good T"; only the appropriate linear combination of the two components (proton and neutron hole) is an acceptable wavefunction.

c. Isospin effects in transition rates

The manner in which the requirement that nuclear states be eigenfunctions of T may affect M1 rates has been briefly

considered by Pelte (1966) and Kanestrøm (1971). These arguments are easily generalized to E1 rates, which we shall consider here. This section shows how "other" selection rules besides the Ellis and Engeland rule considered before may give rise to inhibited E1 transitions.

Consider, for example, the construction of the J^{π} = 1/2- state in O^{17}, and assume it is a state of good total isospin T=½. We write the wavefunction with the hole coupled to a T=1 core as

$$\psi_{T_c=1} = \Sigma(-)^{T-T_z(h)} (\tfrac{1}{2}\, T_z^{p(1)} \tfrac{1}{2} T_z^{p(2)} | 1T_z)(1T_z \tfrac{1}{2} T_z^{(h)} | \tfrac{1}{2}\tfrac{1}{2}) | 2p1h>$$

where the isospin Clebsch-Gordan coefficients give the amplitudes of proton and neutron hole states in the total wavefunction. The factor $(-)^{T-T_z}$ gives the hole the same transformation properties under rotations as for particles. Thus

$$\psi_{T_c=1} = \sqrt{2/3}\,|\nu(p^{-1})\nu(sd)^2> + \sqrt{1/6}\,|\pi(p^{-1})\pi(sd)\nu(sd)>$$

Similarly, coupling to a T=0 core (there is only one way to do this!) we find

$$\psi_{T_c=0} = \sqrt{1/2}\,|\pi)p^{-1})\pi(sd)\nu(sd)> \ .$$

Now since the core isospin is not a good quantum number but the total isospin is, these two states will mix, perhaps strongly, which is dependent on the interaction assumed and on their separation. Writing the mixed wavefunction as

$$\psi = \alpha\psi_{T=1} + \beta\psi_{T=0} \qquad (\beta = \sqrt{1-\alpha^2})$$

the E1 transition to the ground state is proportional to

$$\left| (\sqrt{1/6}\ \alpha + \sqrt{1/2}\ \beta) G_{E1}(\pi) + \sqrt{2/3}\ \alpha\ G_{E1}(\nu) \right|^2 .$$

It is readily seen that for suitable values of α and β the above matrix element may be compelled to vanish, even though $G_{E1}(\pi \text{ or } \nu)$ separately may not.

CHAPTER II

STUDY OF ^{21}Ne

1. Introduction

Among the most realistic calculations that can be carried out on nuclei not too far removed from closed shells are the mixed-configuration shell-model calculations (Ch. I) using either effective interactions (such as the MSDI) or more realistic ones, derived from nucleon-nucleon scattering amplitudes. Since ^{21}Ne is only 5 particles removed from ^{16}O, it is possible using high speed computers with large memories to carry out reasonably exact and realistic calculations in an $(sd)^5$ basis. These calculations are interesting for a variety of reasons: i) one would like to know how much of the currently available experimental data on energy levels, particle transfer spectroscopic factors, and electromagnetic transition rates can be understood in terms of microscopic theory; ii) one can determine which of the currently used interactions are in fact useful for shell-model calculations and iii) one would like to understand the connection between shell model results and those obtained from the phenomenological collective models. A very detailed and comprehensive set of calculations for the A=18 to 22 nuclei (including ^{21}Ne) has recently been completed (Halbert et al. 1971) and we will take

occasion to refer to this outstanding work frequently in our discussion of the ^{21}Ne level structure, with emphasis on points i) and iii) above.

The Nilsson model, however, has long been applied to light nuclei and because of its successes is of more than just historical interest. Fig. 2.1 shows a diagram of the Nilsson level energies applicable to the 2s1d shell as a function of the nuclear deformation δ. The nucleus ^{21}Ne is believed (see, for example, Howard et al. 1965) to be prolate with a deformation $\delta \simeq 0.3$; thus one can deduce from the Nilsson scheme that the ground state of ^{21}Ne consists of an odd neutron in the 3/2+[211] orbital, and gratifyingly, the ground state does indeed have $J^{\pi} = 3/2+$. It is noteworthy in passing that this is one of the few cases where the spherical individual particle model fails to predict the ground state spin of an odd-A nucleus; one would of course expect $J^{\pi} = 5/2+$ since the last nucleon would be in the $d_{5/2}$ subshell. In the Nilsson scheme, a rotational band built on the ground state, characterized by the usual J(J+1) energy spacing and enhanced in-band E2 transitions is expected; it is now believed that the ground state band has been identified up to the $J^{\pi} = 13/2+$ level (Rolfs et al. 1971 and present work). Other low-lying intrinsic states upon which we might expect rotational structure to be superposed are the 1/2+[220], 1/2+[211], 5/2+[202], and 1/2-[101] orbitals - the latter is a hole state formed by promoting a $p_{1/2}$ particle into the

Fig. 2.1

Nilsson level diagram for light nuclei as a function of deformation (ε). Positive values of ε correspond to prolate (cigar) shapes, negative to oblate shape. Levels are labelled by the asymptotic quantum numbers $K[Nn_z\Lambda]$, and by spherical shell model states at zero deformation. Even parity levels are solid, odd parity levels are dashed. Taken from Lederer et al. (1967) p. 590.

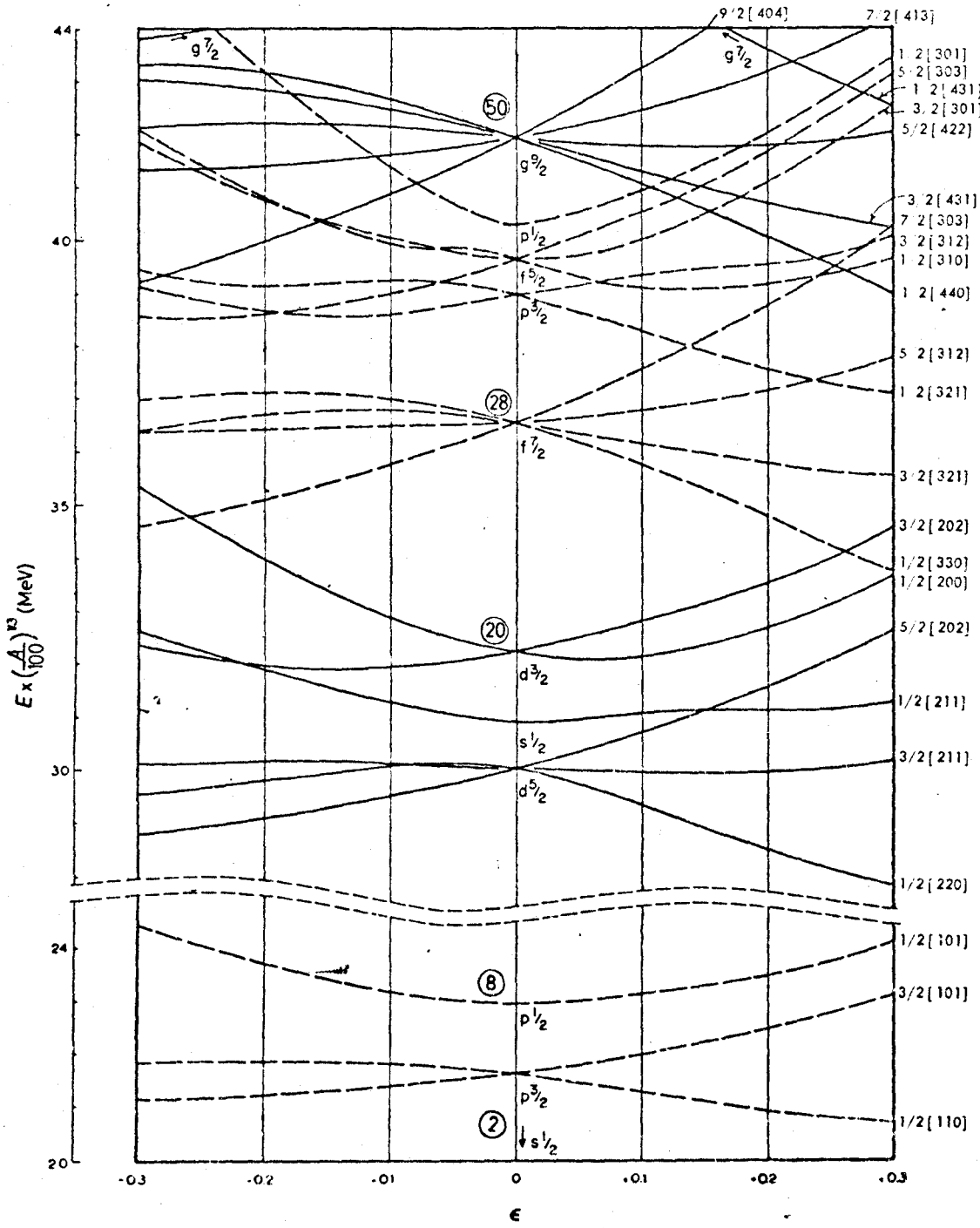
9/2[404]
7/2[413]
g 7/2
g 7/2
1/2[301]
5/2[303]
1/2[431]
3/2[301]
5/2[422]
50
g 9/2
3/2[431]
7/2[303]
3/2[312]
1/2[310]
1/2[440]
p 1/2
f 5/2
p 3/2
5/2[312]
1/2[321]
28
f 7/2
3/2[321]
3/2[202]
1/2[330]
1/2[200]
20
5/2[202]
d 3/2
1/2[211]
s 1/2
3/2[211]
d 5/2
1/2[220]
1/2[101]
8
3/2[101]
p 1/2
p 3/2
2
s 1/2
1/2[110]
44
40
35
30
24
20
-.03
-.02
-.01
0
+.01
+.02
+.03
ε
E x (A/100)^1/3 (MeV)

sd shell. The non-normal parity states are quite interesting because they are found to lie far lower in energy than one would expect from the simple Nilsson model, and as will be shown in the sequel, this can be accounted for by considering the isospin nature of these states.

Many of the levels in ^{21}Ne believed to belong to the above-mentioned bands have in fact been observed in particle transfer reactions to ^{21}Ne, especially in a series of experiments carried out by a group at Yale University and reference to some of their work will be made in the discussion of our results. While spin assignments to ^{21}Ne levels are in some cases established from angular correlation experiments, parities have been to a large extent based on distorted waves analysis of the ^{20}Ne(d,p)^{21}Ne and ^{22}Ne(p,d)^{21}Ne reactions. It was felt that in the light of the importance of accurate spin and parity information to a meaningful comparison with nuclear models, verification of these assignments without recourse to a model of nuclear reactions was desirable. This, then, provided part of the motivation for the present investigation.

Another motivation for this study was the result of a comparison of the low-lying level structure of the nuclei with 11 odd particles (Fig. 2.2). As expected, the mirror pairs ^{21}Na, ^{21}Ne and ^{23}Na, ^{23}Mg are quite similar in their structure. However, there exist significant and annoying differences between ^{21}Ne and ^{23}Na which remain unaccounted for by the simple Nilsson model, whereby both nuclei are

Fig. 2.2

Comparison of the low-lying level schemes of the four $\xi = 11$ nuclei: ^{21}Na, ^{21}Ne, ^{23}Na and ^{23}Mg.

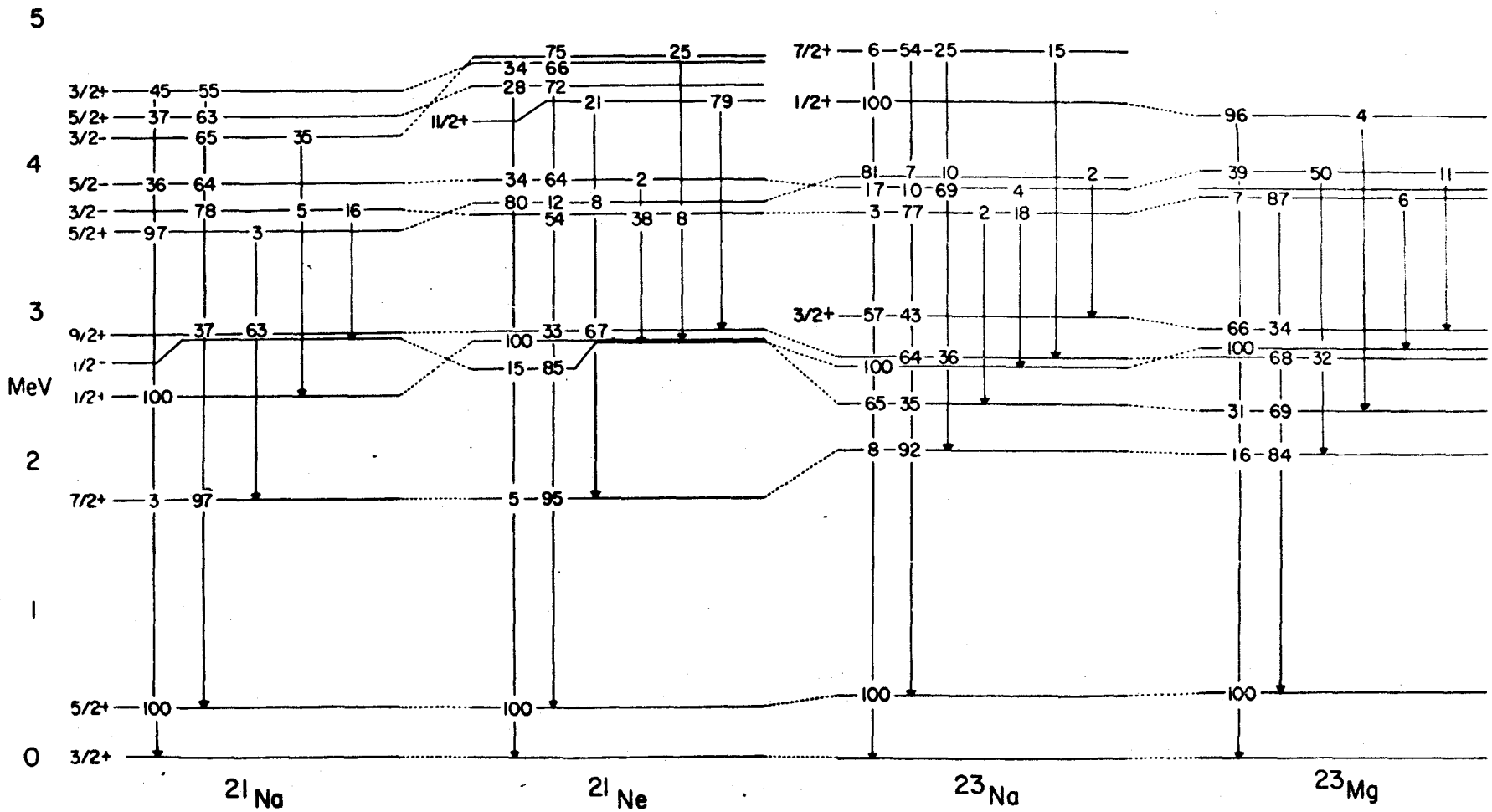
5
4
3
2
1
0
MeV
3/2+ 45 55
5/2+ 37 63
3/2- 65 35
5/2- 36 64
3/2- 78 5 16
5/2+ 97 3
9/2+ 37 63
1/2- 100
1/2+ 100
7/2+ 3 97
5/2+ 100
3/2+
21Na
75 25
34 66
28 72
11/2+ 21 79
34 64 2
80 12 8
54 38 8
100 33 67
15 85
5 95
100
21Ne
7/2+ 6 54 25 15
1/2+ 100
81 7 10 2
17 10 69 4
3 77 2 18
3/2+ 57 43
100 64 36
65 35
8 92
100
23Na
96 4
39 50 11
7 87 6
66 34
100 68 32
31 69
16 84
100
23Mg

considered as consisting of a particle in an $\Omega = 3/2$ orbital outside an inert core, and hence should exhibit quite similar spectra. The immediately evident differences are: i) the lack of a $J^{\pi} = 3/2+$ level in ^{21}Ne at around 3 MeV excitation; ii) lack of a $K^{\pi}=1/2+$ band in ^{21}Ne with the band head near 4 MeV; iii) differences in γ ray branching ratios from several analogous negative parity states. As well, more subtle features prevail in both nuclei which are difficult to explain in the Nilsson model; these involve mainly the properties and decay of the negative parity states. Despite the otherwise remarkable success of the Nilsson model in explaining many features of the low-lying spectra of these nuclei, the above-mentioned discrepancies may provide some further insight into the nature of certain excited states. A discussion of some of the apparent limitations of the model and of the proper treatment of the discrepancies is postponed to the discussion.

2. Experimental Techniques

In this section we discuss in general some of the considerations which must be kept in mind when performing γ-ray angular distribution and linear polarization measurements and which are equally applicable to both the $^{18}O(\alpha,n\gamma)^{21}Ne$ and the $^{26}Mg(\alpha,n\gamma)^{29}Si$ reactions (the latter discussed in detail in the next chapter). This is followed by a discussion of the experimental aspects peculiar to the $^{18}O(\alpha,n\gamma)^{21}Ne$ study.

a. Angular distribution measurements

Gamma ray angular distributions (A.D.) are obtained by measuring the relative γ-ray intensity at a number of angles with respect to the axis of quantization (the beam direction). Although usually only three parameters are sufficient to specify the A.D. uniquely, (the normalization and the Legendre coefficients a_2, a_4) it is customary to obtain the A.D. at a larger number of angles to check the consistency of the data. These angles are frequently chosen at equal intervals of $\cos^2\theta$ (e.g., 0, 30, 45, 60 and 90 degrees) since a plot of $W(\theta)$ vs $\cos^2\theta$ will yield a straight line for $a_4 = 0$, which is often the case. A linear least squares fit of the data to [1.1], i.e. to

$$W(\theta) = a_o + a_2 P_2(\cos\theta) + a_4 P_4(\cos\theta)$$

then yields "best" values for the coefficients a_2 and a_4, as well as the relative intensity a_o.

Evidently, since the measurements at each angle are done sequentially, some means of normalization of the corresponding γ ray intensities is necessary. Furthermore, corrections for effects such as misalignment of the target, absorption in the target backing and chamber walls, and dead time of the analogue-to-digital converters are inevitable. Three methods of normalization are possible: i) to the integrated charge, deposited on the target, ii) to a fixed "monitor" counter, iii) to a known isotropic γ ray coming from the reaction of interest. Of these, i) is the least trustworthy,

since it is difficult to construct extremely accurate current integrators and the misalignment and dead time corrections remain. Method ii) is superior, since it is almost always possible to select a strong γ ray from the reaction of interest to which to normalize the A.D. and minimize the normalization error; furthermore, there is compensation for uncertainties due to the beam spot wandering on the target (usually minimized by suitable collimation) or due to the target deteriorating with time. The best method of all, if feasible, is iii): the use of a known isotropic γ ray. This method compensates for many uncertainties, especially those due to misalignment since the latter will only give rise to an apparent nonisotropic A.D. to the normalizing γ ray. As before, target deterioration is also accounted for and there is some compensation for dead time losses. If there is a known J=0 or 1/2 state in the residual nucleus, its γ decay must be isotropic and hence can be used for such normalization.

b. Linear polarization measurements

The techniques and difficulties of angular distribution measurements are largely duplicated when linear polarizations are measured with the single-crystal detector (to be described presently). However, an additional factor is to be kept in mind: that because the sensitivity of this apparatus to the γ ray polarization is very small, one is frequently looking for intensity differences as small as a few percent. Accor-

dingly, great care must be taken in correcting for finite angle effects and in extracting peak intensities, as well as searching for possible systematic errors. In addition, the experiments are very time-consuming because of the large numbers of counts required to extract the asymmetries with confidence and since the measurements must be repeated a number of times to establish consistency of results.

Previous workers (e.g. Twin et al. 1970) used a three-crystal Compton polarimeter to measure the polarization of γ rays. In such an arrangement, γ rays are Compton scattered from a central crystal (either NaI or Ge(Li) into two analyzing crystals (commonly NaI detectors) placed at $\phi = 0°$ and $90°$, respectively, to the reaction plane. Summing the coincident signals from the scatterer and each analyzer separately, results in two spectra, one associated with the scatterer and the $0°$ detector (say) and the other with the scatterer and the $90°$ detector. From the two γ ray full energy yields $N(\phi)$ the asymmetry and hence polarization may readily be extracted. While having the advantage of quite high polarization sensitivity ($R \simeq 25\%$) this technique suffers from the low counting rate associated with a coincidence experiment and especially from the intrinsically poor resolution of the NaI detectors.

To obviate these difficulties, Ewan et al. (1969) have constructed and described the use of a thin rectangular Ge(Li)

detector as a polarimeter. (Fig. 2.3). Again it operates on the principle that Compton scattering of linearly polarized γ rays occurs preferentially in a plane perpendicular to the electric vector. In a Ge(Li) detector, one class of events contributing to the full energy peak for γ rays with $E_\gamma > 500$ keV arises from Compton scattering of the incident γ ray followed by total absorption of the scattered photon. Consequently, a higher yield in the full energy peak of a polarized γ ray will be obtained with the plane of the detector perpendicular to the electric vector of the γ ray than with it parallel. The polarization asymmetry is then simply obtained by taking γ ray spectra with the plane of the Ge(Li) polarimeter perpendicular to and parallel to the reaction plane, respectively. With this technique one combines the high resolution of a Ge(Li) detector (making it possible to analyze complex spectra) with the simplicity of a "singles" experiment. It is not without disadvantages,however; primarily those caused by its rather low polarization sensitivity ($< 10\%$). This means that for a fully polarized γ ray, there will be only an (at most) 10% difference in the full energy peak intensities measured with the polarimeter in the two orientations. Consequently, it is necessary to perform lengthy experiments to obtain the counting statistics required for accurate determinations of the asymmetry, and to evaluate carefully the possible sources of error. The next few para-

Fig. 2.3

Diagram indicating the experimental arrangement for γ-ray polarization measurements. From Baxter et al. (1970).

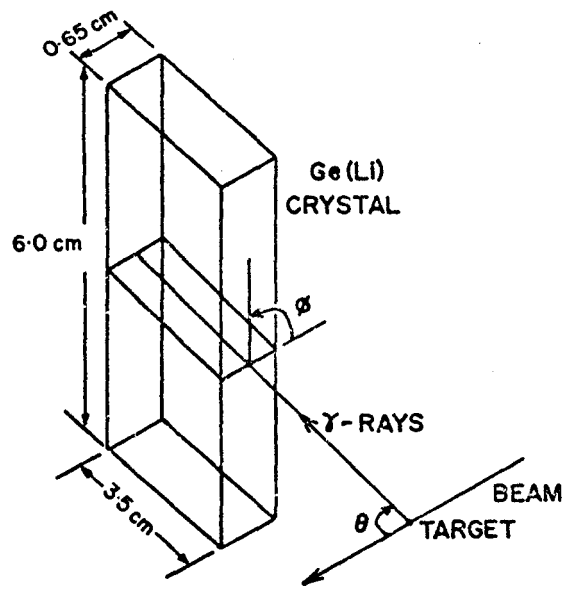
0·65 cm
6·0 cm
3·5 cm
Ge(Li)
CRYSTAL
ø
γ-RAYS
BEAM
θ
TARGET

graphs deal with this latter consideration.

It has already been pointed out that since the polar angle relative to the beam direction subtended by the counter will be different depending whether the plane of the detector is in or out of the reaction plane, spurious asymmetries may result if the γ ray is anisotropic. This is an important effect and an appendix contains an analysis of the corrections to be made.

Spurious asymmetries may also result from i) a large and non-circular beam spot on the target and ii) asymmetrical geometrical arrangements. Condition i) was avoided by the use of a small circular tantalum aperture in front of the target which restricted the diameter of the beam spot to much smaller than the dimensions of the detector, ensuring that the source of γ-rays could be considered a point source. Since the target chamber was a cylinder with a vertical axis perpendicular to the incoming beam, possible asymmetries due to differential absorption were minimized. One small possible source of asymmetry remained: with the plane of the polarimeter vertical there is greater absorption of the γ rays that pass through the target chamber at an angle and are detected off the beam axis. A simple calculation, however, indicates that the resulting asymmetry is very small ($< 0.2\%$) and may be neglected.

c. Calculation of the polarization sensitivity

In the analysis of the polarization data, one considers the asymmetry

$$S = \frac{N(\phi=0°) - N(\phi=90°)}{N(\phi=0°) + N(\phi=90°)}$$

where N(0°) and N(90°) are respectively the number of counts in a γ ray full energy peak with the plane of the single-crystal polarimeter parallel and perpendicular, respectively, to the reaction plane. The polarization is then given by $P = -S/R$ where the sensitivity of the polarimeter, R, is the asymmetry for a γ-ray fully polarized perpendicular to the reaction plane ($P = -1$). It is apparent that for the polarization of an arbitrary γ-ray to be determined, R of the polarimeter must be known as a function of γ ray energy. (R depends also on the solid angle subtended by the detector and the beam spot but this was kept constant during the experiments.) A convenient method of performing this calibration is suggested by Eqn. (1.9) whence the theoretical polarization takes, for pure multipole radiation (say E2), a very simple form depending only on the angular distribution coefficients a_2, a_4. A simultaneous measurement of the angular distribution and polarization asymmetry can readily be carried out for such γ-rays (since most even-even nuclei have $J^\pi = 0^+$ and 2^+ ground and first excited states, there is an abundance of E2 γ rays available, of various energies,

for such a measurement) and a direct comparison of the measured S and the corresponding P (obtained from the angular distribution) immediately yields the sensitivity R. Figure 2.4 shows the sensitivity curve used in the present work. It is worth pointing out that this curve is in excellent agreement with the sensitivity calculated by Ferguson and Lam (private communication, 1972).

d. Analysis of the data

To obtain the areas of the full energy peaks of the various γ-rays in the spectra, a modified version of a non-linear least squares fitting subroutine (Hay 1969) was used to fit the region of each peak of interest in the spectrum to a skew-Gaussian peak shape superimposed on a background taken to be the sum of an exponential and a linear function. The fitted area of the peak less the background was taken as the net intensity; the error in the intensity was calculated in the standard manner

$$\Delta I \simeq \sqrt{P + 2B}$$

where P is the area of the peak alone and B the background underneath. This procedure has the great advantage of treating similar regions in spectra taken at different angles in a uniformly consistent manner - especially important in extracting areas from the polarization spectra where one is seeking only for $\sim$ 5 - 10% effects from spectrum to spectrum.

Fig. 2.4

Polarization sensitivity R of the Ge(Li) polarimeter used in this investigation.

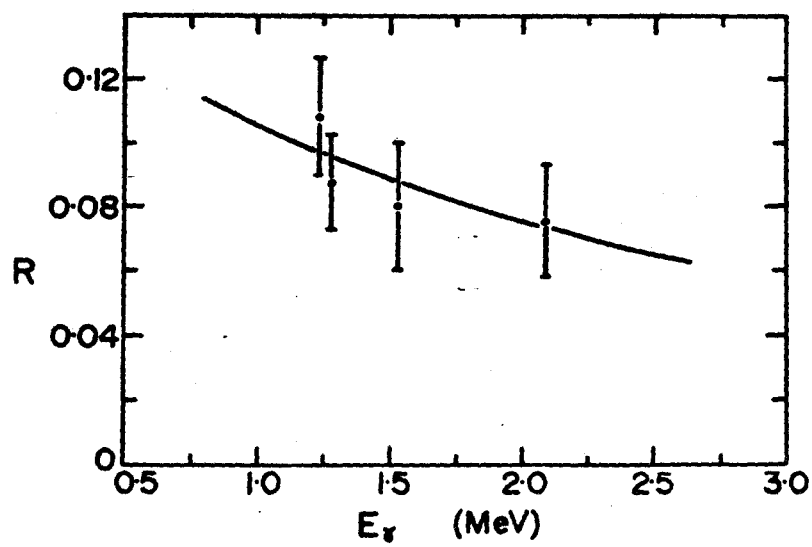
0·12
0·08
0·04
0
R
0·5
1·0
1·5
2·0
2·5
3·0
E_γ (MeV)

The level spins and parities and γ ray multipole mixing ratios were obtained from the angular distribution and linear polarization data using a modified version of a program described by Twin et al. (1970). For specified initial and final spins, parity change and multipole mixture δ a grid-search among the substate population P(m) was carried out to find the combination minimizing χ^2 of the fit. (In some cases the population parameters were restricted using the criteria given in Ch. I.) For a given spin sequence, arc tan δ was varied in 5° intervals from -90° to +90° to obtain the usual χ^2 vs arc tan δ plot. Only solutions for which χ^2 was less than the 0.1% confidence limit were accepted. Errors on the mixing ratio δ were assigned using the 1% confidence limit.

e. $^{18}O(\alpha,n\gamma)^{21}Ne$ experiment

Targets of ^{18}O were prepared by resistance heating of 0.01" thick Ta or W metal in a 99.5% enriched ^{18}O atmosphere at a pressure of 10 Torr. The resulting layer of Ta_2O_5 or W_2O_5 on both sides of the respective metal sheets were approximately 100 $\mu gm/cm^2$ thick as determined from the characteristic interference fringes. Also used in some of the experiments were targets of comparable thickness consisting of Ta sheets anodized in water enriched to 98.8% in ^{18}O, obtained through the generosity of Dr. C. Rolfs of the University of Toronto.

A yield curve of the γ rays from the $^{18}O(\alpha,n\gamma)$reaction

suggested that α-particle bombarding energies of 5.1 and 6.3 MeV be used for the study of the states below and above 3 MeV excitation, respectively. At these bombarding energies, the states in question are well populated and the reaction takes place close to threshhold, so that as discussed in Ch. I, the residual states are well aligned and strong anisotropies in the angular distributions and polarizations may be expected.

The resulting γ rays were detected in an array of three Ge(Li) detectors: a 50 cm^3 detector with resolution 2.5 keV FWHM for 1.33 MeV γ rays for the angular distribution measurements, a 37 cm^3 detector with similar resolution was used as the monitor counter and was placed at 135° to the beam, and the polarimeter, with a resolution of 4.5 keV was placed at 90° to the beam direction. Data from the three detectors were collected simultaneously and stored in separate 2048-channel regions of the analyzer. With a typical beam intensity of 200 nA of doubly charged He ions, angular distribution spectra were taken for 2 h periods and polarization data for 6 h periods. A total of 18 angular distribution and 6 polarization points (3 at each orientation) were taken at each energy. Unfortunately, insufficient statistics in some important γ ray peaks necessitated repeating some of the measurements at a later date; this was done at the Chalk River tandem laboratory where a quite similar experimental setup was used.

A typical spectrum taken at 6.1 MeV with the polarimeter is shown in Fig. 2.5.

In a search for hitherto undetected γ branchings from some of the levels in ^{21}Ne, a γ-γ coincidence experiment was also undertaken. Gamma rays following the bombardment of the ^{18}O target with a 6.2 MeV He beam were observed in the 50 cm^3 detector operated in coincidence with a 3"×3" NaI detector at 90° to the beam. Timing pulses from the Ge(Li) detector were generated by a Canberra "extrapolated zero strobe" unit (model 1426) while leading-edge timing was used on the NaI side. A time resolution of 20 nsec (FWHM) was obtained. The diverse linear pulses were digitized and stored as triplets of 18-bit words in a PDP-9 computer and periodically written on magnetic tape. The sorting was carried out later by a programme which allowed digital windows to be set on peak and background areas in the NaI and time spectra and the corresponding Ge(Li) spectrum to be projected out for analysis.

3. Results

Tables 2.1 and 2.2 summarize the results of the angular distribution and linear polarization measurements. It should be pointed out that the γ transitions from the 2790+2796 keV doublet exhibit isotropic angular distributions and zero polarizations, as expected for J = 1/2 states.

a. The 1747 and 2867 keV levels

The spin of the 1747 keV state was measured by Pronko et al. (1966) to be J = 7/2. The angular distribution co-

Fig. 2.5

Sample γ-ray spectrum obtained at 6.1 MeV beam energy using the Ge(Li) polarimeter. The spectrum was taken over a period of 4 hours. The assignment of the γ-rays is illustrated in the level diagram. Unprimed, single and double primed notations represent full energy, first and second escape peaks, respectively. γ-Rays from contaminant reactions are labelled by the nucleus from which they originate.

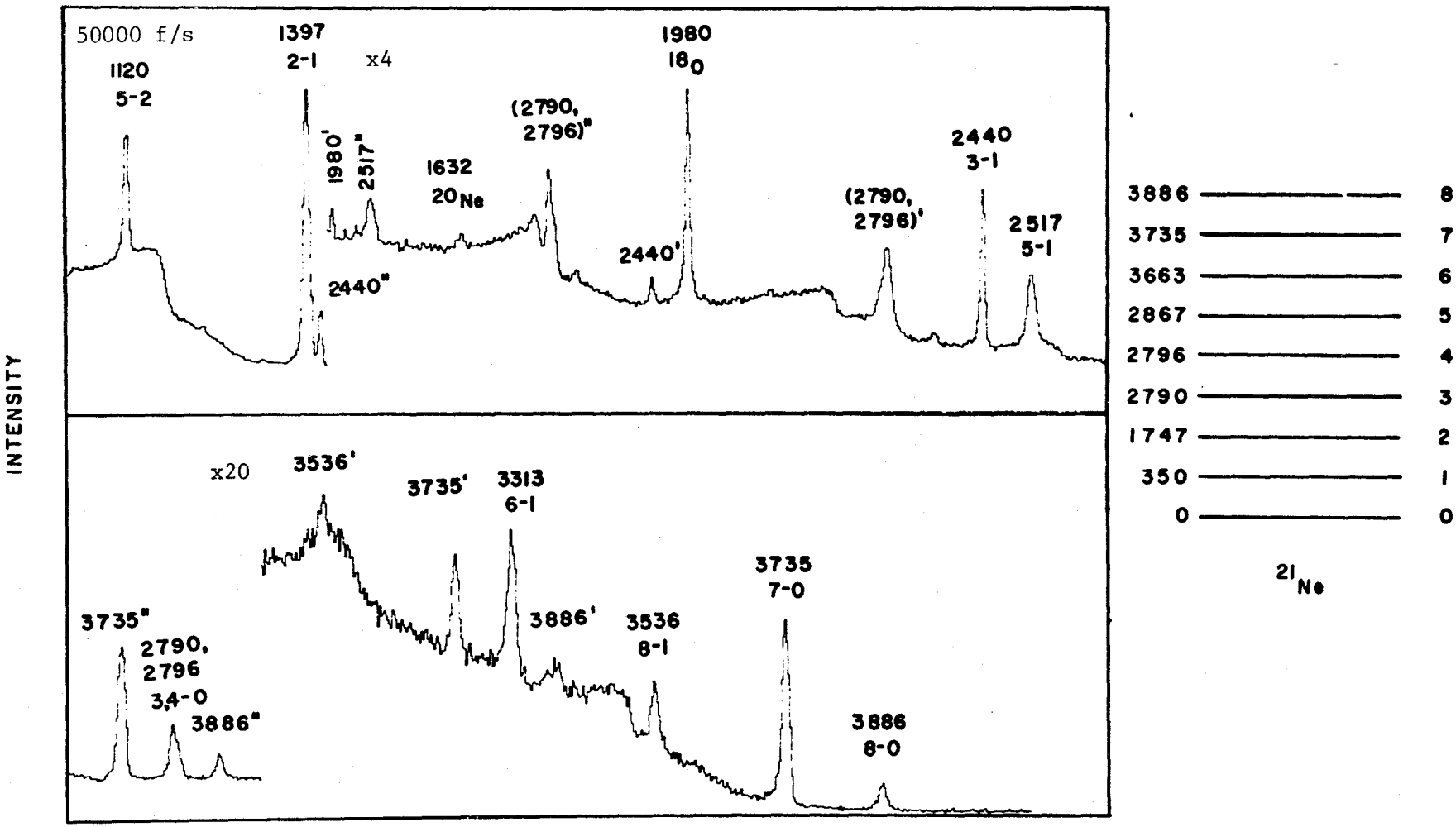
50000 f/s
1397
2-1
x4
1120
5-2
1980
18O
(2790,
2796)"
2440
3-1
1980'
2517"
1632
20Ne
2440"
2440'
(2790,
2796)'
2517
5-1
x20
3536'
3735'
3313
6-1
3735"
2790,
2796
3,4-0
3886"
3886'
3536
8-1
3735
7-0
3886
8-0
INTENSITY
3886
3735
3663
2867
2796
2790
1747
350
0
8
7
6
5
4
3
2
1
0
21Ne

Table 2.1

Results of angular distribution and polarization measurements

Transition (keV)	E_α (MeV)	a_2 [a]	a_4 [a]	Polarization P [b]
1747 → 350	5.2	-0.61±0.02	0.00±0.02	-0.21±0.07
2790 → 350	5.2	0.01±0.03	0.00±0.03	0.03±0.10
	6.1	-0.02±0.03	0.01±0.03	0.05±0.09
2790 → 0 [c]	5.2	0.02±0.04	-0.01±0.04	0.00±0.08
2796	6.1	0.00±0.03	0.02±0.04	-0.06±0.10
2867 → 350	5.2	0.41±0.01	-0.21±0.02	0.70±0.18
2867 → 1747	5.2	-0.43±0.02	0.05±0.02	-0.20±0.08
3663 → 350	6.1	-0.11±0.01	-0.02±0.02	+0.30±0.25
3735 → 0	6.1	-0.45±0.01	0.03±0.01	-0.09±0.05
3886 → 0	6.1	-0.29 0.02	-0.02±0.03	0.89±0.40
3886 → 350	6.1	0.28±0.02	0.01±0.02	-0.19±0.20

a) Corrected for solid angle

b) Corrected for angular distribution effects

c) Not resolved in polarimeter spectra

Table 2.2

Summary of mixing ratios of ^{21}Ne γ-rays from low-lying states [d]

Transition (keV)	J_i^π	J_f^π	Mixing Ratio δ [a]		
			Previous		Present
			Pronko et.al. (1969)	Rolfs et. al.(1972)	
1747 → 350	$7/2^+$	$5/2^+$		b)	+0.15±0.03
2867 → 1747	$9/2^+$	$7/2^+$	+0.06±0.03		+0.09+0.03
3663 → 350	$3/2^-$	$5/2^+$	0.00±0.1	0.00±0.02	c)
3735 → 0	$5/2^+$	$3/2^+$	+0.15±0.04	+0.17±0.06	+0.15±0.04
3886 → 0	$5/2^-$	$3/2^+$	0.00±0.05	0.00±0.05	-0.03±0.03
3886 → 350	$5/2^-$	$5/2^+$	0.00±0.08	-0.09±0.04	-0.45±0.40

a) Phase convention of Rose and Brink (1967).

b) A value of δ = +0.16±0.03 is reported by Pronko et al. (1966).

c) Undetermined by the present work.

d) A more complete summary of mixing ratios in ^{21}Ne is presented in Table 2.5

efficients of the 1747 → 350 keV γ-ray transition (Table 2.1) were used to calculate the expected polarization P of this γ ray as a function of the mixing ratio δ for the two possible multipolarities, E2/M1 and M2/E1. The resulting curves together with the experimental polarization are shown in Fig. 2.6a. The only solution consistent with previous determinations of the mixing ratio of this γ ray (Table 2.2) yields $J^{\pi} = 7/2^{+}$ and $\delta = +0.15 \pm 0.03$.

Pure multipole transitions are especially suited to polarization measurements since the expected γ-ray polarizations are large and can be directly determined from the a_2 and a_4 coefficients. The J =9/2 state at 2867 keV (Pronko et al. 1966) decays to the $J^{\pi} = 5/2^{+}$, $E_x = 350$ keV state via a pure quadrupole transition. From the angular distribution coefficients (Table 2.1) the polarization of this γ ray is expected to be $P = \pm(0.68\pm0.05)$, the positive and negative values corresponding to E2 and M2 radiation respectively. The experimental value (Table 2.1) of $P = +0.70\pm0.18$ thus requires the positive parity assignment to the 2867 keV level. The data for the 2867 → 1747 keV γ ray together with the previously determined mixing ratio (Pronko et al. 1967) are also consistent only with the $9/2^{+}$ assignment (Fig. 2.6b). The resulting mixing ratio $\delta = +0.09\pm0.03$ is in good agreement with the reported value of $\delta = +0.06\pm0.03$.

The positive parity assignments to the 1747 and 2867

Fig. 2.6

Polarization of the (a) 1747-350 and (b) 2867-1747 keV γ-transitions as a function of the corresponding mixing ratio δ. The a_2 and a_4 coefficients given in table 1 were used to calculate these curves. The experimental values of the polarization are indicated by the dotted region. The dashed area superimposed represents the mixing ratio consistent with the experimental polarization; the cross-hatched area below indicates the mixing ratio of the respective γ-transition as obtained in previous work (table 2).

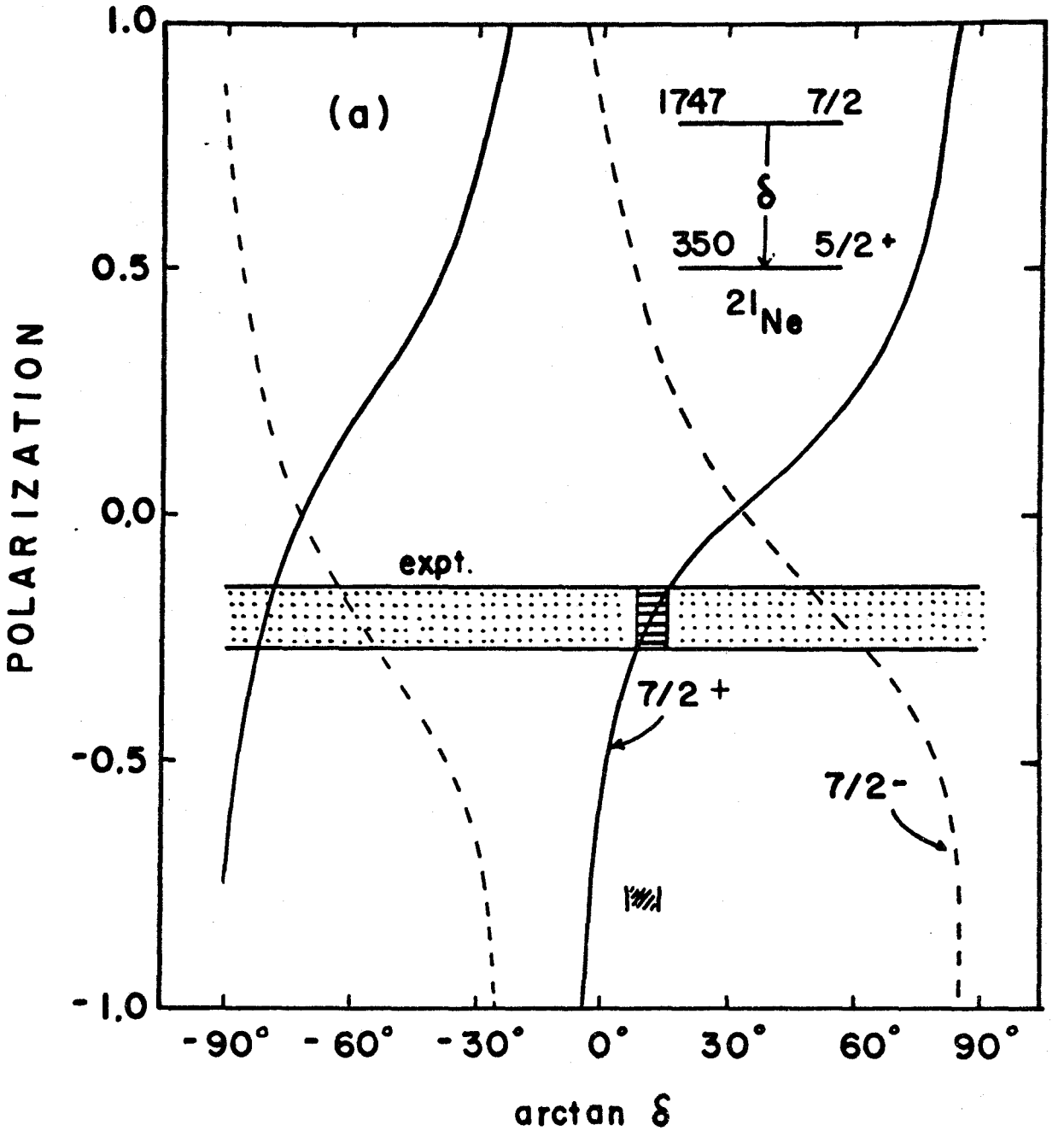
(a)
1747 7/2
δ
350 5/2+
21Ne
expt.
7/2+
7/2-
1.0
0.5
0.0
-0.5
-1.0
POLARIZATION
-90° -60° -30° 0° 30° 60° 90°
arctan δ

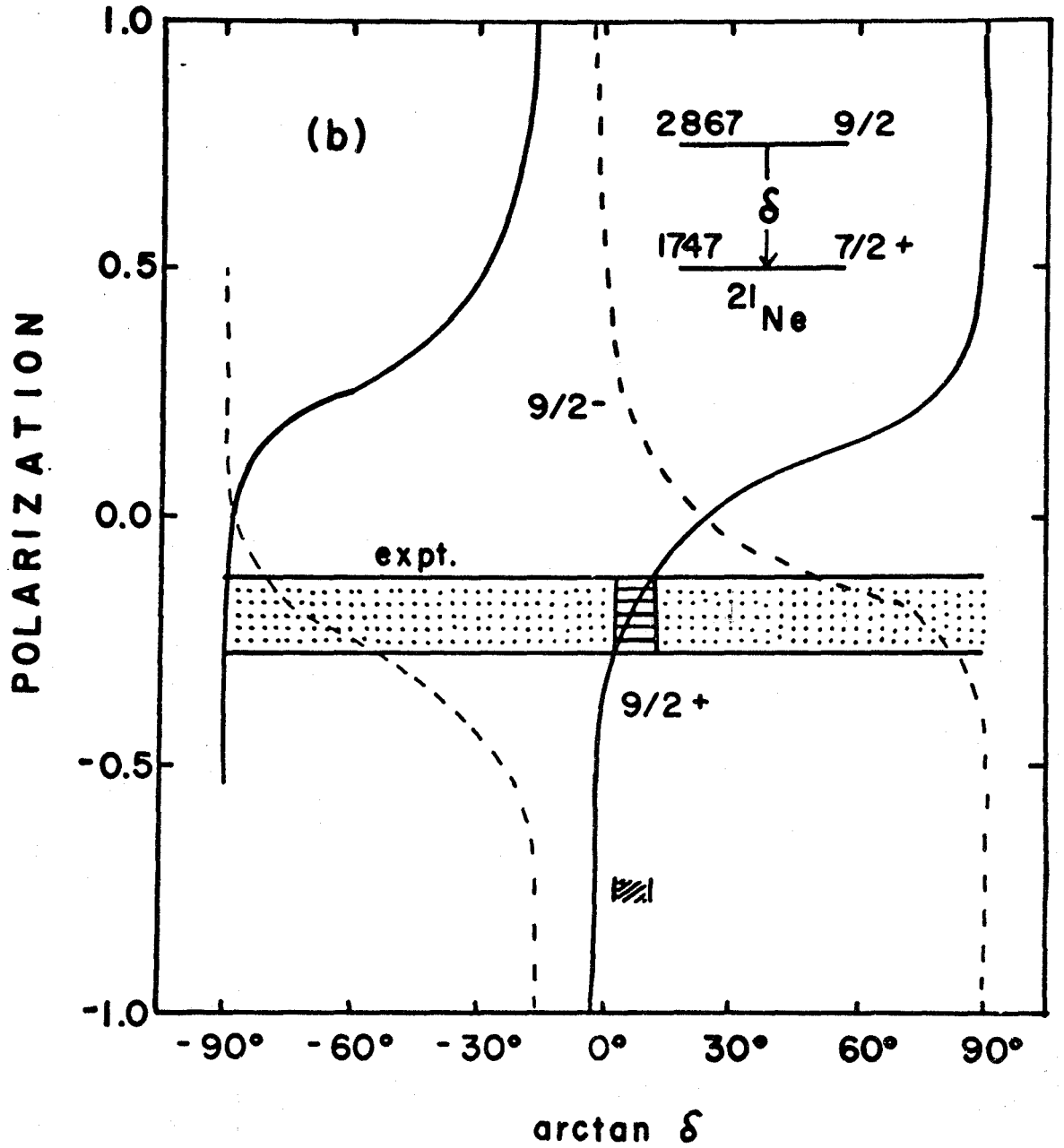
(b)
2867
9/2
δ
1747
7/2+
21Ne
9/2-
expt.
9/2+
1.0
0.5
0.0
-0.5
-1.0
POLARIZATION
-90°
-60°
-30°
0°
30°
60°
90°
arctan δ

keV levels are in agreement with previous assignments based on transition strength arguments (Pronko et al. 1966, 1967).

b. The 3663, 3735 and 3886 keV levels

The J = 3/2 assignment has been reported for the 3663 keV level on the basis of γ-γ angular correlation experiments (Kuhlmann et al.1970). The mixing ratio measured by these authors (δ = 0.00±0.02) for the 3663-350 keV transition and the angular distribution coefficients from the present work (Table 2.1) lead to expected values of the polarization of this γ ray of P = ±(0.16±0.03), positive for E1 and negative for M1 radiation. The measured value (Table 1) of P = +0.30±0.25 favours E1 radiation and consequently $J^{\pi}(3663) = 3/2^{-}$. This is in agreement with the results of Howard et al. (1969), who assigned negative parity on the basis of ℓ transfer in the $^{20}Ne(d,p)^{21}Ne$ reaction.

The angular distribution and linear polarization measurements on the 3735 keV ground state γ transition yield J = 5/2 and furthermore require positive parity for the 3735 keV level (Fig. 2.7a). The angular distributions alone are also consistent with J = 3/2 and a mixing ratio δ = +1.3±0.3; however, this would require a γ-ray polarization of P = ±(0.38±0.02), in serious disagreement with the experimental result of P = 0.09±0.05. The resulting J = 5/2 assignment is in agreement with a recent γ-γ angular correlation measurement by Kuhlmann et al.(1970) and $J^{\pi} = 5/2^{+}$ is consistent with the ℓ = 2 transfer suggested by Howard et al. (1970) to this state in

Fig. 2.7

Polarization of the (a) 3735 → 0, (b) 3886 → 0 and (c) 3886 → 350 keV γ-ray transitions. The notation is given in the caption to fig. 2.6.

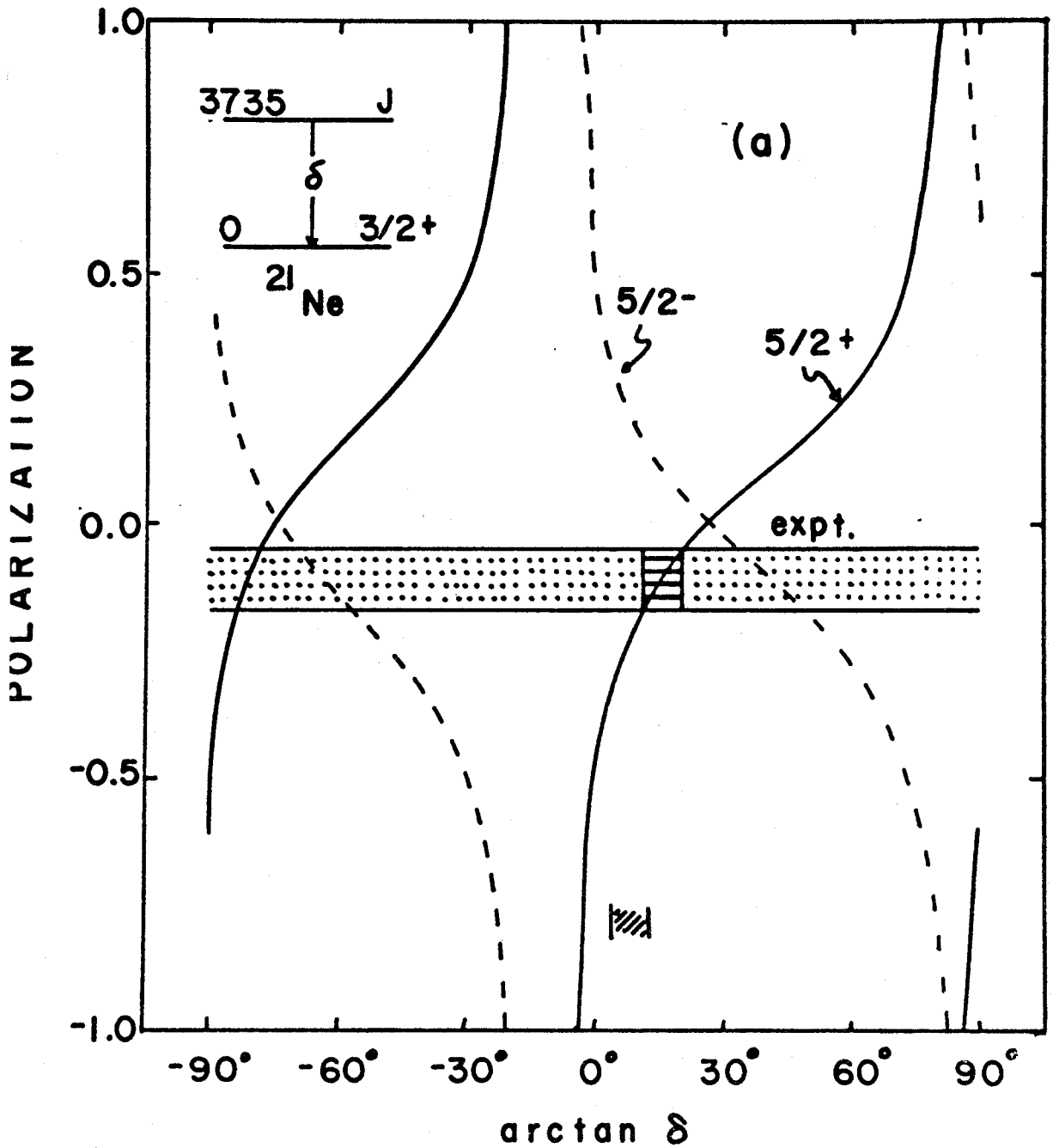
1.0
0.5
0.0
-0.5
-1.0
POLARIZATION
3735
J
δ
0
3/2+
21
Ne
(a)
5/2-
5/2+
expt.
-90°
-60°
-30°
0°
30°
60°
90°
arctan δ

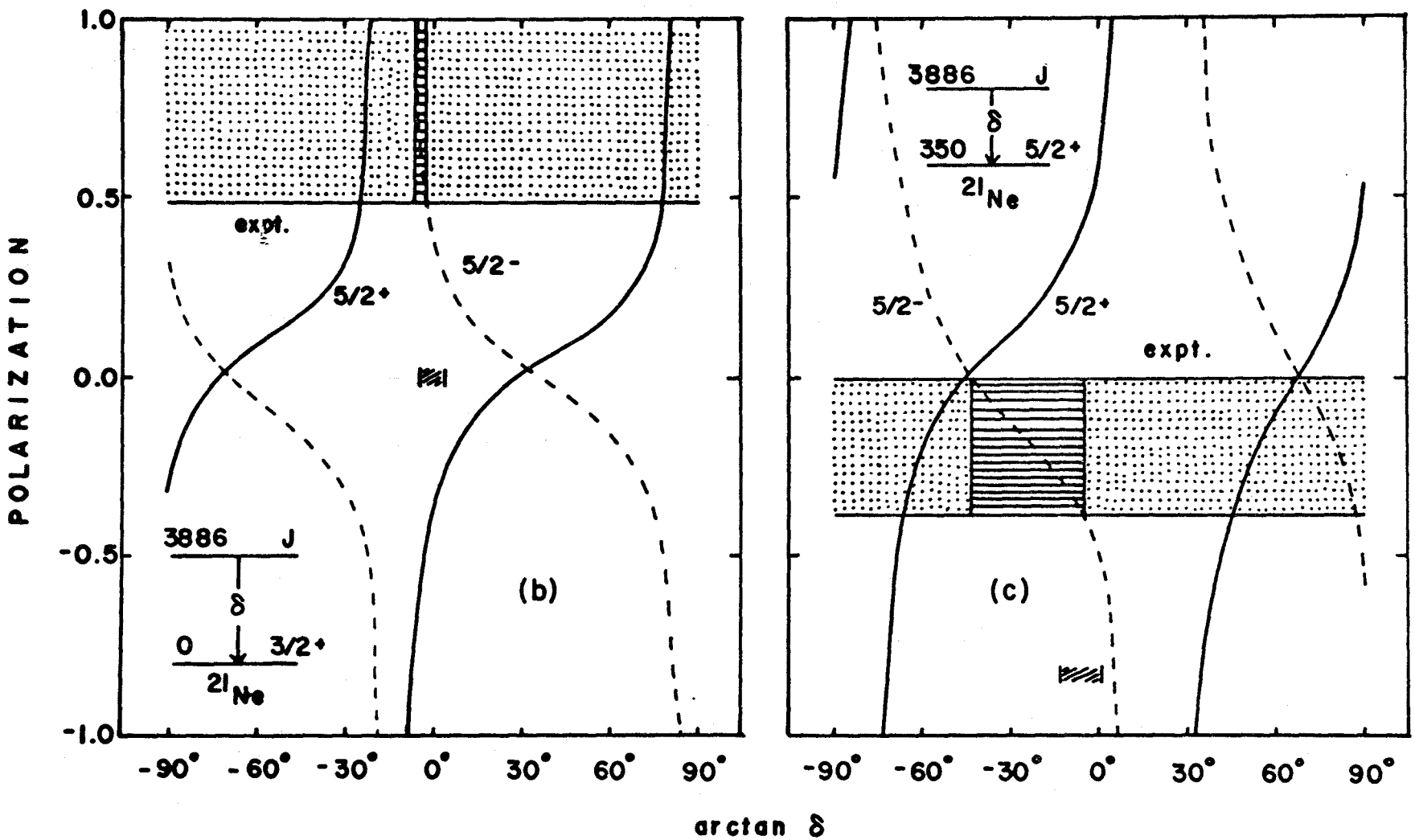
POLARIZATION
1.0
0.5
0.0
-0.5
-1.0
-90°
-60°
-30°
0°
30°
60°
90°
arctan δ
expt.
5/2+
5/2-
3886 J
δ
0 3/2+
21Ne
(b)
3886 J
δ
350 5/2+
21Ne
5/2-
5/2+
expt.
(c)

the $^{20}Ne(d,p)^{21}Ne$ reaction.

Angular correlation measurements by Kuhlmann et al. (1970) of the decay γ rays from the 3886 keV level have resulted in a J = 5/2 spin assignment to this state. The data from the present work on the 3886 → 0 and 3886 → 350 keV γ decays (Table 2.1 and Fig. 2.7b,c) are in agreement with the J = 5/2 assignment and require that the parity of the state be negative. Table 2.2 shows the mixing ratios of the γ rays from this state deduced from these measurements.

c. γ-ray decay of the 3886 keV level

The Ge(Li) spectrum measured in coincidence with the 2440 keV γ ray (resulting from the decay of the 2790 keV level), with background coincidences subtracted, is shown in Fig. 2.8. In addition to the 873 keV line arising from the known 3663-2790 keV decay, a weak line at 1096±2 keV is observed. This γ ray appeared convincingly only in association with the 2440 keV window and is here ascribed to the 3886 → 2790 keV decay. The branching ratio of this transition was determined to be (1.8±0.7)% by comparing the 1096/873 intensity ratio observed in the coincidence spectrum with the 873/3886 and 873/3735 intensity ratios observed in a single γ-ray spectrum taken at the same energy and angle. Since the Ge(Li) detector was placed at $\theta_\gamma = 55°$ to the beam, where $P_2(\cos\theta) \simeq 0$, corrections due to the angular distribution of the 873 and 1096 keV γ rays are small; the uncertainty due to these effects

Fig. 2.8

Partial coincidence γ-ray spectrum from the $^{18}O(\alpha,n\gamma)^{21}Ne$ reaction. During the playback analysis (see text) two windows of equal width were set on the 2.44 MeV γ-ray and a nearby background region in the NaI spectrum (labelled G and B in the inset NaI spectrum, respectively) and projected Ge(Li) spectra recorded. The spectrum is the difference between the two coincidence spectra. The corresponding γ-ray decay scheme is presented in the inset level diagram.

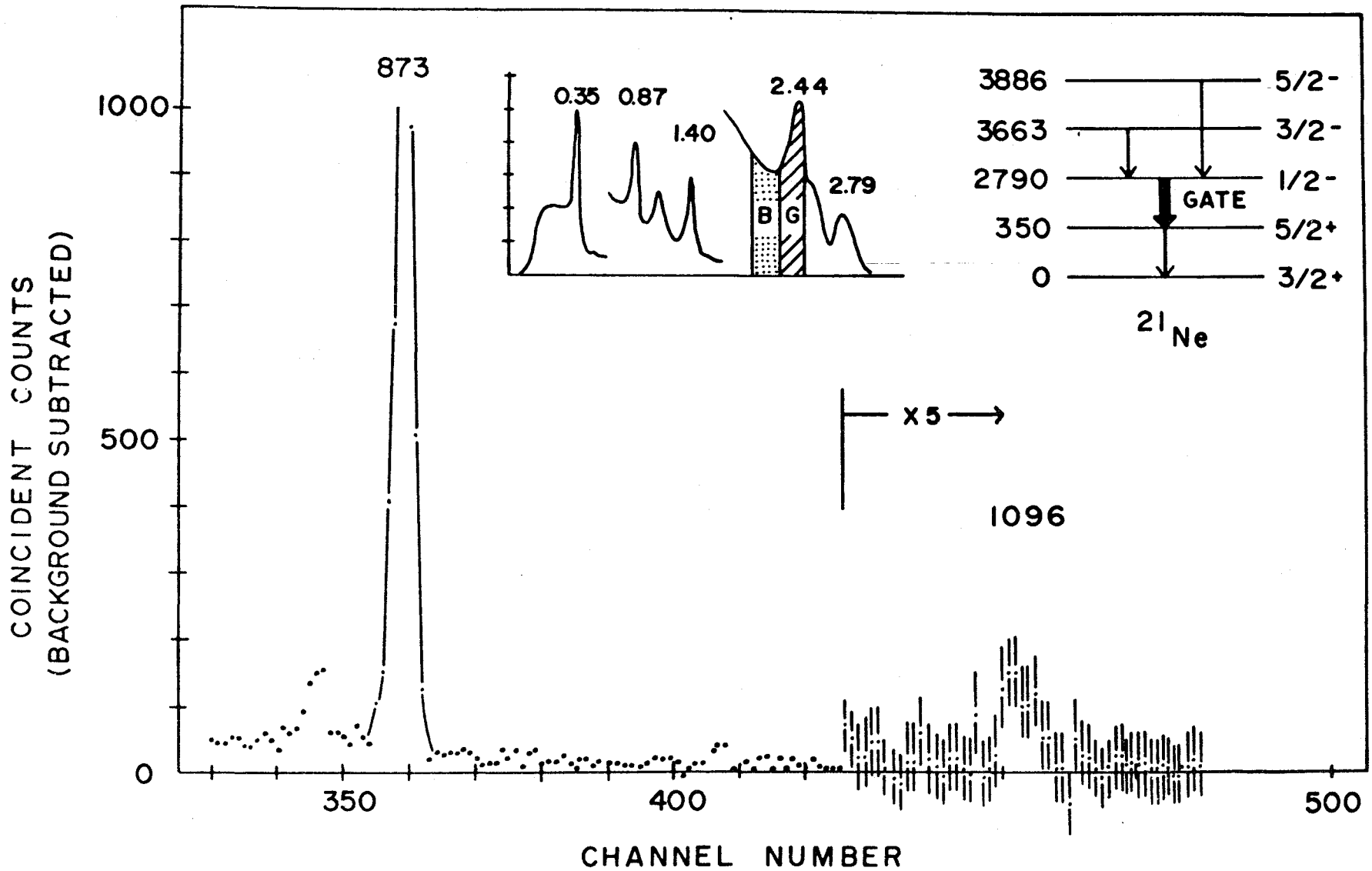
873
1000
500
0
COINCIDENT COUNTS
(BACKGROUND SUBTRACTED)
350
400
500
CHANNEL NUMBER
0.35
0.87
1.40
2.44
2.79
B
G
3886
3663
2790
350
0
5/2-
3/2-
1/2-
5/2+
3/2+
GATE
21 Ne
X5
1096

has been estimated and is included in the error in the branching ratio.

d. Summary of results

The known information on the low-lying levels of ^{21}Ne, obtained from both the present investigations and from the literature, is summarized in Tables 2.3-2.6 as i) spin and parity assignments, ii) branching ratios of level decays, iii) multipole mixing ratios of γ transitions and iv) level lifetimes. This information is used to deduce γ-ray transition strengths and comparison with theoretical calculations is made in a subsequent section.

Fig. 2.9 presents the energies, spins and parities of ^{21}Ne levels below 4 MeV excitation deduced from the present and previous investigations. Not all γ-decay branches are shown (these are given in Fig. 2.2); only those used in the linear polarization and angular distribution analysis.

4. Discussion

a. Rotational band assignments

The $J^{\pi} = 7/2^{+}$ and $9/2^{+}$ assignments to the 1747 and 2867 keV levels respectively strongly support their identification as the third and fourth members of a $K^{\pi} = 3/2^{+}$ ground state rotational band. The properties of both levels in the framework of the collective and shell models have recently been discussed by Rolfs et al. (1971).

The assignment $J^{\pi} = 5/2^{+}$ to the 3735 keV level from

Table 2.3

Spin-parity assignments in ^{21}Ne

E_x(keV)	a)	b)	c)	d)	e)	f)	g)	h)	j)	k)	ℓ)	Accepted
0.350					5/2+	5/2			ℓ=2	3/2+,5/2+		5/2+
1.747	7/2+				7/2+	7/2		7/2				7/2+
2.790		1/2(-)		3/2			3/2		ℓ=0	1/2+	ℓ=1	1/2-
2.796					1/2+			1/2+				1/2+
2.867	9/2+				J≥5/2	(9/2)	9/2					9/2+
3.663	3/2-	3/2-		3/2	3/2			3/2,5/2			ℓ=1	3/2-
3.735	5/2+	5/2		3/2,5/2	(5/2+)			3/2,5/2	ℓ=2	3/2+,5/2+		5/2+
3.886	5/2-	5/2		3/2,11/2				3/2,5/2				5/2-
4.433			11/2(+)	7/2,11/2								11/2+
4.526				3/2,5/2					ℓ=2			(5/2+)
4.686												(3/2+)
6.450			13/2(+)									13/2+

a) Present work
b) Rolfs et al. (1972).
c) Rolfs et al. (1971)
d) Pronko et al. (1969)
e) Howard et al. (1965)
f) Pronko et al. (1966)
g) Pronko et al. (1967)
h) Howard et al. (1967)
j) Howard et al. (1969)
k) Lambert et al. (1968)
l) Howard et al. (1970)

Table 2.4

Branching Ratios of Levels in ^{21}Ne

E_i	E_f	(a)	(b)	(c)	(d)	(e)	(f)	(g)	(h)	(j)	(k)	(l)	Adopted
350	0	100	100	100			100						100
1747	0	4±3	5±2			7	5±2	6			7±1		5±1
	350	96±3	95±2			93	95±2	94			93±1		95±1
2790	0	16±3	15±4		→350(10)			40	15	15	15		15±4
	350	84±3	85±4		→ 0(90)			60	85	85	85		85±4
2796	0	100	100	100							100		100
2867	350	35±5	33±5	41±2		-	37±4	30	31		30±6		34±2
	1747	65±5	67±5	59±2		100	63±4	70	69		70±6		66±2
3663	0	-	<2		<2						<7		
	350	60±7	54±4	54±3	61±3	60					64±3		58±2
	1747		<2		<2						<3		
	2790	40±7	38±4	46±3	35±2	40					36±3		36±3
	2796		8±3		4±2						<5		6±2

(continued next page)

Table 2.4 (continued)

E_i	E_f	(a)	(b)	(c)	(d)	(d)	(e)	(f)	(g)	(h)	(j)	(k)	(l)	Adopted
3735	0	80±8	80±3	87±2	89±2	>90						94±1		81±2
	350	15±8	12±3	13±2	11±2							<9		12±2
	1747	5±3	8±2		<10							6±1		7±2
3886	0	34±5	35±5	29±3	22±2							23±5		29±4
	350	64±5	65±5	71±3	78±2	>60						77±5		69±3
	1747	<2	<3									<10		-
	2790	1.8±0.7	<3									< 6		1.8±0.7
4433	1747	-											21±5	21±5
	2867	-											79±5	79±5
6450	2867	-											20±5	20±5
	4433	-											80±5	80±5

a) Present work
b) Rolfs et al. (1972)
c) Bailey et al. (1972
d) Pronko et al. (1969)
e) Howard et al. (1965)
f) Pronko et al. (1966)
g) Bent et al. (1967)
h) Pronko et al. (1967)
j) Smulders and Alexander (1966)
k) Howard et al. (1970)
l) Rolfs et al. (1971)

Table 2.5

Multipole Mixing Ratios

E_i	E_f	a)	b)	c)	d)	e)	f)	g)	h)	Weighted Average Adopted Value
350	0	-	-	-	$0.02<\delta<0.03$	0.08±0.03	-	(-0.08)-(+0.50) (2.5)-(3.3)		.0.04 ±0.02
1747	0	E2	-	-	-	E2	-	-		E2
	350	0.15±.03	-	-	-	0.18±0.03	-	0.11±0.03		0.15±0.03
2790	0	-	-	-	-	-	-	-		J_i = 1/2 undetermined δ
	350	-	-	-	-	-	-	-		"
2796	0	-	-	-	-	-	-	-		"
2867	350	E2	-	-	-	E2	-	-		E2
	1747	0.09±.03	-	-	-	0.12±0.06	0.06±0.03	-		0.09±0.03
3663	350	-	2.5 ±2.5	0.0 ±0.1	-	-	-	-		0.0 ±0.2
	2790	-	+0.09±0.04 1.5 ±0.6	-	-	-	-	-		+0.09±0.04 1.5 ±0.6
	2796	-	-	-	-	-	-	-		
3735	0	0.15±.04	0.7 ±0.06	0.15±0.03	-	-	-	0→0.62 1.7→2.5		0.16±0.02
	350	-	0.55±0.10	0.57±0.30	-	-	-	-		0.56±0.13
	1747	-	-		-	-	-	-		
3886	0	-0.03±.03	0.00±0.05							-0.03±0.03
	350	-0.45±0.40	0.09±0.04							-0.09±0.07
	2790	E2	-							E2
4433	1747	E2								
	2867		0.13±0.06						0.05±0.05	0.08±0.04
6430	2867	E2								
	4433								0.08±0.03	0.08±0.03

(continued next page)

Table 2.5 (continued)

a) Present work

b) Rolfs et al. (1972)

c) Pronko et al. (1969)

d) Howard et al. (1965)

e) Pronko et al. (1969)

f) Pronko et al. (1969)

g) Howard et al. (1967)

h) Rolfs et al. 1971).

Table 2.6

Lifetime Assignments
(fsec).

Level E_x	a)	b)	c)†	d)	e)	f)	g)	h)	Adopted
350		3600±300	>9000	$<3\times10^{-10}$ sec				22000±3000	22±3 pse
1747	76±12	24±6	150±40		150^{+150}_{-100}				76±12
2790	>3600	>5200	>7000			>1000	84 psec		84 pse
2796	<27	<35	<45			<50			<30
2867	56±14	27±5	100±20		110^{+150}_{-70}				
3663	68±16	63±7	120±20						66±9
3735	<38	<25	<67						<32
3886	43±13	24±10	78±27						34±9
4433	34±6	25±6	78±27						30±4

†) Values superseded by those of ref. b)
a) Rolfs et al. (1971)
b) Bailey et al. (1972)
c) Pronko et al. (1969)
d) Howard et al. (1965)
e) Bent et al. (1967)
f) Smulders and Alexander (1966)
g) Warbuton et al. (1971)
h) Bamberger et al (1968)

Fig. 2.9

Level diagram of low-lying states in ^{21}Ne. The excitation energies and spin assignments in the first column are from previous work and are discussed in the text. Spin and parity assignments obtained in the present work are given in the second column. Only the most intense γ-transitions from these levels were used in the polarization measurements; these are shown in the level diagram.

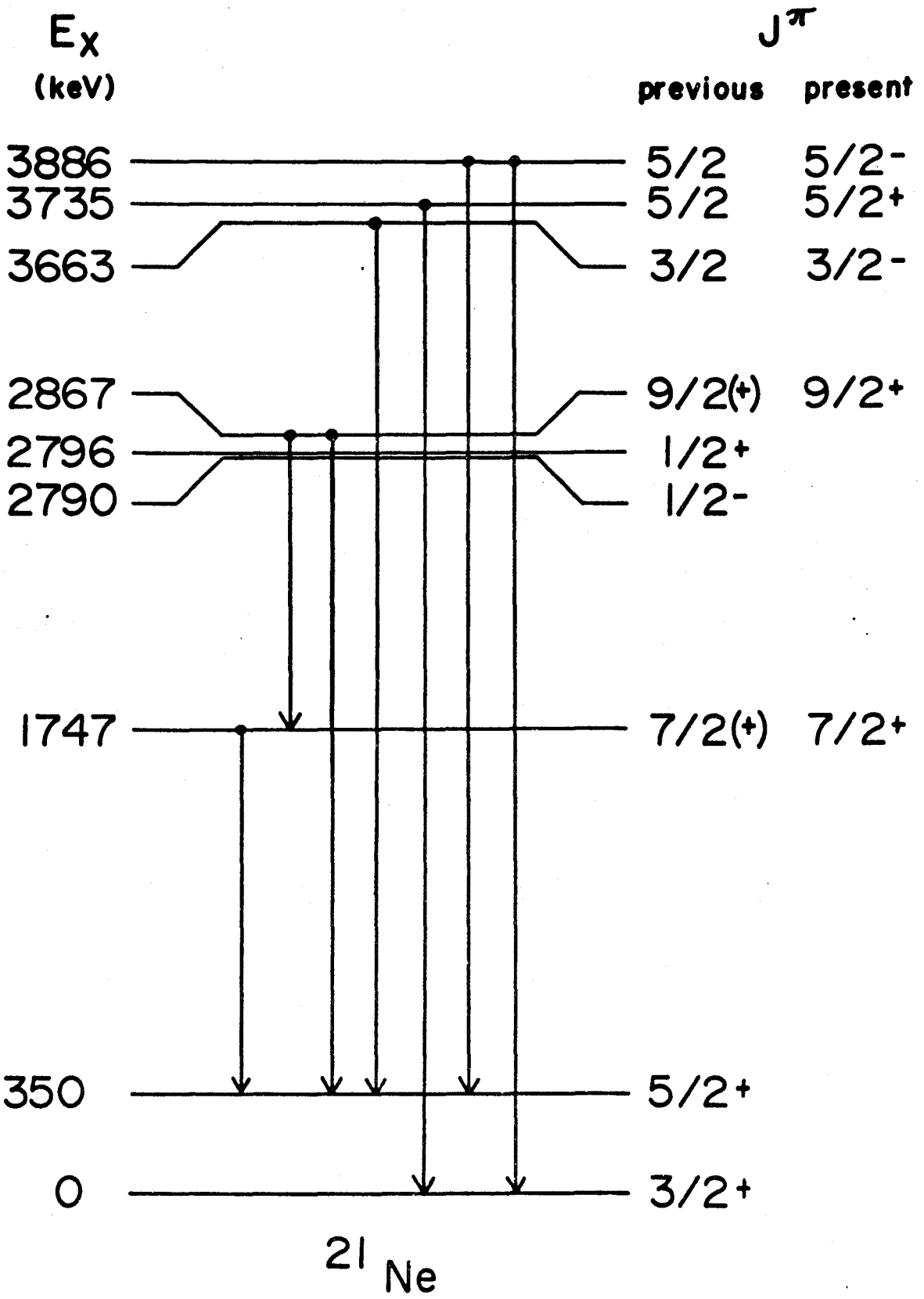
E_x (keV)
J^π
previous
present
3886
3735
3663
2867
2796
2790
1747
350
0
5/2
5/2
3/2
9/2(+)
1/2+
1/2-
7/2(+)
5/2+
3/2+
5/2-
5/2+
3/2-
9/2+
7/2+
^{21}Ne

the present work supports its identification as the head of a $K^{\pi} = 5/2^{+}$ rotational band, as suggested by Rolfs et al. (1971).

There is considerable evidence for regarding the 2790($J^{\pi}= 1/2^{-}$), 3663($J^{\pi}=3/2^{-}$), and 3886($J^{\pi}= 5/2^{-}$) keV levels as members of a $K^{\pi} = 1/2^{-}$ rotational band in ^{21}Ne. This identification was originally suggested by Pronko et al. (1969) on the basis of the energies and spins of these states and by parity determinations based on ℓ-transfer measurements in stripping reactions. Recently the E2 strength of the 3663-2790 keV transition was determined by Rolfs et al. (private communication) to be 20^{+22}_{-15} W.u., lending support to this assignment.

The lifetime of the 3886 keV level has been measured by Rolfs et al. (1971) as 43±13 fs and by Bailey et al. (1972) as 24±10 fs.

The E2 strengths of the weak 1096 keV $5/2^{-} \rightarrow 1/2^{-}$ transition (discussed previously) corresponding to these two lifetime measurements are then 60±30 W.u. and 110±55 W.u. respectively, which represent considerable enhancements over the single-particle rates. In the pure rotational model, the ratio of the $3/2^{-} \rightarrow 1/2^{-}$ and $5/2^{-} \rightarrow 1/2^{-}$ transitions is given by the square of the ratio of the corresponding Clebsch-Gordan coefficients $\langle J_i 2 \frac{1}{2} 0 | \frac{1}{2} \frac{1}{2} \rangle$ with $J_i = 3/2$ and 5/2 respectively; this ratio in this case is unity. The rotational model, then, predicts that the E2 strength of the $5/2^{-} \rightarrow 1/2^{-}$ transition should be the same as that of the $3/2^{-} \rightarrow 1/2^{-}$ transition, i.e. 20^{+22}_{-15} W.u. Of the values given

above, the strength 60±30 W.u. (corresponding to a lifetime 43±13 fs) is in agreement with the rotational model prediction, while the other is rather too strong.

The branching ratio of the 1096 keV transition determined in the present experiment and the lifetime of the 3886 keV state measured previously are in satisfactory agreement with the simple rotational model and place the assignments of the 2790, 3663, and 3886 keV levels to a $K^{\pi} = 1/2$ band on a firmer basis.

b) Level energies

The level scheme of ^{21}Ne given in Figs. 2.2 and 2.9 compares favourably with recent shell model calculations of Halbert et al. (1971) considering 5 particles in the s-d shell and carrying out a full diagonalization with a variety of forces. Naturally, only positive parity levels are predicted in such a calculation; negative parity levels would involve holes in the 1p shell and no such configurations have to date been considered. Table 2.7 presents a comparison of the experimentally observed level energies (col. 3) and the results of Halbert's calculation (col. 4). Also given, for future reference, are the results of two Nilsson-model calculations (cols. 5 and 6) which will be discussed in detail later in this section.

Recent Nilsson-model calculations of ^{21}Ne (see, e.g. Rolfs et al. 1971) have yielded generally satisfactory agree-

Table 2.7

Energies of rotational members in ^{21}Ne experimentally and from the Nilsson model; also results of Halbert's shell model calculation.

K^π	J^π	Expt.[a]	S.M.[b]	Nilsson 1 δ (=0.3)	Nilsson 2 δ (=0.1)
3/2+[211]	3/2+	0.0	0	0.0	0.0
	5/2+	0.350	0.300	0.470	0.410
	7/2+	1.747	1.850	1.456	1.587
	9/2+	2.867	2.900	2.695	2.868
	11/2+	4.431	4.400	4.166	4.300
1/2+[211]	1/2+	2.796		2.796	2.796
	3/2+	(4.687)		3.937	4.613
	5/2+	(4.526)		5.233	4.690
	7/2+	(7.008)		7.826	8.870
	9/2+	(7.043)		10.089	9.010
5/2+[202]	5/2+	3.735		3.735	3.776
	7/2+	(6.177)		5.258	5.301
	9/2+			7.099	7.130
1/2-[101]	1/2-	2.790		2.790	
	3/2-	3.663		3.657	
	5/2-	3.889		3.961	
	7/2-	(5.826)		5.986	
	9/2-	(6.267)		6.532	
	11/2-			9.715	

a) Assignments beyond E_x=4 MeV by Rolfs et al. (1972) on basis of decay scheme.

b) Estimated from Fig. 7 of Halbert et al. (1971) with KB+^{17}O interaction matrix elements.

ment for the positive parity levels if a deformation $\delta = 0.3$ and spin-orbit coupling strength $\kappa = 0.08$ be used.

A difficulty arises, however, with the $K^{\pi} = 1/2+[211]$ band. For a deformation $\beta = 0.3$ the decoupling parameter a of the rotational band is predicted to be very small ($a \simeq 0.1$) and the (d,p) spectroscopic factor of the $J^{\pi} = 1/2^{+}$ band head is also small ($S \sim 0.2$). Furthermore, for an inertial parameter $\hbar^2/2\mathcal{I} \sim 175$ keV (which reproduces the level spacing of the ground state band) the $J^{\pi} = 3/2^{+}$ member of this band is expected to lie at $E_x \simeq 3$ MeV. The lack of such a state in ^{21}Ne labels this band as anomalous. It is now believed (Rolfs et al, 1972) that states at 4.53 and 4.69 MeV have $J^{\pi} = 5/2^{+}$ and $3/2^{+}$, respectively, and these have been assigned to the 1/2+[211] band; this would correspond to a decoupling parameter $a \sim 1.0$ for this band. The (d,p) spectroscopic factor of the 2.796 MeV level has been measured by Howard et al to be $S = 0.8$, larger than predicted. The values for the decoupling parameter and spectroscopic factor are extremely sensitive to the nuclear deformation, however, and calculations predict that if a deformation $\beta \sim 0.10$ be assigned to the intrinsic state, the spectroscopic factor and decoupling parameter would be accounted for. Both the spectroscopic factor and level spacing could also (in principle) be suitably altered by changing the Coriolis mixing strength between this $K^{\pi} = 1/2^{+}$ band and other positive parity rotational bands. This is however an unsatisfactory ad hoc procedure

and an explanation of this anomaly in terms of microscopic models would be desirable.

The Nilsson calculation also predicts that a second, highly decoupled, $K^{\pi} = 1/2^{+}$ band,arising from the promotion of a nucleon out of the lowest K = 1/2 orbital associated with the $d_{5/2}$ shell model state ($K^{\pi} = 1/2+[220]$) should have its band head near 4 MeV. No evidence for such a band in ^{21}Ne has been found, although it is believed (Dubois 1967) that the band head has been identified in ^{23}Na with the $J^{\pi} = 1/2^{+}$ state at 4.43 MeV. A projected Hartree-Fock calculation by Johnstone and Benson (1969) has shown that the corresponding state in ^{21}Ne should lie at high excitation energy ($E_x \simeq 10$ MeV) and this would explain its non-observation. A simple explanation of the high excitation of this state can easily be given, which incidentally illustrates a defect of the Nilsson model: that merely summing single particle energies is inadequate when an excitation involves the breakup of a strongly correlated cluster of nucleons, such as the four particles in the $\Omega = 1/2$ orbital. A great deal of energy is lost by the breakup of this correlated quartet to form the $1/2^{+}[220]$ hole band; hence its high excitation in ^{21}Ne.

Another difficulty arises with the first negative parity state in ^{21}Ne, observed at $E_x = 2.79$ MeV. This is a hole state, formed by the promotion of a particle from the $p_{1/2}$ shell into the s-d shell. The Nilsson model predicts the energy of this state in ^{21}Ne to be $E_x \sim 6$ MeV, in serious

disagreement with experiment. In the following we attempt to show that a suitable choice for the particle-hole interaction can obviate this difficulty and lead to a calculated energy in excellent agreement with the experimental result.

Bansal and French (1964) and Zamick (1965) have investigated the properties of configurations with holes in the 1p shell and particles promoted to the 2s-1d shell. They point out that the particle-hole interaction must be considered to be isospin-dependent; this can be seen from the fact that the T = 1 negative-parity states in ^{16}O lie $\sim$ 5 MeV higher in energy than the corresponding T = 0 states. Consequently, Bansal and French suggested that the interaction be approximated by a monopole potential

$$H_{ph} = a + b\vec{T}_p \cdot \vec{T}_h + c, \qquad (1)$$

where -a is the center of gravity of all states weighted by the factor $(2J + 1)(2T + 1)$, b is the separation of the T = 1 and T = 0 centers of gravity and c is the Coulomb energy which acts between a proton and a proton hole and is taken to be c = -0.5 MeV. As pointed out by Bansal and French, a given set of parameters should be equally applicable for all configurations with holes in the 1p shell and particles in the sd shell.

Following Zamick we consider a nucleus with m holes in the 1p shell and m + n particles in the 2s-1d shell with isospin T_h and T_p, respectively; the nucleus as a whole has

isospin T. The excitation energy of such a configuration relative to the ground state is given by

$$E_{ph} = E((sd^{m+n})T_p) - E(sd^n) + E((p^{-m})T_h) - E(^{16}O)$$
$$+ m(n+m)a + \frac{1}{2}b\,[T(T+1) - T_p(T_p+1) + T_h(T_h+1)]$$
$$+ \text{Coulomb energy between the particles and holes .}$$

In an analysis of the T = 0 and T = 1 negative-parity states in ^{16}O, Zamick suggested the following two sets of parameters: A (a = -0.34, b = 5.50, c = -0.5) and B(a = -0.49, b = 4.9, c = -0.5).

Let us consider the situation in ^{21}Ne. The ground state consists of four particles in a filled $p_{1/2}$ shell, four particles in a filled $\Omega = \frac{1}{2}$ orbital of the $d_{5/2}$ subshell, and the last neutron in the $\Omega = \frac{3}{2}$ orbital. The ground state spin is $J^\pi = \frac{3+}{2}$ and the isospin is $(T,T_3) = (\frac{1}{2},\frac{1}{2})$. In the neutron-proton formalism we may excite either a proton or neutron from the $p_{1/2}$ shell into the $d_{5/2}$ orbital to form the $J^\pi = \frac{1}{2}-$ level. The former configuration has $T_h = \frac{1}{2}$ and $T_p = 0$ or 1; the latter has $T_h = \frac{1}{2}$ and $T_p = 1$. For the case of $T = \frac{1}{2}$, $T_p = 1$, $T_h = \frac{1}{2}$ we may work out the first six terms of (2) readily:

$$E^{T_p=1} = E(^{22}Ne) - E(^{21}Ne) + E(^{15}O) - E(^{16}O)$$
$$- 6a - b + \text{Coulomb energy.}$$

To evaluate the Coulomb energy we must remember that it only acts between protons and proton holes; the component of such

a configuration in the $T_p = 1$ state is given by the square of the relevant Clebsch-Gordan coefficient:

$$(T_o T_{p3} T_h T_{h3} \Big| TT_3)^2 + (10\tfrac{11}{22}\Big|\tfrac{11}{22})^2 = \tfrac{1}{3}.$$

Since we have three protons and one proton hole, the total Coulomb energy is just +c. Similarly, we may evaluate the energy of the configuration with $T_p = 0$; this is

$$E^{T_p=0} = E(^{22}Na) - E(^{21}Ne) + E(^{15}N) - E(^{16}O)$$

$$-6a+0b+3c.$$

An analogous calculation may be carried out for the 8p1h state in ^{23}Na and for the suggested 8p3h state in ^{21}Ne Middleton et al. (1971). The results of these calculations using the two sets of parameters of Zamick are presented in Table 2.8.

From the table, it can be seen that quite good agreement with the experimental energies is obtained for parameter Set B. In ^{21}Ne, it is the 6p1h, $T_p = 1$ state which is the lowest-lying, and for ^{23}Na, the 8p1h, $T_p = 0$ state.

These results are not entirely in agreement with the arguments of Middleton et al. (1971) who give reasons for considering the $J^\pi = \frac{1}{2}^-$ state in ^{21}Ne as primarily an 8p3h configuration, formed by coupling a neutron to a presumed 8p4h state (Nagatani et al. (1971)) in ^{20}Ne at 7.20 MeV. It is interesting to point out in this context that Zamick

Table 2.8

Energies of the lowest-lying $J^{\pi} = 1/2-$ 6p1h and 8p3h states in ^{21}Ne and 8p1h states in ^{23}Na calculated using the particle-hole interaction described in the text

Nucleus	Configuration	T	T_p	T_h	Expt.	Calculated A	Calculated B
^{21}Ne	6p1h	1/2	0	1/2	2.79	5.93	6.83
		1/2	1	1/2		1.35	2.84
	8p3h	1/2	0	1/2		3.83	7.43
^{23}Na	8p1h	1/2	0	1/2	2.64	2.14	3.34
		1/2	1	1/2		5.42	7.41

in his original calculations concluded that the 7.20-MeV state was a 6p2h state; the 8p4h state in fact can be shown to lie about 2-4 MeV in excitation higher than the 6p2h state. Thus, our conclusion that the 2.8-MeV $J\pi = \frac{1}{2}$ - state in ^{21}Ne is a 6p1h state with the 9p3h state about 2 MeV higher up is quite consistent with the latter interpretation of the nature of the 7.2-MeV level in ^{20}Ne.

In the light of the foregoing considerations, Nilsson model calculations for ^{21}Ne were carried out with the following parameters: the band head energies of the ground state, 1/2+[211], 1/2-[101] and 5/2+[202] orbitals were fixed by the experimental data; the deformation δ was chosen to be 0.30 for all bands except the 1/2+[211] orbital, for which $\delta = 0.1$ was chosen in order to reproduce the decoupling parameter of this band. The same rotation parameter $\hbar^2/2\mathcal{J}$ = 175 keV was chosen for all bands except again the 1/2+[211] orbital, for which it was allowed to vary. A possibly disputable point in the preceding is the apparent ad hoc assumptions for the "anomalous" 1/2+ orbital, and the calculations were accordingly also carried out using the standard parameters chosen for the other bands, to study the effect on the energy spectra and transition rates. Table 2.7 shows the experimental and calculated spectra up to 5 MeV excitation for the two calculations. It is evident that $\delta = 0.1$ is necessary to reproduce the level structure of the anomalous 1/2+[211] band.

Noteworthy (perhaps) is the fact that $\hbar^2/2\mathcal{J} = 300$ keV for this band gives the best fit. This is in agreement with the remarkable result that $I\alpha\beta$ (rather than the classical β^2) suggested by Mariscotti et al. (1966) in their phenomenological "variable moment of inertia" model, although it must be admitted that the evidence presented here (one rather dubious case!), is, to say the least, rather tenuous. It is to be emphasized that until the spins and parities of the 4526 and 4687 keV levels are confirmed and the weak in-band transitions to the 2796 keV level measured and the mixing ratios obtained, allowing estimates of E2 strengths to be made, this rotational band assignment must remain tentative.

c. Electromagnetic transition rates

Nilsson, in his original article, presented explicit formulae for the electromagnetic (EM) transition rates between states describable as belonging to pure configurations. For no Coriolis coupling, these formulae are schematically of the form

$$B(E\lambda)=\text{const}\left|\langle I\lambda K\ K'-K|I'K'\rangle+b_{E\lambda}(-)^{I'+K'}\langle I\lambda K-K'-K|I'-K'\rangle\right|^2 G_{E\lambda}^2$$

for a transition $|IK\rangle \rightarrow |I'K'\rangle$. The quantities $b_{E\lambda}$ and $G_{E\lambda}$ are complicated products of radial integrals, Clebsch-Gordan coefficients and expansion coefficients relating deformed and spherical states. A similar relation holds for $M\lambda$ rates, but the corresponding quantities $b_{M\lambda}$ and $G_{M\lambda}$ now also depend

on the proton and neutron magnetic moments and on the core gyromagnetic ratio. Unless one of the bands has K = 1/2, a simplification is introduced as the $b_{(E/M)\lambda}$ vanish.

For mixed bands, the above equations still hold in a slightly modified manner. If we write

$$|I_i> = \Sigma\ a_j\psi_j$$

$$|I_f> = \Sigma\ b_k\psi_k$$

where ψ denotes a pure Nilsson wavefunction, and let

$$E\lambda^{jk} = G_{E\lambda}\{<I\lambda K\ K'-K|I'K'> + b_{E\lambda}(-)^{I'+K'}<I\lambda K-K-K'|I'K'>\}$$

with a similar expression for $M\lambda$, then the transition probability for mixed bands may be written

$$B(E\lambda, I_i \rightarrow I_f) = \text{const}\left|\sum_{jk}\ a_j b_k E\lambda^{jk}\right|^2$$

and similarly for $B(M\lambda)$. Note the coherent sum; this results in quite dramatic alterations to the transition probability even for rather small admixtures of other bands and may even result in almost complete cancellation of certain matrix elements.

The ground-state band.

A number of lifetime measurements of members of the ground state band in ^{21}Ne have of late been carried out (e.g. Pronko et al. 1969, Rolfs et al. 1971, and Bailey et al. 1971) which unfortunately are not in very good agreement. Table 2.6 presents the results of these measurements. The discrepancy for the 350 keV level is especially severe, and it

is difficult to judge the reasons for the differences as ever fewer publications in the literature give sufficient information for a truly critical analysis of such data. It may be pointed out, however, that recoil-distance measurements (which give $\sim$ 22 psec for the 350 keV level) are usually quite reliable, whereas Doppler-shift measurements for low-energy γ rays and long-lived states are difficult to interpret due to the very small shifts involved. Accordingly, for the purposes of the present discussion, we shall accept the $\tau(350) = 22\pm5$ psec value with the caveat that a remeasurement of this lifetime appears highly desirable.

To extract the required dipole and quadrupole transition strengths from the experimental data, the multipole mixing and branching ratios of the γ transitions are required. These are presented in Table 2.4 and 2.5 and have been obtained from a variety of sources, including the present work, as indicated. In general, the agreement between the various detdeterminations is quite good.

The Coriolis-mixed wavefunctions obtained from the Nilsson-model calculation described previously as given in Table 2.9 for the positive parity bands were used to obtain transition rates between the levels of the ground-state band in ^{21}Ne. The parameters $b_{E\lambda}$ and $G_{E\lambda}^{KK'}$ were not allowed to vary, but were fixed at the values obtained from the expressions given by Nilsson (1955). For magnetic transitions, free-

Table 2.9

Nilsson wavefunctions for positive parity states in ^{21}Ne

E_x experimental (MeV)	E_x calculated	J^π	1/2+[211]	3/2+[211]	5/2+[202]
0.00	0.00	3/2+	+0.1219	-0.9925	-
0.350	0.497	5/2+	-0.1638	0.9497	0.2669
1.747	1.389	7/2+	-0.1600	0.9188	0.3608
2.796	2.796	1/2+	1.000	-	-
2.867	2.590	9/2+	-0.1704	0.8925	0.4175
	3.937	3/2+	-0.9925	-0.1219	-
	5.234	5/2+	0.9754	0.1964	-0.1001
3.735	3.768	5/2+	0.1475	-0.2440	0.9585
4.431	4.167	11/2+	-0.1511	0.8740	0.4618

nucleon g-values were used, but a value of $g_R = 0.3$ was used (Rolfs et al. 1971) for the core gyromagnetic ratio instead of the semiclassical $g_R = Z/A$. Because ^{21}Ne consists of only one kind of particle (neutron) outside a scalar ^{20}Ne core, there are no isospin-dependent modifications to the M1 rates of the kind discussed by Kanestrøm (1971) and Frank (1972) applicable to ^{23}Mg and ^{23}Na, respectively. The results of the transition rate calculation (using the wavefunctions given in Table 2.9) are presented in Table 2.10. The agreement between the experimental and predicted E2 and M1 rates is quite satisfactory and lends strong support to the Nilsson-model interpretation of the positive-parity levels of ^{21}Ne.

The 350 keV transition rate is not in as good agreement with the experiment but it is to be noted that the errors on the mixing ratio of this transition are quite large. Since $|M(E2)|^2 \sim \delta^2/1+\delta^2 \cong \delta^2$ (for small δ) this results in a poor determination of the E2 strength. About all one can say is that the larger values for δ (350) give better agreement. Unfortunately, a more precise measurement for this mixing ratio than the quoted $\delta = 0.05 \pm 0.03$ appears quite difficult, especially since the correct method of assigning meaningful errors to δ appears to be so unclear.

Halbert et al. (1971) also calculated some E2 and M1 rates for the "ground state rotational band" of ^{21}Ne in the framework of the shell model. These results are presented in the final column of Table 2.10. As is evident, the shell

Table 2.10

Experimental and Calculated Transition Strengths in ^{21}Ne

Transition E_i	E_f	Expt a) L=2	Expt a) L=1	Expt b) L=2	Expt b) L=1	Nilsson Model c) L=2	Nilsson Model c) L=1	Shell Model L=2	Shell Model L=1
350[d]	0	$3.0^{+4.14}_{-2.1}$	0.034±0.005			19.0	0.064	21.9	0.10
1747	350	12±6	0.14 ±0.02	40±15	0.45±0.10	14.0	0.11	15.4	0.17
	0	30±14	-	10±4	-	9.0	-	9.1	-
2790[e]	350	-	$<1.1\times10^{-7}$ (E1)	-	-	0.11	6.3×10^{-3}		
	0	0.69±.05 (M2)	-	-	-	3.9	-		
2796	0	-	>0.05	>0.05	-	0.85	2.0		
2867	1747	15±9	0.27±0.07	30±18	0.55±0.10	7.3	0.14	8.3	0.20
	350	14.2±3.6	-	29.5±5.7	-	12.2	-	12.1	-
3663	2790	20^{+22}_{-14}	0.26±0.04	-	-	17.7	0.095		
	350	-	3.09×10^{-4} (E1)	-	-	9.0×10^{-2}	8.7×10^{-3}		
3735	1747	-	>0.01			0.02	0.064		
	350	>0.60	>0.005			0.75	0.041		
	0	>0.60	>0.015			0.18	0.205		
3886	2790	62±30	-	112±65		11.7	-		
	350	-	4.7×10^{-4} (E1)		8.3×10^{-4}	0.31	6.0×10^{-4}		
	0	-	1.5×10^{-4} (E1)		2.6×10^{-4}	0.025	5.8×10^{-5}		

(continued next page)

Table 2.10 (continued)

a) Lifetimes of Rolfs et al unless otherwise specified (see Table 4.8)

b) Lifetimes of Bailey et al. where appreciably different from a)

c) No isospin adjustment to M1 rates

d) τ = 22±5 psec

e) τ = 85±15 psec

model results also agree reasonably well with experiment. Since these shell-model calculations proceed from a more satisfactory basis than those based on the Nilsson model, this is a highly gratifying result. It is, of course, to be hoped that the microscopic shell model should be able to reproduce nuclear properties as well as more phenomenological models, but it is still pleasant to see this result conclusively shown. The agreement between the shell and Nilsson models might also imply that the Nilsson model somehow "picks out" the important parts of the shell-model wavefunctions and focusses attention on "rotation-like" parts thereof. Thus, it might be instructive to compute overlaps between shell-model and Nilsson-model wavefunctions to see what features of these wavefunctions are common to both models.

The $K^{\pi} = 1/2-$ band.

Table 2.10 also presents the E1 transition rates from members of the $K^{\pi} = 1/2-$ band to a number of other states, primarily those belonging to the ground state band. The marked inhibition of these E1 rates is noteworthy, especially for the highly hindered 2.790 → 0 and 3.663 → 0 (not even seen!) transitions. In fact, the value quoted for the 2.79 → 0 E1 rate must be taken as an upper limit, since for a retardation of such magnitude, M2 radiation may well be significant. A number of model-dependent explanations have been proposed to indicate, in a general way, why E1 inhibition is to be expected (e.g. Chapter I of this thesis) but it is

clear that these are insufficient to explain the remarkable variation in transition strengths throughout the band.

A microscopic interpretation of these data is highly to be desired. A comparison between the nuclei ^{21}Ne and ^{23}Na indicates immediately the severity of the dissimilarity between the two supposedly identical rotational bands -- in particular, the lifetime of the band head in ^{23}Na is ≈ 100 fsec, leading to a "normal" E1 inhibition of 10^{-3} -- 10^{-4} W.u., whereas in ^{21}Ne the 80 psec lifetime implies the 10^{-8} W.u. retardation in Table 2.10. The fundamental difference between these bands could be connected with the fact that in ^{21}Ne the hole state may be formed by exciting <u>either</u> a proton <u>or</u> a neutron from the $p_{1/2}$ shell to the $\Omega = 3/2$ orbital of the $d_{5/2}$ shell, whereas in ^{23}Na this orbital is filled, thus "blocking" the neutron excitations. Thus isospin may play a crucial role. It is interesting to note that by constructing states of good isospin in a manner analogous to that done by Pelte (1966) for the positive parity states, we obtain a modified E1 transition operator for the 1/2- decay:

$$E1 \rightarrow \frac{1}{\sqrt{2}} \{\theta^{n}_{E1} + \theta^{p}_{E1}\}$$

where as before, the superscript n and p refer to neutron and proton single-particle operators, respectively. Writing the effective neutron and proton operators proportional to

$-Z/A$ and N/A, respectively, it is clear that the E1 matrix element, as constructed above, almost vanishes as $Z \simeq N \simeq A/2$. In ^{23}Na we cannot construct such a state since, as pointed out, the neutron excitations are not allowed. This simplified picture is not necessarily complete or even entirely accurate in all its details; it is, however, included to demonstrate how isospin dependent effects may bring such cancellations about.

Next, we consider an alternative, phenomenological, model for the E1 decays from the negative parity states. The method was suggested in Chapter I , where the single particle matrix element for the Nilsson model

$$m_{\pm} = \langle \alpha K | j_{\pm} | \alpha' K \mp 1 \rangle$$

instead of being calculated, was allowed to be a free parameter. If we now consider explicitly the E1 amplitude between states of a $K^{\pi} = 1/2-$ band and states of the ground $K^{\pi} = 3/2^{+}$ band with a $K^{\pi} = 1/2+$ admixture (recalling that the $K^{\pi} = 5/2$ admixture to the ground state band cannot affect the E1 rates) we obtain

$$B(E1) \alpha \left| \langle J_1 \tfrac{1}{2} 1 1 | J_2 \tfrac{3}{2} \rangle + \sqrt{3}\, m \{ \langle J_1 \tfrac{1}{2} 1 0 | J_2 \tfrac{1}{2} \rangle + (-)^{J_2 - \frac{1}{2}}\, m' \langle J_1 \tfrac{1}{2} 1 -1 | J_2 -\tfrac{1}{2} \rangle \} \right|^2$$

where the parametrized matrix elements m and m' contain the single-particle matrix elements and replace the usual quantities G_{E1} and b_{E1}. The next step is to estimate m and m' from

experimental data on the low-lying band members and use these values to make further predictions for higher band members. We see that the transitions 1/2- → 3/2+ and 3/2- → 3/2+ are both severely inhibited; therefore we approximate the corresponding E1 strengths by letting them vanish identically. Then

$$\left|\left\langle \frac{11}{22}11 \middle| \frac{33}{22}\right\rangle + \sqrt{3}\, m\left(\left\langle \frac{11}{22}10 \middle| \frac{31}{22}\right\rangle + m'\left\langle \frac{11}{22}1{-1} \middle| \frac{3}{2}\frac{1}{2}\right\rangle\right)\right|^2 = 0$$

and

$$\left|\left\langle \frac{31}{22}11 \middle| \frac{33}{22}\right\rangle + \sqrt{3}\, m\left(\left\langle \frac{31}{22}10 \middle| \frac{31}{22}\right\rangle + m'\left\langle \frac{31}{22}1{-1} \middle| \frac{3}{2}\frac{1}{2}\right\rangle\right)\right|^2 = 0 \ .$$

The solution of these two equations yields

$$m = -\sqrt{2}, \quad m' = -1/\sqrt{2}.$$

We can then work out the E1 branching ratios of the higher spin members of the band and compare with the known experimental information. Unfortunately, states with spin greater than 5/2- are as yet only tentatively identified (Rolfs et al. 1972); further experiments are presently under way in this laboratory to confirm these assignments. Table 2.11 presents the results of the above analysis. It will be observed that the agreement between experiment and the two-parameter model (henceforth called the generalized adiabatic model) is exceedingly good for ^{21}Ne. It has been noted (Frank et al. 1972) that the agreement with the Nilsson model for the ^{23}Na E1 transitions is quite good, if band mixing be included in the treatment. For ^{21}Ne however the Nilsson model gives an exceedingly poor fit to the data (Table 2.11) - in particular, the highly

Table 2.11

El Decays in ^{21}Ne

(Relative reduced El strengths)

J^{π} initial	final	Expt.	Nilsson Model Pure Bands	Mixed	Generalized adiabatic model
1/2-	3/2+	∿ 0	100	100	0*
3/2-	5/2+	100	60	91	100
	3/2+	∿ 0	40	9	0*
5/2-	7/2+	<10	48	92	10
	5/2+	72	45	7	57
	3/2+	28	7	7	33
(7/2-)	9/2+	94	42	86	92
	7/2+	6	48	10	3
	5/2+	< 2	10	4	5
9/2(-)	11/2+	<19	38	79	10
	9/2+	36	48	18	37
	7/2+	64	14	3	53

*) Transition assumed to vanish identically.

inhibited 1/2- - 3/2+ transition is not reproduced at all, as previously noted. Setting this transition equal to 0 in the generalized adiabatic model has the effect, because of the signs and magnitudes of certain Clebsch-Gordan coefficients in the coherent sum, of enhancing $J^- \rightarrow (J+1)^+$ transitions for (2J+1)/2 = even and inhibiting them for (2J+1)/2 = odd; a feature which is experimentally verified. It can be shown that the $J^- \rightarrow (J+1)^+$ enhancements observed by Frank et al. (1972) for ^{23}Na predicted by the Nilsson model are also reproduced by the generalized adiabatic model and can be attributed to a similar effect - the differences arising from a change in sign of a matrix element $m_{\pm}$.

It appears that we are faced with a rather puzzling situation. The discrepancies between E1 rates in ^{23}Na and ^{21}Ne do not end with the $1/2^-$ levels, but continue right up the band, whenever (2J+1)/2 = odd. They remain unexplained by the Nilsson model (though the generalized adiabatic model works quite successfully) and indicate deviations from Nilsson-model wavefunctions. It is likely that the anomalies for transitions with (2J+1)/2 = odd are closely related and that a proper explanation of the 1/2 → 3/2+ inhibition (perhaps, but not necessarily, along the lines of the isospin arguments outlined previously) will lead to an increased understanding of these, and other, interesting features in ^{21}Ne.

CHAPTER III
STUDY OF ^{29}Si

1. Introduction

The nuclei in the mass region 27-29 are of particular interest because of the current evidence (Hirko 1969, Mermaz et al. 1969) that the nuclear deformation is changing from prolate to oblate in this region of the 2s-1d shell. Lighter nuclei, especially those with $20 \leq A \leq 25$ are well described in terms of the strong coupling rotational model (e.g. Ch. II), while only a few mass numbers past A=29 the nuclei are probably spherical and better described by vibrational models. Accordingly, the nuclei with A=29 are especially interesting since it is not clear whether the best description is given by the Nilsson model or the intermediate coupling model applicable to vibrational cores, and if the evidence for deformation (if any) points to prolate or oblate. To solve ^{29}Si "exactly" in the shell model would require the distribution of 13 particles in the sd shell, and such a problem would entail the diagonalization of $10^4 \times 10^4$ matrices - a formidable problem indeed! Recently, however, the results of a "truncated" calculation have been reported (de Voigt et al. 1972).

The experimental information on the low-lying states

of ^{29}Si (up to 4 MeV) at the beginning of this work was reasonably detailed, while little or no information was available on the states above 4 MeV. Bromley et al., as long ago as 1957, concluded from the known information on the states below 3.6 MeV that the Nilsson model, which had recently been successfully applied to ^{25}Mg and ^{25}Al by Litherland et al. (1956), was applicable to ^{29}Si if an oblate deformation was assumed. The states at 0, 2.426 and 2.028 MeV were described as the J^{π} = 1/2+, 3/2+ and 5/2+ members of the 1/2+[211] band while states at 1.273 and 3.069 MeV were suggested to be the J^{π} = 3/2+ and 5/2+ members of the 3/2+[202] band. The strongest single piece of experimental evidence for oblate deformation was the existence of a J^{π} = 7/2(-) state at 3.623 MeV. If this state be assigned to the 7/2-[303] orbit of the Nilsson model, it can only be the lowest negative parity state if δ is negative. The J=7/2 assignment for the 3.62 MeV state has been confirmed from angular correlation studies of ^{28}Si(d,pγ)^{29}Si (Becker et al. 1967) and ^{29}Si(p,p'γ)^{29}Si (Ferguson et al 1967). The negative parity assignment was based on the observation of possibly questionable ℓ=3 stripping patterns in the ^{28}Si(d,p)^{29}Si reaction (Blair and Quisenberry 1961, Betigeri et al 1966) and in the ^{28}Si(t,d)^{29}Si reaction (Barros et al. 1961).

The apparent success of the Nilsson model in explaining the low-lying level scheme did not extend to the electromagnetic transition rates, however. Hirko (1969) has performed a

comprehensive calculation including the effects of Coriolis mixing and has obtained quite satisfactory agreement with the then known information. Unfortunately, he has used a large number of free or quasi-free parameters (up to 12) which in the opinion of this author should not be necessary and detracts from an otherwise excellent work. Nevertheless, the results were most encouraging and prompted us to repeat the calculations using a more realistic and limited choice of parameters.

The objectives of the present work, when it began over two years ago, were as follows. In view of the importance of the negative parity assignment to the 3.62 MeV level, it seemed desirable to confirm it by model-independent techniques such as a γ-ray linear-polarization measurement. Bardin et al. (1970) had observed a state at 5.26 MeV to which they assigned J=9/2 and proposed it as the next member of a rotational band based on the 3.62 MeV level; this claim was investigated and a search later made for higher spin members of this band. Finally, a search was carried out for higher spin members of the low-lying positive parity bands and their decay was studied.

These investigations proved fruitful and their results were published in due course in two articles: Spear et al. (1971) and Pilt et al. (1971). At about the same time, an article appeared by a group at Liverpool University (Main et

al.1970) who measured a number of level spins in ^{29}Si from a study of the $^{29}Si(p,p'\gamma)^{29}Si$ and $^{26}Mg(\alpha,n\gamma)^{29}Si$ reactions and reached conclusions similar to ours. Two further articles, one on spins and lifetimes (Bardin et al. 1971) and one on lifetimes and branching ratios (Bailey et al. 1972) have appeared since. Aside from the work of Hirko (1969), no detailed Nilsson model calculations on ^{29}Si have recently appeared.

The remainder of this chapter incorporates the two articles written by us, mentioned above, with some new experimental and theoretical results obtained since their publication.

2. Experiment

The $^{26}Mg(\alpha,n\gamma)^{29}Si$ reaction was used to produce ^{29}Si nuclei in their excited states. Because the Q value of the $^{26}Mg(\alpha,n)^{29}Si$ reaction is only 36 keV, a suitable choice of incident α-particle energy leads to near-threshold population of the states of ^{29}Si of interest. With an incident channel spin of 0 and low orbital angular momentum of the emitted neutrons, only the lowest magnetic substates of these levels will be populated.

The ^{26}Mg targets were prepared by vacuum evaporation of MgO enriched to $\geq$ 99% in ^{26}Mg onto a tantalum backing 0.010 in. thick. Lanthanum metal was added to the MgO in stoichiometric proportions as a reducing agent during the evaporation.

Several successive evaporations onto the same substrate were required to obtain targets of the desired thickness (about 200 $\mu g/cm^2$).

Angular distribution spectra were accumulated for approximately 1h periods. A total of three spectra were measured at each of the angles 0, 20.7, 30, 37.8, 45, 52.2, 60, 69.3 and 90 degrees corresponding to equal intervals of $\cos^2\theta$. Polarimeter spectra, because of the reduced efficiency of the small crystal, were collected for approximately 3 h periods at each orientation (parallel and perpendicular), the crystal being rotated once for each measurement of three angles with the movable detector. A total of three spectra at each orientation were taken. All spectra were written on magnetic tape for analysis following each run.

The alignment of the correlation table was determined at the end of the experiment using the strong 1.273 MeV γ ray in ^{29}Si resulting from the decay of 6.5 min ^{29}Al produced by the $^{26}Mg(\alpha,p)^{29}Al$ reaction. The target was irradiated for approximately 10 min periods after which the beam was turned off and spectra collected during the following 10 min at several angles. The resulting angular distribution normalized to the fixed monitor counter was isotropic to within 2%.

Because there is no well-known spin 1/2 state (other than the ground state) in ^{29}Si, normalization cannot be done internally. The consequent necessity of using a monitor detector leaves open the possibility of certain systematic

errors due to such effects as misalignments in the geometry and wandering of the beam spot on the target. Errors due to these are difficult to estimate but the consistency of both the angular distribution and polarization data after other corrections had been made indicates that they were very small. Consequently, γ-ray yields were normalized to the strong 2028 keV gamma ray resulting from the decay of the second excited state in ^{29}Si as detected in the monitor counter. This state is rather weakly fed ($\sim$ 4%) in the β decay of ^{29}Al which is produced in the very weakly competing ^{26}Mg(α,p)^{29}Al reaction and hence the presence of resulting 2028 keV γ-rays is not expected to confound the results appreciably. The normalized γ-ray angular distribution data were corrected for attenuation in the target backing and for the finite solid angle effects. A correction to the polarization asymmetry resulting from the γ-ray angular distribution was also made.

3. Results

The present study concentrated on the states at 3.623, 4.081, 4.742, 5.255 and 5.283 MeV, whose spins and parities were determined. Multipole mixing ratios of the γ rays de-exciting these and some other states in ^{29}Si were also determined; in some cases, the angular distribution and polarization data were able to distinguish between alternative hypotheses made on the basis of previous measurements. Branching ratios

were also measured at $\theta=55°$, (where $P_2(\cos\theta)=0$ and compared with previous work. Tables 3.1-3.3 and Fig. 3.1 summarize the results obtained. Table 3.1 lists the Legendre polynomial coefficients of the angular distributions and the polarizations of various γ rays measured; table 3.2, the spins and mixing ratios deduced from the data in table 3.1 and comparison with other measurements; and table 3.3 γ branching ratios of the states in ^{29}Si. For completeness, table 3.4 presents the results of two recent measurements of lifetimes in ^{29}Si.

a. Negative parity levels

The lowest-lying negative parity state in ^{29}Si is believed to be the J=7/2 level at 3.623 MeV. In an attempt to confirm this assignment, the 1595 keV transition from the 3.623 MeV state to the J=5/2+ 2.028 MeV state was studied at bombarding energies E_α = 5.54 and 6.30 MeV in the ^{26}Mg$(\alpha,n\gamma)^{29}$Si reaction. The angular distributions obtained at each energy were quite similar (Table 3.1) and corresponded to a quadrupole/dipole mixing ratio of δ = 0.03±0.03 for J=7/2, in good agreement with previous measurements (Becker et al. 1967, Ferguson et al. 1967) indicating a pure dipole transition. The polarization of this γ ray (using the sensitivity curve presented in Ch. II and the data from Table 3.1) was measured to be P = (0.42±0.08). Since the predicted polarization for a pure dipole transition at $\theta=90°$ is, from Ch. I,

$$P_t = \pm \frac{3\,a_2}{2 - a_2} = \pm(0.48\pm0.03) \begin{matrix} + \text{ for E1} \\ - \text{ for M1} \end{matrix}$$

Table 3.1

Bombarding energy (MeV)	Initial State (keV)	Final State (keV)	Transition Energy (MeV)	Legendre Coefficients a_2	Legendre Coefficients a_4	Polarization P
5.54	2028	1273	0.765	0.31±0.04	-0.08±0.05	-0.25±0.13
	2426	0	2.426	-0.57±0.02	-0.02±0.04	+0.12±0.19
	2426	1273	1.153	-0.23±0.05	-0.09±0.06	0.12±0.19
	3623	2028	1.595	-0.38±0.01	0.02±0.02	0.42±0.08
	4081	1273	2.808	0.37±0.02	-0.13±0.03	0.60±0.25
	4081	2028	2.053	-0.17±0.04	-0.10±0.04	0.09±0.17
6.30	4742	2028	2.714	0.44±0.02	-0.18±0.03	0.40±0.27
	5283	1273	4.010	-0.66±0.03	0.02±0.03	0.20±0.25
	5255	3623	1.632	0.46±0.02	0.09±0.02	-0.73±0.19

Table 3.2

Mixing ratios of γ-transitions in ^{29}Si

$E_x^{(i)}$ (keV)	$E_x^{(f)}$ (keV)	$J_x^{(i)}$	$J_x^{(f)}$	δ(E2/Ml) a)	b)	c)	d)
1273	0	3/2+	1/2+	-	-0.20±0.02	-0.23±0.03	
2028	0	5/2+	1/2+	∞	∞	∞	
	1273	5/2+	3/2+	0<δ<0.6	-	-	0.09±0.18 e) 3.5 ±2.5
2426	0	3/2+	1/2+	0.65±0.15	0.26±0.08	{0.38±0.06 0.18±0.10	
	1273	3/2+	3/2+	-0.15±0.15		{-0.07±0.10 -2.8 ±1.0	
3069	1273	5/2+	3/2+	-	-0.27±0.02	-0.21±0.05	
	2028	5/2+	5/2+	-	-0.04±0.02	-	
4081	1273	7/2+	3/2+	∞	∞	∞	
	2028	7/2+	5/2+	-0.10±0.02	-0.14±0.04	-	
4742	2028	9/2+	5/2+	∞	∞	∞	
	4081	9/2+	7/2+	-	-	-	
5284	1273	7/2+	3/2+	∞	∞	∞	
	2028	7/2+	5/2+	0.21±0.10	$0.09 \leq \delta \leq 0.58$	-	

a) Present work
b) Bardin et al. (1971)
c) Main et al. (1970)
d) Other measurements
e) Becker et al. (1967)

Table 3.3

Branching ratios of γ-transitions in ^{29}Si

$E_x^{(i)}$ (keV)	$E_x^{(f)}$ (keV)	B.R. a)	b)	c)
2028	1273	7±1	5	4
	0	93±1	95	96
2426	1273	13±1	12	13
	0	87±1	88	87
3069	2426	<2		
	2028	34±3	22	22
	1273	66±3	78	78
3623	3069	10±1	9	11
	2028	88±2	90	86
	1273	2±0.5	1	3
4081	2028	50±8	60	40
	1273	50±8	60	60
4742	4081	8±2	6	-
	2028	91±2	94	100
4838	1273	24±10	10	-
	0	76±10	90	100
4896	2028	36±4	24	-
	1273	50±4	56	82
	0	14±2	20	18

(continued next page)

Table 3.3 (continued)

$E_x^{(i)}$ (keV)	$E_x^{(f)}$ (kev)	B.R. a)	B.R. b)	B.R. c)
4933	1273	11±5	5	4
	0	89±5	95	96
5255	3623	100	100	100
5283	3067		9	-
	2426		13	-
	2028		67	96
	1273		11	4

a) Present work

b) Bardin et al. (1971)

c) Main et al. (1970)

Table 3.4

Lifetimes in ^{29}Si

E_x	T_m (fsec) a)	b)
1273	360±70	470±35
2028	360±70	490±40
2426	13±3	29±11
3069	20±7	20^{+25}_{-10}
3623	4000±1000	4200±500
4081	48±8	40±8
4742	45±10	33±10
4838	<5	<10
4896	10±3	<10
4933	<10	<10
5255	100±20	80±10
5283	<10	<10

a) Bardin et al. (1971)

b) Bailey et al. (1972)

Fig. 3.1

Energy levels and decay of ^{29}Si for $E_x \leq 5.3$ MeV. The excitation energies and branching ratios were obtained in the present work. Errors on energies are believed to be $\leq$ 2 keV; those on branching ratios are given in Table 3.3. The spin assignments are discussed in the text.

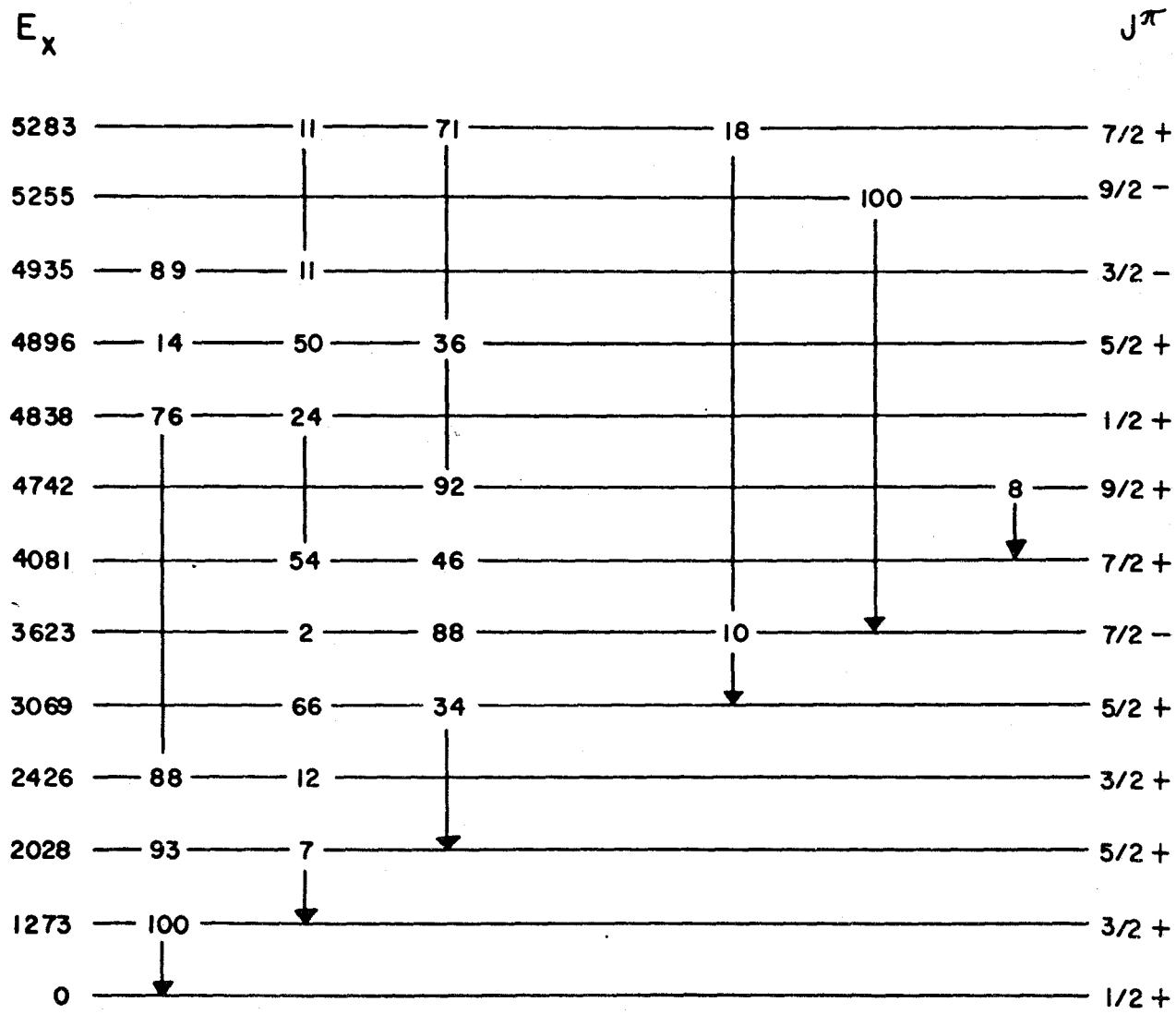
E_x
J^π
5283
5255
4935
4896
4838
4742
4081
3623
3069
2426
2028
1273
0
11
71
18
100
89
11
14
50
36
76
24
92
8
54
46
2
88
10
66
34
88
12
93
7
100
7/2 +
9/2 −
3/2 −
5/2 +
1/2 +
9/2 +
7/2 +
7/2 −
5/2 +
3/2 +
5/2 +
3/2 +
1/2 +

29
Si

we see that negative parity is unambiguously established for the 3.623 MeV level,confirming the assignments based on direct reaction studies.

Recently Bardin et al. (1970) have reported that the 5.255 MeV state has $J^{\pi} = 9/2-$. They have proposed that it may belong to a $K^{\pi} = 7/2-$ band based on the 3.623 MeV 7/2 state; their measurements of the lifetime of the 5.255 MeV state and of the multipole mixing ratio for the 1.632 MeV transition to the 3.623 MeV state indicate that the E2 component of the transition has an enhancement of 27±7 Weisskopf units (W.u.). The sign of the mixing ratio is consistent with an oblate shape for the nucleus.

Bardin et al. deduced their J = 9/2 assignment from measurements of the angular distribution of the 1.632 MeV gamma ray from the reaction $^{26}Mg(\alpha,n\gamma)^{29}Si$ at $E_{\alpha} = 6.4$ MeV. Since this energy is only 300 keV above threshold it was assumed that the neutrons emitted were predominantly s wave and hence that the ^{29}Si nuclei were strongly aligned. Assuming population parameters $P(\pm 1/2) = 0.9$ and $P(\pm 3/2) = 0.1$, they obtained a good fit for J = 9/2, and all other possibilities were rejected at the 0.1% confidence limit; an analysis assuming $P(\pm 1/2) = 0.67$ and $P(\pm 3/2) = 0.33$ made no significant change to these results. A negative parity assignment was inferred because positive parity would require an M2 transition of 838±232 W.u. A close examination of the data of Bardin et al.

indicates that the exclusion of J=5/2 at the 0.1% confidence level is marginal, particularly if P(±1/2) is allowed to vary and become greater than 0.9.

Angular distribution data for the 1.632 MeV gamma ray obtained at E_α = 6.3 MeV in the present work are shown in Fig. 3.2. The Legendre polynomial coefficients are a_2 = 0.46±0.02, a_4 = 0.09±0.02, in reasonable agreement with the results of Bardin et al. The measured polarization is -(0.75±0.22).

The data were analyzed using a modified version of a program described by Twin et al. (1970). The results of a χ^2 analysis of the angular distribution are shown in Fig. 3.2. The population parameters were restricted so that P(±3/2) <0.25 and P(±5/2)<0.10; these limits are more than twice the values obtained from simple penetrability calculations. Fits within the 0.1% confidence limit were obtained only for J(5.255) = 5/2 or 9/2; with mixing ratios $\delta = 1.19^{+0.21}_{-0.57}$ and δ = (0.49±0.05) respectively. The best fits for J = 3/2, 5/2, 7/2, 9/2 and 11/2 are shown in Fig. 3.2. The value of the mixing ratio obtained for J = 9/2 is in excellent agreement with the value (δ =-0.49±0.07) reported by Bardin et al. (1970).

In Fig. 3.2 the experimentally determined and predicting polarizations are compared; for each value of δ the polarizations was calculated using the population parameters which gave the best fit to the angular distribution for that

Fig. 3.2

(top) Angular distribution of the 1632 keV transition between the 5.26 MeV and 3.62 MeV levels in ^{29}Si. Best fits for various possible spin assignments for the 5.26 MeV level are shown.

(bottom) (a) Plots of χ^2 vs. δ for the angular distribution of the 1632 keV transition for various spin assignments to the 5.26 MeV level.

(b) Comparison of experimental and predicted polarizations of the 1632 keV γ ray. The shaded portion represents the experimental value with errors. The polarization was calculated for each value of δ using the population parameters giving the best fit to the angular distribution at that δ-value.

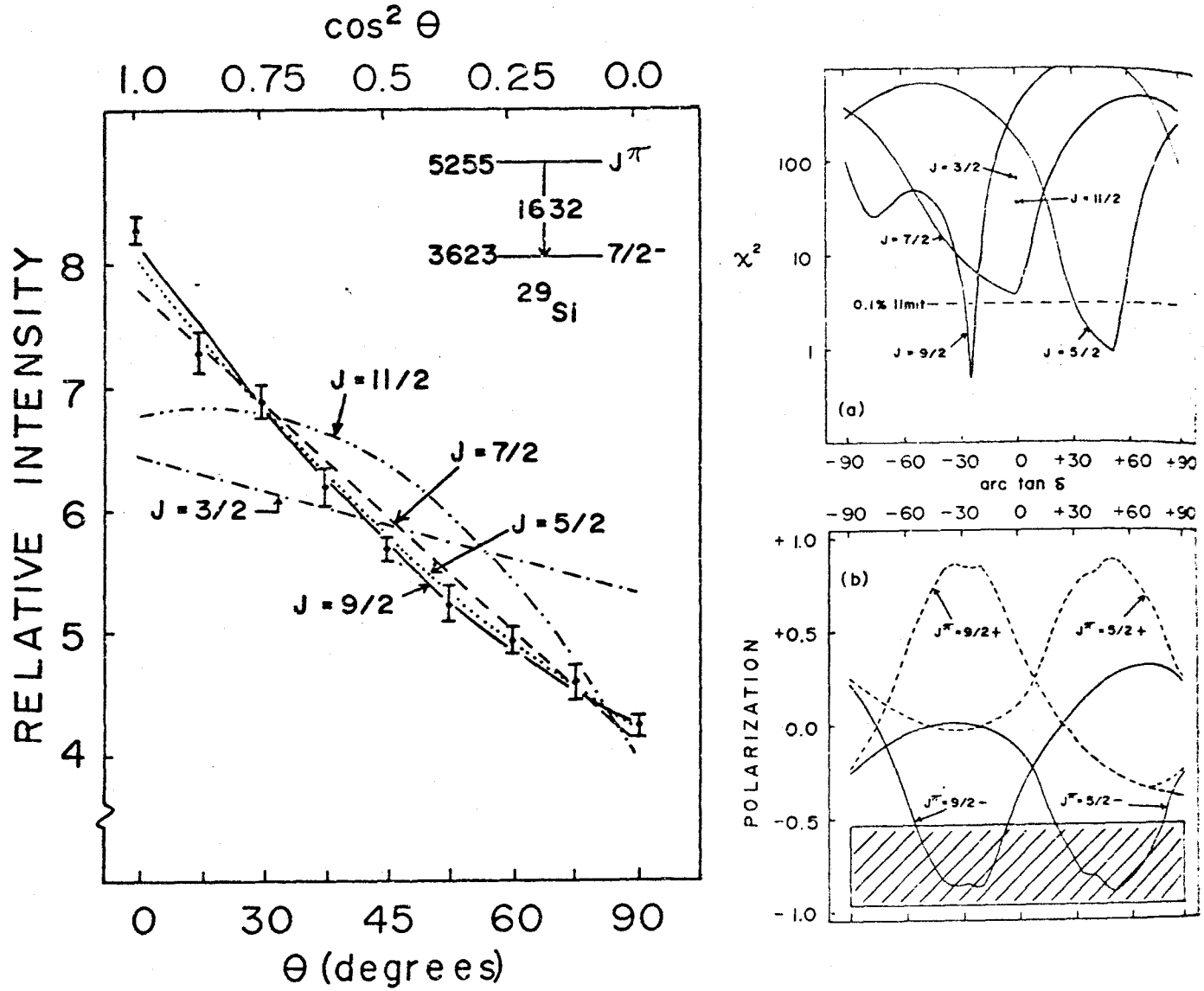
cos² θ
1.0 0.75 0.5 0.25 0.0
5255 — Jπ
1632
3623 — 7/2-
29Si
RELATIVE INTENSITY
8
7
6
5
4
J = 11/2
J = 7/2
J = 3/2
J = 5/2
J = 9/2
0 30 45 60 90
θ (degrees)
χ²
100
10
1
J = 3/2
J = 11/2
J = 7/2
0.1% limit
J = 9/2
J = 5/2
(a)
-90 -60 -30 0 +30 +60 +90
arc tan δ
-90 -60 -30 0 +30 +60 +90
+1.0
+0.5
0.0
-0.5
-1.0
POLARIZATION
(b)
Jπ = 9/2+
Jπ = 5/2+
Jπ = 9/2-
Jπ = 5/2-

value of δ. Examination of Fig. 5.2 shows that only J^{π} = 5/2- or 9/2- are allowed by the data.

A further check on the parity assignments was made by analyzing the angular distribution and polarization data simultaneously, but allowing the population parameters P(±1/2), P(±3/2), P(±5/2), and P(±7/2) to vary without restriction. No significant differences in the conclusions resulted; a fit below the 0.1% limit could be obtained for J^{π} = 5/2+, but the mixing ratio required would correspond to an M2 strength greater than 4000 W.u.

Thus, for the 3.623 MeV state, J^{π} = 7/2-. For the 5.255 MeV state, the present experiment indicates that J^{π} = 5/2- or 9/2-; it does not permit an unambiguous J^{π} = 9/2- assignment.

Nevertheless, assuming J^{π} = 9/2- (as appears likely from other considerations, as shown in a subsequent section) and that the 3.623 MeV level forms the head of a K^{π} = 7/2- rotational band, it is natural to search for the next member of such a band. Extrapolating the known energies of the J=7/2 and (9/2) levels using the rotational formula, we find E_x(J=11/2) = 7.3 MeV. The expectations are that it should decay to the 7/2- and 9/2- levels via $\sim$ 3.6 and 2.0 MeV γ rays, respectively. Accordingly, γ spectra of the $^{26}Mg(\alpha,n\gamma)^{29}Si$ reaction were taken at bombarding energies

from 7.0 to 9.5 MeV and studied for the presence of 2 γ rays at the expected energies but separated by exactly 1.632 MeV (the 9/2-7/2 separation). Although a large number of new γ rays was observed as the bombarding energy was increased, no sign of the expected γ rays was detected. This can be attributable to a) the 11/2- level is very weakly populated, if it at all exists, or b) only one of the branches is appreciable. The K-selection rule should greatly inhibit possible E1 transitions to positive-parity levels.

A γ-γ coincidence measurement was then carried out in a further search for the 11/2- level. It will be noted from the level scheme (Fig.3.1) that the 9/2- level decays $\sim$ 100% to the 7/2- level via a 1.632 MeV γ ray; the latter state in turn decays primarily (91%) to the 5/2+ level via a 1595 keV γ ray. Thus if a coincidence "window" is put on the 1595+1632 keV doublet, one should observe, besides the expected γ rays de-exciting the 7/2- and 5/2+ levels, γ rays feeding either the 9/2- or 7/2- levels, or both. The necessity of using a high bombarding energy ($\sim$ 10 MeV) precluded the possibility of using Ge(Li)-NaI coincidences as had been done in the $^{18}O(\alpha,n\gamma)^{21}Ne$ reaction since the γ ray spectra were quite complicated, with many peaks, and proper identification of the γ rays was of the essence. Thus, the measurement was carried out using Ge(Li)-Ge(Li) coincidences, despite the much lower efficiency of the Ge(Li)

detectors. Fig. 3.3 shows part of a γ ray spectrum in coincidence with the 1595+1632 keV doublet. Since these two γ rays are in coincidence with one another, they both appear in the gated spectrum. As well, there is a new line at 1524 keV which has heretofore remained unobserved, and which is assigned to the decay of a level at 6.78 MeV to the J=9/2 state at 5.255 MeV. It should be pointed out that the 2028 keV line (not shown in the spectrum), which is rather strong, has its first escape peak at 1517 keV, and it is reasonable to ask whether this might not be the explanation of the new line. A comparison of the intensities of 1595'/1595 and 1524/2028 indicated,however, that the 1524 keV line was too strong by a factor $\simeq$ 3 to be the 2028' line. Accordingly we conclude that the 1524 keV line is no more than $\simeq$ 25% in intensity attributable to 2028'. We should also point out that it is not possible to establish definitely whether we are seeing a (6.78-5.25) or a ("5.15"-3.62) MeV decay. However, the second possibility is most unlikely as there has been no previous experimental evidence for a level at 5.15 MeV while the existence of the 6.78 MeV level is well documented (Endt and van der Leun 1967). Very recently (Bailey et al. 1972) have also reported the decay of the 6.78 MeV level to the 5.255 and 3.623 MeV states; however, they did not measure coincidence spectra and because of the complex γ ray spectra in singles experiments, their assignment must remain tentative. The second

Fig. 3.3

Partial Ge(Li)-Ge(Li) coincidence spectrum obtained from a gate on the 1595-1632 keV doublet. The 1524 keV line is discussed in the text.

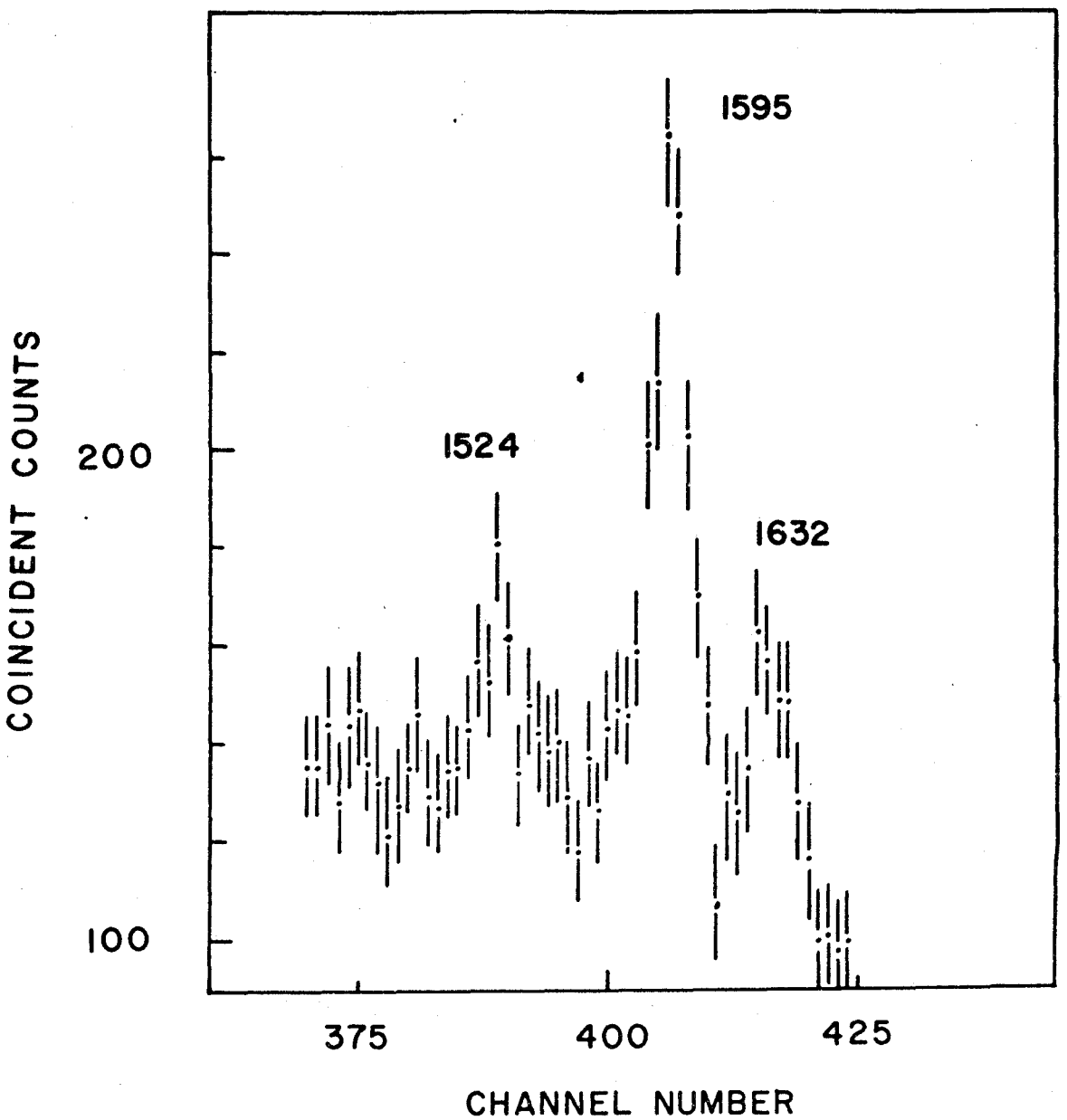
1595
1524
1632
200
100
COINCIDENT COUNTS
375
400
425
CHANNEL NUMBER

γ branch from the 6.78 MeV level, i.e. a 3157 keV γ ray to the 3.62 MeV level, was not observed in our coincidence spectrum. However, the efficiency of the Ge(Li) detectors is much lower at this energy and an upper limit of 40% of the total feed from the 6.78 MeV level was assigned to this decay. This is in reasonable agreement with the value quoted by Bailey et al. (1972) of 60% to this cascade.

b. Positive-parity levels

As mentioned earlier, spin and parity assignments to the five lowest excited states of ^{29}Si (up to the 3.069 MeV level) had been given in earlier work. Some of the multipole mixing ratios of the γ rays had also been obtained; however, a few remained undetermined, and these were delimited in the present work.

If the Nilsson-model description of states in ^{29}Si is valid, J^{π} = 7/2+ and 9/2+ states should exist at $E_x \simeq 6$ MeV which belong to the K^{π} = 1/2+ and 3/2+ bands. Levels which are given this interpretation are also described in this section.

The 2.028 MeV level

This state is assigned J^{π} = 5/2+ on the basis of a number of angular correlation measurements and is the J^{π} = 5/2 member of the decoupled K^{π} = 1/2+ ground state band, (e.g. Becker et al. 1967). Its decay proceeds 93% to the ground state via an E2 transition and 7% via a weak 755 keV γ ray

to the J^{π} = 3/2+ 1.273 MeV level. The mixing ratio of this weak γ ray was limited by Becker et al. (1967) to $\delta = -0.009 \pm 0.18$ or $\delta = 3.49^{+2.48}_{-1.24}$. Despite its weakness in the $^{26}Mg(\alpha,n\gamma)$ spectra, this line proved tractable to an angular distribution and polarization analysis; the results are given in Table 3.1. In the analysis, J^{π} = 5/2+ was assumed for the initial state and all population parameters were allowed to vary since the 2.028 MeV level is fed both directly and through cascade γ rays from higher levels. In this way, the mixing ratio of the 755 keV γ ray was limited to $0 \leq \delta \leq 0.5$. Combining with Becker's work, we obtain $0 \leq \delta \leq 0.09$.

The 2.426 MeV level

This state is known (Becker et al. 1967) to have J^{π} = 3/2+ and is also assigned to the ground state rotational band. The decay is (86.5±0.5)% to the ground state and (13.5±0.5)% to the first excited state (1.273 MeV). Angular correlation experiments have been relatively unsuccessful in determining the mixing ratio of the γ rays since for an initial spin of 3/2+, one can fit the angular correlation data for almost any value of δ. Main et al. (1970) have used both the $^{29}Si(p,p'\gamma)$ and $^{29}Si(\alpha,\alpha'\gamma)$ reactions to assign δ=0.38±0.10 or $\delta = 0.81 \pm 0.10$ to the 2426 keV γ ray and $\delta = -0.07 \pm 0.10$ or $\delta = -2.8 \pm 1.0$ to the 1153 keV γ ray. In the present experiment, the γ ray angular distributions were equally inconclusive but the addition of the rather strong polarization

data was sufficient to give reasonably unique values for the mixing ratios: $\delta = 0.65 \pm 0.20$ for the 2426 keV γ ray and $\delta = -0.10 \pm 0.10$ for the 1153 keV γ ray. These values are in very good agreement with one of the alternate solutions given by Main et al. for each γ ray.

The 3.069 MeV level

Several angular correlation experiments (most recently, Main et al. 1970) fix the spin at $J^{\pi} = 5/2+$, and positive parity is indicated from the decay and the 20±9 fsec lifetime (Bardin et al. 1971, Bailey et al. 1972) of this state. The 18±5 W.u. decay to the $(J^{\pi},K^{\pi}) = (3/2+,3/2+)$ state at 1.273 MeV is strongly suggestive that this state may be the $J^{\pi} = 5/2+$ member of this band, as originally proposed by Bromley et al. (1957). Other information concerning this state is given in Tables 3.2 and 3.3.

The 4.081 keV level

The only spin assignment to this state existing in the literature appears to be that of Ferguson et al. (1967) who assign $J = 7/2$ from the results of a $^{29}Si(pp'\gamma\gamma)$ angular correlation measurement.

Becker et al. (1967) measured the particle-gamma angular correlation from $^{28}Si(d,p\gamma)^{29}Si$ reaction but were unable to reach any conclusion other than $J \geq 3/2$. A recent measurement of the $^{29}Si(p,p'\gamma)$ angular correlation (Main et al.

1970) is in agreement with the 7/2 spin assignment. No direct measurement of the parity of this state has been made; however, a measurement of the lifetime of the state by Wozniak et al. (1969) suggests positive parity.

An α-particle bombarding energy of 5.54 MeV was used to populate this state in the $^{26}Mg(\alpha,n)^{29}Si$ reaction, corresponding to approximately 800 keV above threshold. The γ-ray angular distribution of the 2808 keV γ ray yielded the values $a_2 = 0.37 \pm 0.02$ and $a_4 = 0.13 \pm 0.03$. The nonzero value of a_4 immediately eliminates J = 3/2 from consideration for the spin of the state. J = 9/2 can be eliminated because of the decay to the J = 3/2 level, thus limiting the spin to 5/2 or 7/2. Best fits of the angular distribution with these two spin hypotheses yielded for J = 7/2 and pure E2 multipolarity a value $\chi^2 = 1.3$ and for J = 5/2 a value $\chi^2 = 6.1$ at $\delta = 1.0$. The latter χ^2 is considerably higher than the 0.1% confidence limit, thus confirming the spin assignment of 7/2. Figure 3.4 shows the angular distribution and the best fits for spins 7/2 and 5/2.

Since the 2808 keV γ ray is assumed to be pure quadrupole, the formula for polarization takes on a particularly simple form, namely

$$P = \pm \frac{3a_2 + 5/4a_4}{2 - a_2 + 3/4a_4}$$

\+ for no parity change

\- for parity change

Fig. 3.4

top: Angular distribution of 2808 keV transition and the best fits, assuming J = 5/2 and 7/2 assignments to the 4.08 MeV level. The fit for J = 7/2 assumes pure quadrupole radiation.

bottom: χ^2 vs arc tan δ plot for the 2053 keV transition from the 4.08 MeV level, assuming J = 7/2 for the initial state (see above figure and text) and using the substate populations derived from that transition. A close inspection of the χ^2 curve shows that the minimum falls at $\delta = -0.10$.

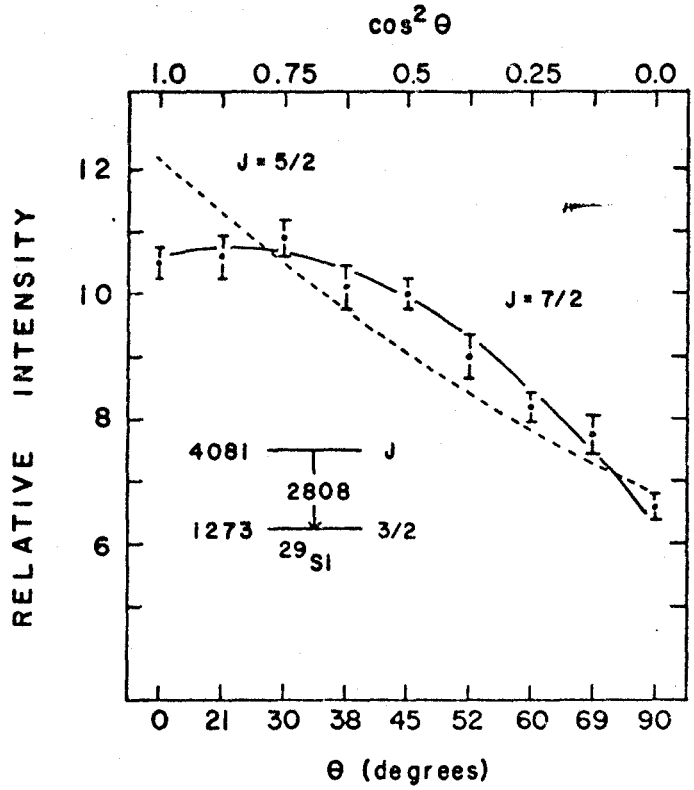
cos² θ
1.0
0.75
0.5
0.25
0.0
RELATIVE INTENSITY
12
10
8
6
J = 5/2
J = 7/2
4081
J
2808
1273
3/2
29Si
0
21
30
38
45
52
60
69
90
θ (degrees)

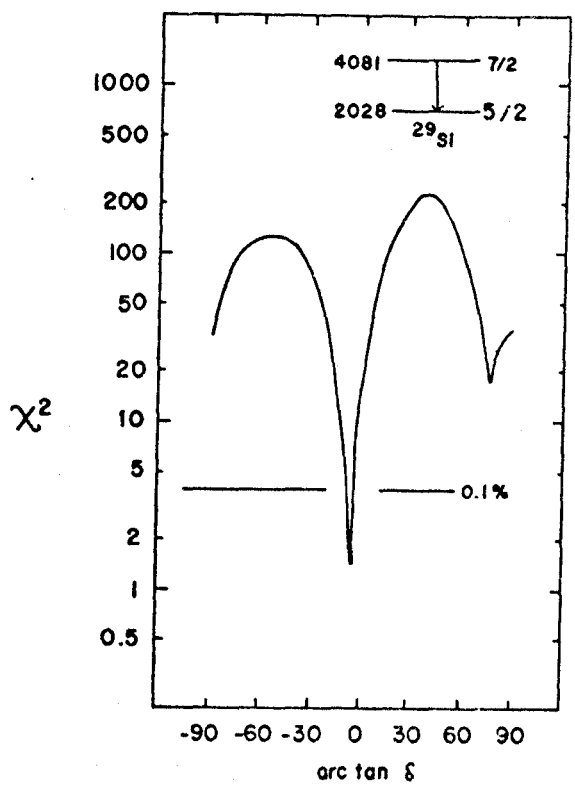
4081
7/2
2028
5/2
29Si
1000
500
200
100
50
20
10
5
2
1
0.5
χ²
0.1%
-90
-60
-30
0
30
60
90
arc tan δ

(cf. Ch.I). Substitution for the above values of a_2 and a_4 yields polarization values of $\pm(0.72\pm0.06)$, negative for a parity change and positive for no parity change. Experimentally, the measured polarization (assuming a sensitivity R of 0.065 ± 0.015) was 0.60 ± 0.25. Thus the parity change in the transition and the parity of the 4081 keV level is established as positive, confirming the suggestion of Wozniak et al. (1969).

With the spin and parity of the 4081 keV level thus determined, the angular distribution and polarization of the second γ branch from this state, namely the 2053 keV γ ray to the $J^{\pi} = 5/2+$ 2028 keV level was analyzed to determine the multipole mixing ratio of the transition. The same population parameters for the 4.08 MeV level were used which gave the best fit to the 2808 keV γ-decay. The resulting χ^2 plot is shown in Fig. 3.4 (lower), and a value $\delta = -(0.10^{+0.02}_{-0.03})$ is obtained using the 1% confidence limit of χ^2 (the errors on δ then correspond to $\sim$2 standard deviations). This value is in good agreement with $\delta = -(0.05\pm0.02)$ reported by Ferguson et al. (1967).

The 4742 keV level

This level was observed to decay only to the spin 5/2 state at 2028 keV. The corresponding 2714 keV γ ray was highly anisotropic ($a_2 = 0.44\pm0.02$, $a_4 = -0.18\pm0.03$). The χ^2 analysis of the angular distribution data alone yielded

fits below the 0.1% confidence limit only for J = 9/2 and quadrupole radiation, and for J = 5/2, with $\delta = -(1.4\pm0.30)$. For spin 7/2, the minimum of χ^2 was 19.8 and thus could be readily excluded (Fig. 3.5).

The measured polarization of the 2714 keV γ ray was $+0.40 \pm 0.27$. For a pure quadrupole transition the above values of the a_2 and a_4 coefficients imply $P = \pm(0.77\pm0.05)$, positive for E2 radiation and negative for M2. The measured value of the polarization is in satisfactory agreement with the predicted value and requires positive parity for the 4742 keV level, if we assume J(4742) = 9/2. For the spin 5/2 possibility, we may calculate the expected polarization P_t from the formulae in Chapter I:

$$P_t\ (90°) = \pm \frac{3(a_2+b_2) + 5/4a_4}{2 - a_2 + 3/4a_4} \quad \begin{matrix} + \text{ electric} \\ - \text{ magnetic} \end{matrix}$$

where b_2 is the combination of a_2, a_4, δ and Wigner-coefficients defined in Ch. I. Using this relation, we find

$$P_{J=5/2}(90°) = \pm(0.84\pm0.08)$$

positive for a parity change and negative for no parity change. Neither of the above values is in very good agreement with the experimental value of $P = 0.40\pm0.27$; however, if the spin 5/2 assignment is correct, its parity must be negative and the transition to the 2028 keV state must be M2/E1. The mixing ratio solution of $\delta = -(1.4\pm0.3)$, however, renders this highly unlikely as in conjunction with the lifetime mea-

Fig. 3.5

top: χ^2 vs. arc tan δ for the 2714 keV γ ray from the 4.74 MeV to 2.03 (J = 5/2) MeV level.

bottom: Angular distribution and χ^2 vs arc tan δ plots for the 3255 keV γ ray deexciting the 5.28 MeV level in ^{29}Si.

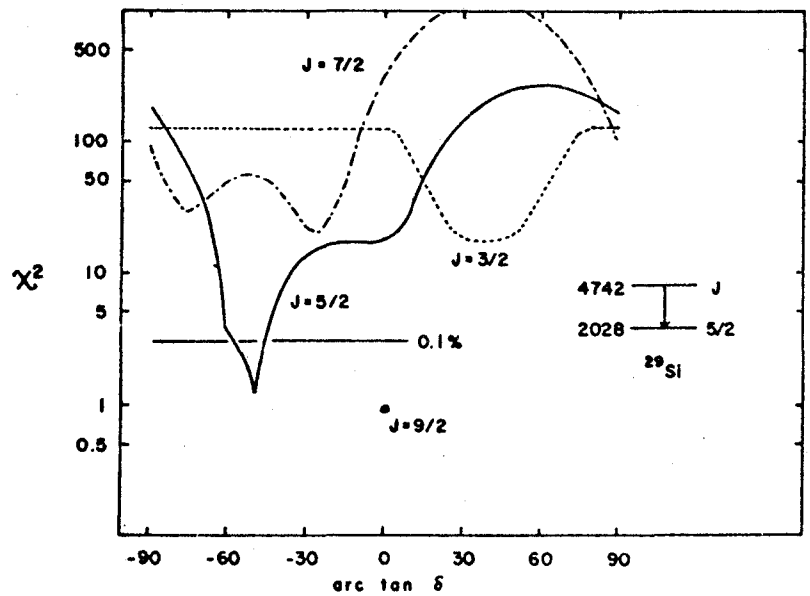
500
100
50
10
5
1
0.5
χ^2
J = 7/2
J = 3/2
J = 5/2
0.1%
J = 9/2
4742
J
2028
5/2
^{29}Si
-90
-60
-30
0
30
60
90
arc tan δ

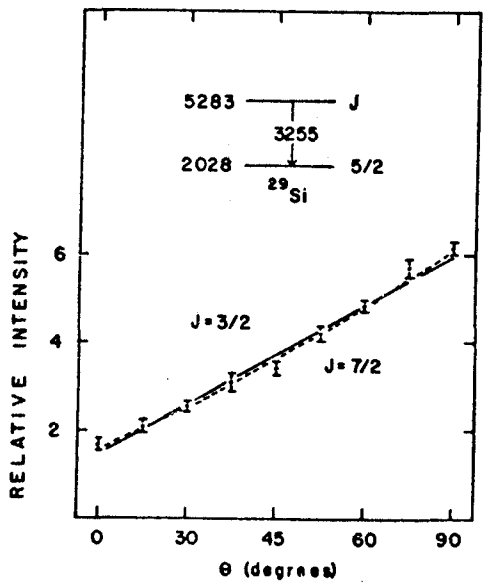
5283
J
3255
2028
5/2
^{29}Si
J = 3/2
J = 7/2
RELATIVE INTENSITY
6
4
2
0
30
45
60
90
θ (degrees)

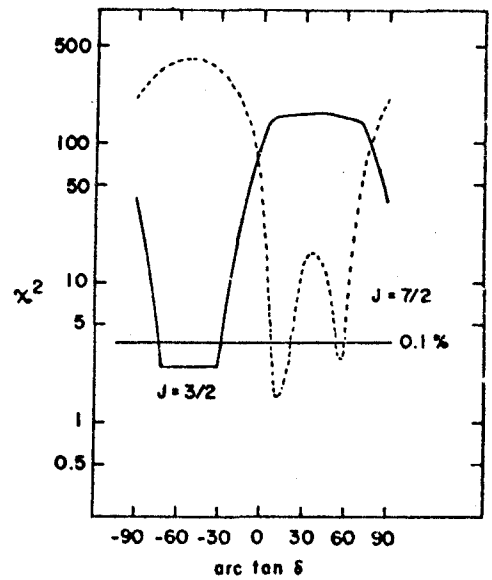
500
100
50
10
5
1
0.5
χ^2
J = 7/2
0.1 %
J = 3/2
-90 -60 -30 0 30 60 90
arc tan δ

surements of Fisher et al. (1970) of $(0.45\pm0.15)\times10^{-13}$ s for the 4742 keV level, an M2 strength of 40±15 Weisskopf units (W.u.) would be required.

We thus conclude that the spin and parity of the 4742 keV level is 9/2+ with 5/2- an extremely remote possibility. Main et al. (1970) have recently measured the $^{29}Si(p,p'\gamma)$ angular correlation and obtained J = 9/2 for the 4742 keV level,in agreement with our results.

Levels at 4.838, 4.896 and 4.935 MeV

Betigeri et al. (1966) have assigned $J^{\pi}(4.84) = 1/2+$ on the basis of $\ell_n = 0$ transfer observed in the $^{28}Si(d,p)^{29}Si$ reaction. This conclusion is supported by the isotropic γ ray angular distributions observed from this level both in the present work and by Bardin et al. (1971). Main et al. (1970), however, observed anisotropic γ ray angular correlations in the $^{29}Si(p,p')$ reaction and instead concluded $J^{\pi} = 3/2+$. However, it is conceded in their paper that the coincidence γ ray spectrum for the 4.84 MeV gate contained radiation from the 4.89 MeV level which was unresolved in their proton spectrum. This latter state has a substantial ground state transition; ground-state radiation from the 4.84 and 4.89 MeV levels would not be resolved in the NaI spectrum. Thus, accurate angular correlation measurements of the 4.84 MeV transition would have to take into account the 4.89 MeV intensity and there is no evidence in the

paper of Main et al. (1971) that this was done. Accordingly, we do not believe the $J^{\pi} = 3/2+$ assignment has been proven and hold that $J^{\pi}(4.84) = 1/2+$.

The $J^{\pi}(4.90) = 5/2+$ and $J^{\pi}(4.93) = 3/2-$ assignments have been confirmed by Bardin et al. (1970) from their angular distribution measurements and are non-controversial.

Although the present experiment did not concern itself directly with these levels, we mention the known experimental information on them here, firstly for completeness, and secondly since they will be briefly mentioned in the following discussion on model calculations.

The 5.283 keV level

The primary decay ($\sim$90%) of this state is to the $J^{\pi} = 5/2+$ 2028 keV level, with a weak branch to the 1273 keV level. The angular distribution of the 3255 keV γ ray is anisotropic (Table 3.1) and the χ^2 analysis (Fig. 3.5) is compatible with either spin 7/2 or 3/2. Even incorporating the measured values of the γ-ray polarization ($P = 0.20\pm0.25$), one cannot distinguish between the two possibilities. Furthermore, one cannot even make an unambiguous parity assignment to this state, both negative and positive parities being allowed for either spin assignment. However, considerations based on the measured lifetime of this state ($<0.1\times10^{-13}$s) by Fisher et al. (1970) and on the allowed ranges of the

multipole mixing ratio from the angular distribution measurements allow one to make arguments based on partial radiative widths. Table 3.5 summarizes the experimental information on the 5283 keV level and the partial radiative widths for each spin and parity assignment. It is clear that for all allowed solutions, the M2 strengths are so large as to render the corresponding negative parity assignments highly unlikely. Certainly for spin 3/2, negative parity can be rejected on this basis; for spin 7/2 and the smaller value of δ, the M2 strength of > 24 W.u. is much larger than comparable strengths in this region of the sd shell.

Thus one can be reasonably confident in limiting the spin and parity of the 5283 keV state to 7/2+ or 3/2+ on the basis of these arguments.

The 5.565 MeV level

Bardin et al. (1971) have observed approximately equal feeds from this state to the 4081 (J^{π}=7/2+) and 3069 (J^{π}=5/2+) keV levels. The rigorous conclusion was J^{π} = 5/2+ or 9/2+ but the angular distribution systematics, γ-decay branching, and mixing ratios all supported the J^{π} = 9/2+ assignment. This state was unfortunately too weakly populated in the present experiment to allow a polarization measurement to be made; the analysis of the angular distributions yielded results similar to those given above.

Table 3.5

Allowed ranges of the multipole mixing ratio δ for the 3255 keV radiation and possible spin hypotheses J = 3/2 and 7/2 for the 5283 keV level in ^{29}Si.

Spin	δ(3255)	Strengths in W.u.			
		E1	M1	E2	M2
7/2	$0.21^{+0.15}_{-0.07}$	$>3\times10^{-3}$	>0.09	>0.79	>25
	1.46±0.27	$>1.2\times10^{-3}$	>0.04	>25	>740
3/2	$-2.75<\delta<-0.6$	$>2\times10^{-3}$	>0.07	>11	>340

4. Discussion

As mentioned above, the large model spaces involved render impractical complete spherical shell model calculations for ^{29}Si, and to date, only one truncated calculation has been reported (de Voigt et al., 1972). Predictions based on the strong-coupling Nilsson model and the intermediate coupling model (Castel et al 1970) do exist, however, and it is interesting to compare these predictions with our results.

Nilsson model

It will be recalled that Bromley et al (1957) concluded that the then available information on the low-lying states of ^{29}Si could be explained by assigning the levels to rotational bands based on Nilsson orbits #9 (K^{π}=1/2+) and #8 K^{π}(3/2+) with a deformation β= -0.15. If this interpretation is maintained, the 7/2+ and 9/2+ states at 5.28 and 4.74 MeV, respectively, may be assigned to the K^{π} = 1/2+ band and the J^{π} = 7/2+ 4.08 MeV state to the K^{π} = 3/2+ band. These assignments are supported by i) the energies of the levels and the spin sequences are approximately what would be expected, ii) the corresponding in-band E2 transitions are strongly enhanced over the Weisskopf estimates (Table 3.7).

Hirko (1969) has carried out a Nilsson-model calculation of theenergies and γ-transitions in ^{29}Si and obtained good agreement with the then available data. However, he used a large number of parameters to obtain this agreement and this

fact, together with the new data available as a result of the present and concurrent work, suggested that these calculations should be repeated, both for the level energies and electromagnetic transition strengths. The following parametrization was chosen: the band head energies of the 3/2+[202], 1/2+[211] and 1/2+[200] orbitals were chosen to agree with experiment (normalized to 1/2 1/2+[211] at zero excitation); the deformation was first obtained approximately by a minimization procedure and then allowed to vary slightly from this value to yield the best fit; the moment of inertia parameter $h^2/2\mathcal{J}$; and the intrinsic electric quadrupole moment (which cannot be obtained from the quadrupole interaction since ^{29}Si has a $J^{\pi} = 1/2$ ground state) was chosen to give the best fit to the E2 rates. Free nucleon magnetic moments and $g_R = 0.30$ (e.g. Rolfs et al.,1971) were used for the M1 strengths and are not regarded as additional free parameters since no variation of them was carried out. The total number of free parameters used in the calculation was $\simeq 5$ as compared with 12 for Hirko (1969). The final values of the parameters used are given in Table 3.6. The details of the calculation have been outlined briefly in a previous section and by a number of other authors (Price 1971, O'Neil 1972, Frank 1972) and need not be repeated here.

The results of the calculations are summarized in Fig. 3.6 and Tables 3.6 and 3.7. Figure 3.6 shows a comparison between the experimental and calculated level scheme;

Fig. 3.6

Comparison of the known positive parity levels of ^{29}Si with the results of a Nilsson model calculation including Coriolis band mixing. The Nilsson parameters used are given in Table 3.6 and were the same for all three bands. Dotted lines connecting states represent tentative identifications of observed and calculated levels.

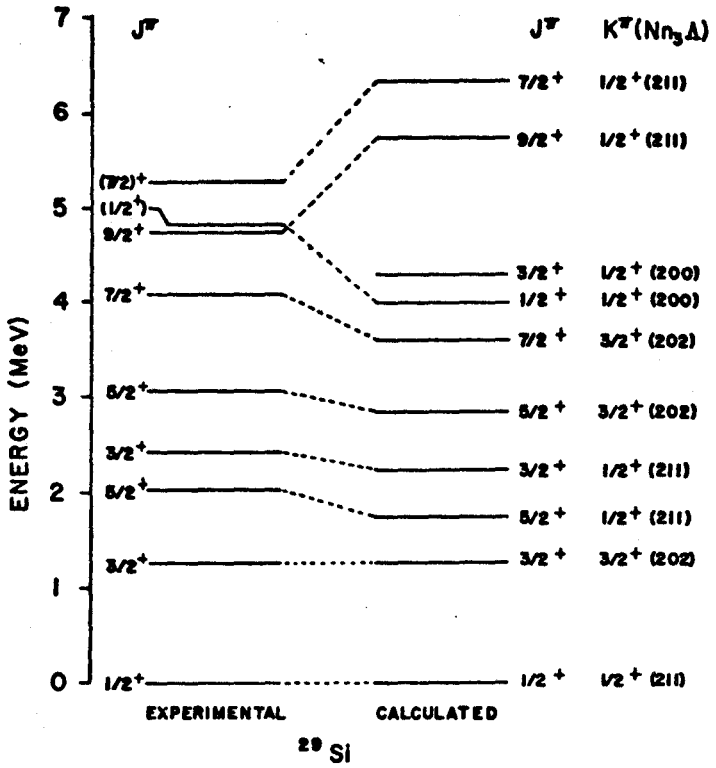
ENERGY (MeV)
7
6
5
4
3
2
1
0
J^π
J^π
$K^\pi(Nn_z\Lambda)$
(7/2)+
(1/2+)
9/2+
7/2+
5/2+
3/2+
5/2+
3/2+
1/2+
7/2+
9/2+
3/2+
1/2+
7/2+
5/2+
3/2+
5/2+
3/2+
1/2+
1/2+ (211)
1/2+ (211)
1/2+ (200)
1/2+ (200)
3/2+ (202)
3/2+ (202)
1/2+ (211)
1/2+ (211)
3/2+ (202)
1/2+ (211)
EXPERIMENTAL
CALCULATED
29 Si

Table 2.6

Wavefunctions of Coriolis-mixed states in ^{29}Si

J^{π}	E_x^{expt}	E_x^{calc}	1/2+[211]	1/2+[200]	3/2+[202]
1/2+	0	0	-0.9966	0.0823	-
3/2+	1.273	1.261	-0.3457	-0.3327	-0.8774
5/2+	2.028	1.434	0.9793	-0.1887	-0.0730
3/2+	2.426	2.204	-0.8978	-0.1545	0.4124
5/2+	3.069	2.866	-0.1170	-0.2334	-0.9653
7/2+	4.081	3.797	-0.3429	-0.5734	-0.7440
9/2+	4.741	5.369	0.9569	-0.2560	-0.1373
7/2+	5.283	6.691	-0.7992	-0.2382	0.5519

Parameters for Coriolis mixing calculation

$\hbar^2/2\mathcal{J}$ = 300 keV

δ = -0.20

H = 0.08

Table 2.7

^{29}Si Transition rates

J_i^π	E_x^i		E_x^f	Expt.		Nilsson		Int. Coupl.		Shell	
				M1	E2	M1	E2	M1	E2	M1	E2
	1273	→	0	0.035±0.003	4.3 ±0.3	0.038	4.31	3.0×10^{-5}	2.8	0.055	5.9
5/2+	2028	→	0	-	9.8 ±0.8	-	12.9	-	14.6	-	8.8
		→	1273	0.01 ±0.003	25	0.018	0.04	0.013	0.02	7×10^{-4}	1.1
3/2+	2426	→	0	0.064±0.01	22±7	0.10	10.0	2×10^{-5}	6.2	0.063	4.9
		→	1273	0.13 ±0.04	<10	0.08	5.7	0.013	0.5	0.096	8.7
5/2+	3069	→	1273	0.20 ±0.08	22±8	0.16	16.8	0.10	4.6	0.028	7.2
		→	2028	0.28 ±0.11	2.0 ±0.8	0.31	4.9	0.008	0.1	0.073	0.17
7/2+	4081	→	1273	-	10±3	-	13.2	-	18.8	-	6.8
		→	2028	0.041±0.006	0.47±0.07	0.03	0.20	1×10^{-5}	0.3	0.011	3.2
9/2+	4741	→	2028	-	25±5	-	18.2			-	11
		→	4081	0.22 ±0.07	-	0.14	0.005				
7/2+	5283	→	1273(*)	12±2		2					
		→	2028	70±5		71					
		→	2426	<3							
		→	3069	18±6		27					

(*) Lifetimes of 5.28 MeV not known; numbers given are branching ratios.

the details of the Coriolis-mixed wavefunctions for each state are given in Table 3.6; and Table 3.7 presents a comparison of the experimentally deduced and calculated transition strengths between the positive-parity levels. Table 3.7 also gives, for completeness, the results for the intermediate-coupling and shell model calculations; these will be discussed subsequently.

It is clear that though the energies of the low-lying states are quite well predicted by the Nilsson model, those for the higher states (J^{π} = 7/2+ and 9/2+ members of the K^{π} = 1/2+ band) are in poorer agreement. No reasonable change in the parametrization used was able to yield any meaningful improvement for these states. The deviations are probably due to admixtures of other, higher-lying rotational bands into the J^{π} = 7/2+ and 9/2+ levels which may be sufficiently great to cause the required energy shifts. The large number of states above E_x = 5.5 MeV of (as yet) unknown spin and parity makes attempts at identifying these other bands rather futile. Alternatively, the successes of the intermediate coupling model (Castel et al. 1970; to be discussed subsequently) suggest that there may well be substantial mixtures of vibrational states in these poorly described levels. The sequence 1/2+, 5/2+, 3/2+, 9/2+, 7/2+ with small spacing between the 5/2+ - 3/2+ or 9/2+ - 7/2+ doublets may be explained by the simple coupling of a j = 1/2+ neutron to

the 0+, 2+, 4+ states of ^{28}Si, which lie at 0, 1.78 and 4.61 MeV, respectively, in remarkable agreement with the centroids of the corresponding particle-coupled states in ^{29}Si, which turn out to be at 0, 1.59, and 4.95 MeV. Thus,deviations from the expected rotational spacings in ^{29}Si can be attributed to deviations from rotational flow in the corresponding even-even core ^{28}Si. Despite these difficulties, the calculation of energy levels agrees sufficiently well with experiment to be, at least, encouraging.

Stronger support for the rotational-model assignments may be obtained from the comparison of the electromagnetic transition strengths presented in Table 3.7. The magnitudes of the E2 rates are well reproduced by the Nilsson model and, as expected, "in-band" rates are enhanced by 10-20 W.u., and "out-band" transitions are of the order of the single-particle rate. It is interesting (and heartening!) to note that the surprisingly strong 4 W.u. E2 strength of the 1273 keV transition is well predicted and arises as a consequence of strong mixing between the 1/2+ and 3/2+ bands in the 1.27 MeV state (of Table 3.6).

The M1 rates calculated with the Nilsson model are also in excellent agreement with the experimental values for the deformation chosen. It became apparent in the course of the calculations that the M1 strengths were the most sensitive of any of the experimental data to the deformation and these were accordingly used to obtain the final 'best'

value of the deformation β. The agreement obtained for both the E2 and M1 rates is indeed remarkable considering the small number of free parameters used in the calculation; 18 transition strengths and the branching ratios of the 5.28 MeV level are quite well reproduced.

Thus, the Nilsson rotational model with Coriolis-mixing of the low-lying positive parity bands appears to give a remarkably faithful description of the properties of the levels of ^{29}Si.

Intermediate coupling model

Castel et al. (1970) have calculated the energy spectra and electromagnetic transition of a number of odd-A nuclei, including ^{29}Si, in the framework of the intermediate coupling model modified to include the anharmonic vibrations of the core. The energies are in acceptable agreement with the experiment (up to about 3 MeV), as are the E2 strengths (Table 3.7) but the M1 rates are, in many cases, too small by a considerable amount. The interpretation of ^{29}Si has, in the past, generated difficulties in both the rotational and vibrational models and Castel et al. find that their model gives improved results for nuclei of slightly greater mass (A = 33,35) which are in the known vibrational region.

Shell model

Very recently, de Voigt et al (1972) have published the results of a shell model calculation on ^{29}Si in a truncated

space. The transition rates obtained are also presented in Table 3.7. The agreement with the experimental data is generally good, except for a consistent underestimation of E2 rates. This is presumably due to the fact that "collective" transitions in a shell model arise from constructive interference of many small components of the wavefunctions and thus in an extended (and more realistic) model space larger E2 strengths would be obtained. The M1 strengths are in rather surprisingly good agreement when it is realized that they arise from constructive or destructive interference of a few large components; thus it is difficult to predict the behaviour of the M1 rates in an extended space. The excitation energies of the low-lying states, however, are not very well reproduced by the shell model calculations.

CHAPTER IV

CONCLUSIONS

The simultaneous measurement of γ-ray angular distributions and linear polarizations following near-threshold nuclear reactions has proved a useful tool for determining the spins and parities of nuclear states and deducing γ-ray multipolarities in the nuclei ^{21}Ne and ^{29}Si. Measurement of γ-γ coincidences, using both Ge(Li) and Na(I) detectors, revealed the presence of hitherto unobserved γ-ray transitions in both nuclei that were important for their theoretical significance.

The results of the experiments performed were combined with previous data on level lifetimes to extract γ-ray transition strengths. The level energies, spins and parities and transition amplitudes were compared, for both ^{21}Ne and ^{29}Si, with predictions based on the Nilsson strong-coupling rotational model. For ^{21}Ne, which is known to be strongly deformed, the good agreement generally obtained was not unexpected. However, a number of properties of a $K^{\pi} = \frac{1}{2}$ - band, in particular its anomalously low energy and extremely inhibited E1 transition rates to the positive parity states, could not be satisfactorily explained. However, it was suggested that both features might be the result of the peculiar structure of these states in an isospin formalism. The

nucleus ^{29}Si was of interest because it lies in a region where the nuclear shapes are unclear: the deformation appears to change abruptly as more nucleons are added. The results of the present experiments and calculations were able to confirm the oblate shape of ^{29}Si, and showed that remarkably good agreement between the Nilsson model and experiment could be obtained with surprisingly few variables.

Shell model calculations have also recently been carried out on both nuclei by groups at Oak Ridge, Michigan and Utrecht. The results are in (again) strikingly good agreement with the experiment and with the Nilsson model. The agreement is particularly gratifying (though not necessarily as good) for ^{29}Si, since as has been pointed out, a sizeable truncation of the configuration space used is necessary to keep the calculation within reasonable limits of computer time and memory. The success with which ^{29}Si (with its 13 "valence" nucleons) has been treated in such a limited manner leads one to hope that other "complex" nuclei, heretofore considered intractable by shell-model calculations, may also be as amenable to analysis.

It is of great interest to note that the shell model and the Nilsson model lead to essentially similar conclusions on energy levels, transition strengths, etc. This is particularly remarkable because one model is an attempt at a complete, microscopic description of the nucleus while the other is a semiclassical treatment (with its only one active

nucleon!) laden with approximations and limitations. Nevertheless, the end results of both calculations are quite similar. In an attempt to explore deeper into the foundations of the Nilsson model (which will certainly continue to be used for nuclei where shell model calculations are still unthinkable) it would be most interesting to carry out a detailed comparison of the shell model and Nilsson-model wavefunctions for a particular nucleus. For example, in Halbert's (1971) calculation of ^{21}Ne, mention is made of "rotation-like bands" which appear as a result of the massive $(sd)^5$ diagonalization. Why do these appear? What is the relationship between the structure of these bands and rotational motion of nuclei? Can one write a microscopic rotational wavefunction which has almost exactly unity overlap with a given part of the shell-model state (ie. can we "project" out a part of each state of a band a constant, "intrinsic", part, leaving the rest to describe the motion of the nucleus as a whole)? These questions are bound to be answered in the future (some are already partly understood) and will hopefully lead to a new, improved understanding of the nucleus transcending our present limited knowledge.

References

D. C. Bailey et al., J. Phys. A. 4 (1971) 908.

D. C. Bailey et al., J. Phys. A. 5 (1972) 596.

R. K. Bansal and J. B. French, Phys. Lett. 11 (1964) 145.

T. T. Bardin, J. A. Becker, T. R. Fisher and A.D.W. Jones, Phys. Rev. Lett. 24 (1970) 772.

T. T. Bardin, J.A. Becker, T.R. Fisher and A.D.W. Jones, Phys. Rev. C4 (1971) 1625.

F. Barros, P. D. Forsyth, A. A. Jaffe and I.J. Taylor, Proc. Phys. Soc.(London) 77 (1961) 853.

A. M. Baxter, B.W.J. Gillespie and J.A. Kuehner, Can. J. Phys. 48 (1970) 2434.

J. A. Becker, L. F. Chase and R. E. McDonald, Phys. Rev. 157 (1967) 967.

R. D. Bent et al., Nucl. Phys. A90 (1967) 122.

M. Betigeri et al., Z. Natur. 21a (1966) 980.

A. G. Blair and K. S. Quisenberry, Phys. REv. 122 (1961) 869.

D. M. Brink and G. R. Satchler, Angular Momentum. Oxford: The Clarendon Press, 1968.

D. A. Bromley, H.E. Gove and A.E. Litherland, Can. J. Phys. 35 (1957) 1057.

G.E. Brown, Unified Theory of Nuclear Models and Forces, Amsterdam: North-Holland, 1967.

B. Castel, K.W.C. Stewart and M. Harvey, Can. J. Phys. 48 (1970) 1490.

P.M. Endt and C. van der Leun, Nucl. Phys. A105 (1967) 1.

T. Engeland and P.J. Ellis, Nucl. Phys. A181 (1972) 368.

G.T. Ewan, G.I. Andersson, G.A. Bartholomew and A.E. Litherland, Phys. Lett. 29B (1969) 352.

L.W. Fagg and S.S. Hanna, Rev. Mod. Phys. 31 (1959) 711.

A.J. Ferguson, Angular correlation methods in gamma ray spectroscopy. Amsterdam: North-Holland, 1965.

A.J. Ferguson et al., Proceedings of the International Conference on Nuclear Structure, Tokyo, 1967.

A.J. Ferguson and S.T. Lam, Chalk River Nuclear Laboratories, 1972.

G.G. Frank, M.W. Green, D.T. Kelly, A.A. Pilt and J.A. Kuehner, Phys. Rev. Lett. 28 (1972) 571.

G.G. Frank, McMaster University, 1972.

H. Frauenfelder and R.M. Steffen, in Alpha, beta and gamma-ray spectroscopy, K. Siegbahn, ed. Amsterdam: North-Holland, 1966.

M.W. Greene, J.A. Kuehner and A.A. Pilt. Phys. Lett. 35B (1971) 560.

E.C. Halbert, J.B. McGrory, B.H. Wildenthal and S.P. Pandya, Advances in Nuclear Physics 4 (1971) 315.

R. G. Hirko, Ph.D. Thesis, Yale University, 1969.

A.J. Howard, D.A. Bromley and E.K. Warburton, Phys. Rev. 137 (1965) B32.

A. J. Howard, H.P. Allen, D. A. Bromley, J. W. Olness and E. K. Warbuton, Phys. Rev. 157 (1967) 1022.

A. J. Howard, J. G. Pronko and C. A. Whitten, Phys.Rev. 184 (1969) 1094.

A. J. Howard, J. G. Pronko and C. A. Whitten, Nucl. Phys. A152 (1970) 317.

J. M. Joyce, R. W. Zurmühle and C. M. Fou, Nucl. Phys. A132 (1969) 629.

I. Kanestrøm, Phys. Lett. 35B (1971) 283.

A. K. Kerman, Kgl. Danske Vidensk. Selsk, Mat-Fys. Medd. 30 (1956) 15.

P. D. Kunz, University of Colorado, 1965.

M. Lambert et al., Nucl. Phys. A112 (1968) 161.

C. M. Lederer, J. M. Hollander and I. Perlman, Table of Isotopes (Sixth edition) New York: Wiley and Sons, 1966.

A. E. Litherland, H. McManus, E. B. Paul, D. A. Bromley and H. E. Gove, Can. J. Phys. 36 (1958) 378.

A. E. Litherland, G. T. Ewan and S. T. Lam, Can. J. Phys. 48 (1970) 2320.

I. G. Main et al., Nucl. Phys. A158 (1970) 364.

M. C. Mermaz, C. A. Whitten and D. A.Bromley, Phys. Rev. 187 (1969) 1466.

S. G. Nilsson, Kgl. Danske Vidensk. Selsk., Mat-Fys. Medd. 29 (1955) 16.

R. A. O'Neil, McMaster University, 1972.

D. Pelte, Phys. Lett. 22 (1966) 448.

A. A. Pilt, M.Sc. Thesis, University of Alberta, 1969.

A. A. Pilt, R. H. Spear, R. V. Elliott and J. A. Kuehner, Can. J. Phys. 49 (1971) 1263.

R. H. Price, Ph.D. Thesis, McMaster University, 1971.

J. G. Pronko, W. C. Olsen and J. T. Sample, Nucl. Phys. 83 (1966) 321.

J. G. Pronko, C. Rolfs and H. J. Maier, Nucl. Phys. A94 (1967) 561.

J. G. Pronko, C. Rolfs and H. J. Maier, Phys. Rev. 186 (1969) B1174.

C. Rolfs, E. Kuhlmann, F. Riess and R. Krämer, Nucl. Phys. A167 (1971) 449.

C. Rolfs and H. P. Trautvetter, University of Toronto, and E. Kuhlmann and F. Riess, University of Freiburg, 1972.

H. J. Rose and D. M. Brink, Rev. Mod. Phys. 39 (1967) 306.

P.J.M. Smulders and T.K. Alexander, Phys. Lett. 21 (1966) 664.

S. J. Skorka, J. Hertel and T. W. Retz-Schmidt, Nuclear Data A2 (1966) 347.

E. Sheldon, S. Mathur and D. Donati, Comp. Phys. Comm. 2 (1971) 272.

E. Sheldon and D. M. van Patter, Rev. Mod. Phys. 38 (1966) 143.

R. H. Spear, J. E. Cairns, R.V. Elliott, J. A. Kuehner and A. A. Pilt. Can. J.Phys. 49 (1971) 355.

P.J. Twin, W.C. Olsen and D.M. Sheppard, Nucl. Phys. A143 (1970) 481.

M.J.A. de Voigt, P.W.M. Glaudemans ,J. de Boer and B. H. Wildenthal, Nucl. Phys. A186 (1972) 365.

E. W. Vogt, D. McPherson, J. A. Kuehner and E. Almqvist, Phys. Rev. 136 (1964) B99.

E. K. Warburton, J. W. Olness, G.A.P. Engelbertink and K. W. Jones, Phys. Rev. C3 (1971) 2344.

M. J. Wozniak, R. L. Hershberger and D. J. Donahue, Phys. Rev. 181 (1969) 1580.

L. Zamick, Phys. Lett. 19 (1965) 580.

APPENDIX I

CORRECTION TO THE POLARIZATION DUE TO ANGULAR DISTRIBUTION EFFECTS

In both the analysis of the polarization of unknown γ-rays and the determination of detector sensitivity using the planar polarimeter account must be taken of the variation in count rate in the "parallel" and "perpendicular" orientation due to the angular distribution of the γ-ray. For example, a pure E2 γ-ray with a minimum in the angular distribution at 90° will give an excess of counts in the "parallel" direction since proportionately more counts will be detected at $(90\pm\theta)°$ than at 90°. An expression for the correction to be made is derived here.

For a detector subtending a horizontal angular range $\pm\theta_o$ radians from 90°, the mean integrated intensity is

$$N_{||} = \int_{\frac{\pi}{2}}^{\frac{\pi}{2}+\theta_o} a_o(1+a_2P_2(\cos\theta)+a_4P_4(\cos\theta)d\theta \Big/ \int_{\frac{\pi}{2}}^{\frac{\pi}{2}+\theta_o} d\theta \qquad (1)$$

Using $P_2(\cos\theta) = \frac{1}{2}(3\cos^2\theta-1)$

$P_4(\cos\theta) = \frac{1}{8}(35\cos^4\theta-30\cos^2\theta+3)$

we find

$$N_{||} = a_o^{(||)}\{1 - \tfrac{1}{2}a_2 + \tfrac{3}{8}a_4 + \theta_o^2(\tfrac{1}{2}a_2 - \tfrac{5}{4}a_4) + \theta_o^4(-\tfrac{1}{10}a_2 + \tfrac{9}{8}a_4)\}. \qquad (2)$$

The angle subtended in the horizontal plane when the detector is in the vertical direction is very small and we may assume $\theta_o = 0$. The intensity is then

$$N_{\perp} = W(90) = a_o^{(\perp)}\{1 - \tfrac{1}{2}a_2 + \tfrac{3}{8}a_4\} \quad . \qquad (3)$$

The difference in counting rates due to the γ-ray polarization is expressed by the different normalization factors $a_o^{(\parallel)}$ and $a_o^{(\perp)}$. Thus the correct asymmetry (S) is expressed as

$$S = \frac{a_o^{(\parallel)} - a_o^{(\perp)}}{a_o^{(\parallel)} + a_o^{(\perp)}} \quad .$$

$N_{\parallel}$ and $N_{\perp}$ are the experimental intensities observed in the two orientations. Thus the asymmetry S in terms of these quantities and the angular distribution coefficient (assumed to have been measured in a simultaneous experiment) is

$$S \sim \frac{N_{\parallel}(1-\frac{1}{2}a_2+\frac{3}{8}a_4)-N_{\perp}[1-\frac{1}{2}a_2+\frac{3}{8}a_4+\theta_o^2(\frac{1}{2}a_2-\frac{5}{4}a_4)+\theta_o^4(-\frac{1}{10}a_2+\frac{9}{8}a_4)]}{N_{\parallel}(1-\frac{1}{2}a_2+\frac{3}{8}a_4)+N_{\perp}[1-\frac{1}{2}a_2+\frac{3}{8}a_4+\theta_o^2(\frac{1}{2}a_2-\frac{5}{4}a_4)+\theta_o^4(-\frac{1}{10}a_2+\frac{9}{8}a_4)]} \quad .$$

APPENDIX II

PUBLICATIONS BASED ON WORK DONE AT McMASTER

1. R. H. Spear, J. E. Cairns, R. V. Elliott, J. A. Kuehner and A. A. Pilt, Can. J. Phys. 49 (1971) 355.
2. A. A. Pilt, R. H. Spear, R. V. Elliott and J. A. Kuehner, Can. J. Phys. 49 (1971) 1263.
3. M. W. Greene, J. A. Kuehner and A. A. Pilt, Phys. Lett. 35B (1971) 560.
4. G. G. Frank, M. W. Greene, D. T. Kelly, A. A. Pilt and J. A. Kuehner, Phys. Rev. Lett. 28 (1972) 571.
5. A. A. Pilt, Phys. Rev. C5 (1972) 1786.
6. A. A. Pilt, R. H. Spear, R. V. Elliott, D. T. Kelly, J. A. Kuehner, G. T. Ewan and C. Rolfs, Can. J. Phys. 50 (1972) in press.